

HYDROGEOCHEMICAL AND MICROBIOLOGICAL FACTORS
AFFECTING THE HEAVY METAL CHEMISTRY
OF AN ACID MINE DRAINAGE SYSTEM

A DISSERTATION
SUBMITTED TO THE DEPARTMENT OF APPLIED EARTH SCIENCES
AND THE COMMITTEE ON GRADUATE STUDIES
OF STANFORD UNIVERSITY
IN PARTIAL FULFILLMENT OF THE REQUIREMENTS
FOR THE DEGREE OF
DOCTOR OF PHILOSOPHY

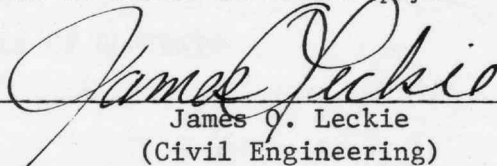
By
Darrell Kirk Nordstrom
March 1977

© Copyright 1977

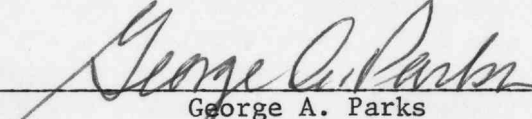
by

Darrell Kirk Nordstrom

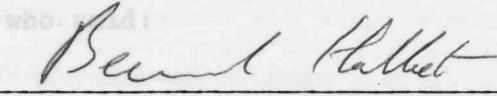
I certify that I have read this thesis and that in my opinion it is fully adequate, in scope and quality, as a dissertation for the degree of Doctor of Philosophy.


James O. Leckie
(Civil Engineering)

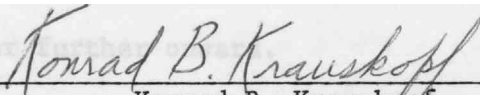
I certify that I have read this thesis and that in my opinion it is fully adequate, in scope and quality, as a dissertation for the degree of Doctor of Philosophy.


George A. Parks

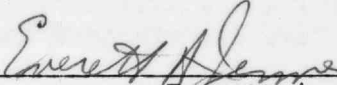
I certify that I have read this thesis and that in my opinion it is fully adequate, in scope and quality, as a dissertation for the degree of Doctor of Philosophy.


Bernard Hallet

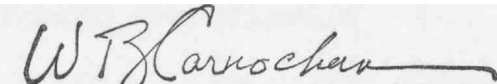
I certify that I have read this thesis and that in my opinion it is fully adequate, in scope and quality, as a dissertation for the degree of Doctor of Philosophy.


Konrad B. Krauskopf

I certify that I have read this thesis and that in my opinion it is fully adequate, in scope and quality, as a dissertation for the degree of Doctor of Philosophy.


Everett A. Jenne
(U. S. Geological Survey)

Approved for the University Committee
on Graduate Studies:


Dean of Graduate Studies

To Pierre Teilhard

who said:

"Sense of Earth" should be understood
to mean the passionate concern for our
common destiny which draws the thinking
part of life ever further onward.

TABLE OF CONTENTS

	Page
LIST OF FIGURES	vi
LIST OF PLATES	viii
LIST OF TABLES	ix
PREFACE	xi
ACKNOWLEDGEMENTS	xiii
ABSTRACT	xv
INTRODUCTION	1
Project Background	1
Major Objectives	2
Interrelationship of the Environmental Factors	3
THE SPRING CREEK DRAINAGE AND THE SAMPLING PROGRAM	5
The Spring Creek Drainage Basin	5
Outline of Sampling Program	11
Sampling Methods and Discharge Measurements	13
ANALYTICAL PROCEDURES	16
GEOLOGY	18
Geomorphology	18
Tectonic History and Petrogenesis	19
Major Rock Units	22
Summary of Rock Types and Compositions	26
Ore Deposits	28
Structural Features at Iron Mountain	33
Hydrothermal Alteration	34
Hydrogeology: A Unique Reactor	36
MINING HISTORY: INITIATING THE REACTOR	39
THE AQUEOUS OXIDATION OF SULFIDE ORES	51
MICROBIOTA AND THEIR EFFECT ON FERROUS IRON OXIDATION IN ACID MINE WATERS	57

	Page
Microbial Ecology of Acid Mine Waters: Literature Review	58
Microbial Ecology of Acid Mine Waters: Field Observations	68
Isolation of the Iron-oxidizing Bacterium: <i>Thiobacillus ferrooxidans</i>	77
Oxidation Rates of Acid Mine Waters on Site and in the Laboratory	84
OXIDATION-REDUCTION EQUILIBRIA IN ACID MINE WATERS	99
Eh Measurements in Natural Waters: Equilibria or Disequilibria?	99
Experimental Method	101
The Redox Chemistry of ZoBell's Solution	102
Correlation of Measured Eh with the Ferrous-Ferric Redox Couple	120
The Control of pH by Redox Reactions	123
HYDROCHEMICAL PATTERNS	129
Climate	129
Distribution of Stream Discharges, Solute Concentrations, and Solute Loads within the Drainage Area	130
Seasonal Variations in Rainfall, Discharge and Solute Concentrations	137
Solute-Discharge Variations During a Mild Rainstorm	147
Rate of Chemical Weathering	150
MINERAL EQUILIBRIA CONTROLS ON THE COMPOSITION OF ACID MINE WATERS	152
Thermodynamic Data for Metal Sulfate and Hydroxide Complexes	155
Thermodynamic Data on Jarosite, Gypsum and Other Sulfate Minerals	157
Modifications of a Water-Mineral Equilibria Computing Program for Acid Mine Water	159
Activity Product Trends and Mineral Equilibria in the Richmond-Hornet, Boulder Creek and Spring Creek Drainages	161
CONCLUSIONS	174
REFERENCES	177
APPENDICES	191
I. Tables of water analyses	191
II. Measured potentials in ZoBell's solution from 8° to 84°C	210

LIST OF FIGURES

Figure	Page
1. Location of the Spring Creek drainage	6
2. Geologic map of the Spring Creek drainage	27
3. Cross section of ore bodies	29
4. Cross section of Richmond ore body	35
5. Change in ferrous iron, Eh and pH during oxidation of 9 K culture media by <i>T. ferrooxidans</i>	82
6. Dependence of ferric iron concentration on bacterial cell count	83
7. Location of sample sites for iron oxidation study . . .	87
8. Oxidation of acid mine waters	96
9. Measured potentials of ZoBell's solution	104
10. Comparison of calculated with measured Eh values	122
11. pH convergence of oxidizing mine waters and 9 K media	126
12. pH, iron and conductance variations with discharge . . .	140
13. Correlation of the aluminum concentrations with the specific conductance	141
14. Correlation of the cadmium concentrations with the specific conductance	142
15. Correlation of the sulfate concentrations with the specific conductance	143
16. Correlation of the zinc and cadmium concentrations . . .	145
17. Correlation of the dissolved iron with discharge and specific conductance	146
18. Variation in sulfate concentrations at sites G, J and D during a mild rainstorm	148

Figure	Page
19. Saturation indices for melanterite as a function of the log conductivity showing that supersaturation is reached in the Hornet-Richmond effluent	166
20. Saturation indices for amorphous iron hydroxide showing that saturation is reached by the diluted downstream waters	168
21. Saturation indices for goethite demonstrating supersaturation for nearly all of the samples	169
22. Saturation indices for gypsum indicating saturation is reached in the undiluted mine waters issuing directly from the mines	172
23. Saturation indices for epsomite showing that saturation is never reached by these waters	173

LIST OF PLATES

Plate		Page
1.	Green filamentous algae (<i>Ulothrix</i> ?) growing in acid spring in the open pit at Iron Mountain	69
2.	"Acid slime streamers" covering bottom of Boulder Creek as seen through about 5 to 10 cm of water	71
3.	Green filamentous algal (<i>Ulothrix</i> ?) growth along the banks of Spring Creek	75
4.	Mosslike clumps of green algae growing at base of Spring Creek Dam outlet	78
5.	Intense red-brown color of Spring Creek between sites J and K caused by the oxidation and hydrolysis of high dissolved iron concentrations	86
6.	Precipitation of jarosite minerals and efflorescent sulfate minerals in Boulder Creek at site G	164

LIST OF TABLES

Table	Page
1. Selected hydrologic characteristics of the Spring Creek drainage basin	7
2. Description of reconnaissance and long-term sampling sites	12
3. Methods of analysis	17
4. Major rock units	30
5. Sulfide minerals used as substrates for <i>T. ferrooxidans</i>	65
6. Water analysis of Boulder Creek before and after infiltrating an embankment	76
7. Composition of 9 K medium	80
8. Composition and velocity of Spring Creek water at selected sites downstream before rainstorm	89
9. On site ferrous iron oxidation rates before and after a rainstorm	93
10. Linear least square equations fitted to the emf measurements for $T < 55^{\circ}\text{C}$	106
11. Complex association in the aqueous potassium ferro-ferricyanide system at 25°C	111
12. Half-cell potentials for the saturated KCl silver-silver chloride and Orion combination redox reference electrodes	117
13a. Thermodynamic value for equimolar potassium ferro-ferricyanide solutions at 25°C	118
13b. Temperature dependent equations for the thermodynamic functions	119
14. Comparison of dissolved metal and sulfate loads	132
15. Composition of Iron Mountains tailings spring compared to Boulder Creek	133

Table	Page
16. Composition of Slickrock Creek at Iron Mountain	136
17. Composition of Spring Creek at mouth of reservoir under a range of flow conditions	138
18. Log K and enthalpies of association for sulfate complexes used to calculate mineral equilibria in acid mine waters	156
19. Thermodynamic data for three major jarosites	158

PREFACE

In this thesis I have examined the geological, chemical and microbiological aspects of a stream environment severely affected by acid mine drainage. Valuable water quality information, essential to the design and management of treatment procedures, is presented, and it is in regard to proposed treatment plans that I would like to remind readers of the warning from Reinow and Reinow (1967):

Once there dwelt a King in a tiny but very fruitful kingdom, bordered all round about by cruel and barren lands. But the King was sick unto death. Brought to his bed by all manner of self-indulgence he groaned in his suffering and irritably bid his court physicians to heal him. Now, the leeches (as the physicians were yclept) had long known the true remedy for the King's malady, but it was an unpleasant one--so unpleasant they feared the King's ire should they apply it.

So they quickly applied expedients--pain-killing drugs and unctuous reassurances. But while these dulled the King's misery for an hour, they soon left him feeling more wretched than before. Then the leeches resorted to opium, but this, while it furnished the ailing King with periods of blissful fantasy, also passed away, leaving him worse off in stomach and temper than ever.

Then the wisest of the leeches said, "The King is our Protector. Without him we are destroyed. We must bravely abandon expedients; we must concoct the ancient herbal remedy and forthrightly puke and purge the King; it is our only chance." So this they did, and the King, now deathly sick, was surprisingly unresisting.

Within seven days the King began to improve. Finally, he rose from his bed feeling like new. But as soon as he felt recovered, the King, in his ignorance, returned to the unrestrained dining and carousing, as was his wont, and the tumefaction returned upon him worse than before.

Now, what all these sycophants--leeches and wise men--at the King's bedside knew well was this: that no cleansing herbs or remedies ever devised could restore lasting health to their ruler unless he ceased glutting himself and reduced his swollen girth. But who would tell the King what to do? Frightenedly, they

conferred together and wrung their hands, but not one among them could muster the hardiness to tell his Sire the blunt and unwelcome truth, or seek to curb him. And so, for risk of offending the royal temper, they cravenly let him die.

The world today is a sick world, drained of its life-giving waters and toxic with the wastes of too many people crowded into too many congested areas. All the river dredging, diversion of streams, poisoning of phreatotypes, the cloud-seeding, much of the dam-building, the re-use of waste water and sewage--all the frenetic busy work of a foolhardy civilization whose water resources are on a permanent decline but which refuses to admit it--are merely the treatment of symptoms. They are temporary pain-killers--the aspirin of science.

Any proposed solution to the acid mine drainage problems of Shasta County must contain the assurance, through a carefully thought-out strategy, that the consequences of the cure will not be worse than the present predicament.

ACKNOWLEDGEMENTS

A thesis of this scope could not have been completed without the generous assistance of several people. Bob Averett, Everett Jenne and Rich Fuller (U. S. Geological Survey) conspired to make this project possible. George Parks, my chief advisor, was an unfailing source of encouragement, support and constructive criticism. I am particularly grateful to Leland George, consultant for Stauffer Chemical Company, for his willingness to assist with the field work and to correct several discrepancies in the mining history. The support of Stauffer Chemical Company and Leland George made the investigations of Slickrock Creek and Boulder Creek a much easier task. It is a pleasure to have worked with Jo Burchard, Dave Vivit, Don Girvin and Doris York (U. S. Geological Survey) whose technical assistance made it possible to meet deadlines. No one person gave as unselfishly of their time as Jim Ball (U. S. Geological Survey) did on analytical methods and especially on computer programming aspects of WATEQ2. Valuable help on stream gaging and sampling was provided by Malcolm Weston, Michael Friebe, Pete Shelton, Bruce Webb, Greg Tom, Ray Hoffman and Rodger Ferreira, all of the Water Resources Division, U. S. Geological Survey. June Parker of the Redding field office (U. S. Geological Survey) kept track of the confusion I created whenever I embarked on a field trip. Several other members of the Survey offered welcome advice but the most important of these were Vance Kennedy, Charles Christ and Robert Potter. Lily Young and Jim Leckie (Stanford University) gave valuable advice with

the microbiological and chemical aspects of the project. I want to thank Anne Berry for completing the grim task of final typing and seeing the thesis through to binding. The continuous support of Everett Jenne throughout all phases of this project made it possible for me to carry out my intended goals. Finally, I really owe my deepest gratitude to my wife, Karen, who not only provided much needed encouragement but who also helped with lab work, typing and editing.

ABSTRACT

Abandoned copper mines in Shasta County, California, contain massive sulfide ores and tailings which are being weathered and oxidized to form strongly acidic mine drainage. The massive sulfides are composed dominantly of fine-grained pyrite with variable amounts of chalcopyrite, sphalerite, greenockite, tetrahedrite-tennantite and galena emplaced in the middle horizon of the Balaklala Rhyolite. Effluents issuing from these ore bodies reach pH values as low as 0.3 and contain solute concentrations as high as 10,000 mg/l iron, 300 mg/l copper, 1200 mg/l zinc, 1000 mg/l aluminum, 10 mg/l cadmium and 40,000 mg/l sulfate due to the oxidation of the sulfides to sulfuric acid. Over 16 km (10 mi) of stream distance in one watershed are affected by acid mine waters draining from one major complex of ore bodies. The periodic occurrence of high runoff from the polluted streams has resulted in fish kills at nearby recreational areas for several decades.

To determine the major sources and variations of acid discharges within a single watershed, an 18 month sampling program was carried out at critical points along the major streams. Water samples were analyzed for all major constituents and the results, along with discharge measurements and microbiological samples, were used to identify the major controls on the dissolved solute concentrations from their sources to their entrance to a reservoir several kilometers downstream.

High concentrations of iron, copper, zinc, cadmium and sulfate in the initial effluent are governed by the oxidative breakdown of massive

fine-grained pyritic ore by groundwaters infiltrating faults and stopped out areas within a gentle syncline. High concentrations of sodium, potassium, calcium, magnesium and aluminum result from contact of these acid waters with the rhyolitic wall rock. Gypsum solubility provides an upper limit to the calcium concentrations whereas the other major cations are limited only by the solubility of such readily dissolved minerals as epsomite, alum, goslarite, chalcantite and melanterite, and the natural abundance of the original rock.

During downstream transport, the solute concentrations are controlled by the rainfall-discharge history under changing conditions of transient flow. Solute concentrations have been found to increase with the initial rise in discharge due to (1) the dissolution of soluble sulfate minerals which have precipitated along stream banks and (2) the rapid rise in the discharge of a polluted tributary relative to the more slowly rising, unpolluted main stream. The tributary discharge rises more rapidly than that of the main stream because its smaller drainage area allows it to respond to rainfall more quickly. For conditions of low stream flow, solute concentrations are limited by the solubility of oxide, hydroxide and sulfate minerals such as melanterite, gypsum and amorphous iron hydroxide. Mineral equilibria calculations were carried out on water analyses by extensive modification of the computerized chemical model known as WATEQ, which outputs activities of solute species and saturation indices for 186 minerals. Punched card output was used for plotting water quality parameters and mineral stability diagrams. Rapid rates of iron oxidation in the streams, which force the precipitation of ferric iron minerals, are controlled by the growth of *Thiobacillus ferrooxidans*, an iron-oxidizing bacterium. An average oxidation

rate of 2.8 mM/hr measured on site agrees quite well with the average rate measured in 9K culture media, suggesting that these bacteria are growing under near optimum conditions in these streams.

Field Eh measurements proved to be in reasonable agreement with redox potentials calculated from ferrous-ferric analyses. A consistent discrepancy, however, suggests that some complexes may be unaccounted for in the equilibria computations. In the course of the Eh studies, the temperature dependence for the Eh of ZoBell's solution was found to be: $Eh (v) = 0.430 - 0.0023 (T - 25) - 0.0000038 (T - 25)^2$. These measurements permitted the estimation of the enthalpy, entropy and heat capacity of the ferro-ferricyanide couple at 0.15 molar ionic strength.

"The farther and more deeply we penetrate into matter, by means of increasingly powerful methods, the more we are confounded by the interdependence of its parts. . . . It is impossible to cut into this network, to isolate a portion without it becoming frayed and unravelled at all its edges."

--Pierre Teilhard (1959)

Frontispiece. ERTS color photo of Shasta Lake and Whiskeytown Lake;
Iron Mountain is located at the white spot northeast of Whiskeytown
Lake and west of the Sacramento River; Redding is at bottom, right
of center.

PLEASE NOTE:

Frontispiece is a very dark color photo and will not reproduce well in xerographic copies. Filmed in the best possible way.

UNIVERSITY MICROFILMS.



INTRODUCTION

Project Background

Shasta Lake, at the head of the Sacramento Valley in California, is well known for its recreational availability, water storage capacity for irrigation, flood control and hydroelectric power output. Less well known are the periodic fish kills associated with acid mine drainage in the Shasta Lake-Keswick Reservoir area. On at least nine separate occasions during the last 20 years more than a thousand fish have been reported dead, highlighted by a fish kill of 100,000 on April 22, 1955, and again in 1963 and 1964 (Nordstrom and others, 1977). The severity of the problem has effected a series of written reports, chiefly by the California Fish and Game Department and the California Water Quality Control Board, on the sources of contamination and the effects on native fish (Appendix III; Nordstrom and others, 1976).

In nearly every report, the high copper concentrations present in the acid mine waters were said to be the cause of the fish kills. This conclusion was inevitable because (1) the mines were primarily opened up for copper production, (2) only iron and copper (and rarely zinc) were analyzed in the state studies, and (3) the toxicity of copper at high concentrations is well known. Several questions remained unanswered: (a) Are all possible toxic metals accounted for? (b) Are all sources of acid mine drainage which end up in the Sacramento River accounted for? (c) What is chiefly responsible for the observed relationship between high discharges and fish kills? (d) What is the

variation in dissolved metal concentrations and discharges throughout the year? (e) What factors control these variations?, and ultimately, (f) What can be done to prevent further pollution?

On July 26, 1976, the California Regional Water Quality Control Board (Central Valley Region) adopted a resolution to support a demonstration project for the correction of mine pollution under a cooperative studies program with the U. S. Geological Survey. The initial stage of this project was a reconnaissance survey of trace metals input to Shasta Lake and Keswick Reservoirs (Nordstrom and others, 1976). Following this survey the most contaminated stream, Spring Creek, was chosen for detailed study as part of the present Ph.D. thesis. These studies should contribute significantly toward answering the previously posed questions.

Major Objectives

The principal aim of this thesis is to define the hydrogeochemical processes which determine the observed variations in dissolved solute concentrations of an acid mine drainage system. The major factors which will be shown to control solute concentrations in the study area are:

1. equilibrium or near-equilibrium states of mineral saturation during normal low-flow conditions of discharge;
2. the seasonal rainfall-discharge patterns and dilution trends during moderate to high flow, non-steady state conditions of discharge;
3. the amount of microbial activity present in the streams.

These factors are developed from a long-term field and laboratory program which involved:

1. an 18 month water sampling and stream gaging program at several sites;
2. analytical determination of all major constituents;
3. X-ray identification of fresh mineral precipitates;
4. identification of iron-oxidizing bacteria;
5. modification of a chemical model to test calculated mineral equilibria against field observations.

Interrelationship of the Environmental Factors

A primary goal for any environmental science is to understand the specific processes by which a measurable quantity undergoes change by a spatial or temporal displacement in the natural environment. At least two fundamental aspects of natural processes need to be considered for the interpretation of changes occurring in the environment:

- (1) the thermodynamic and kinetic constraints on a chosen system and
- (2) the interdependence of all the chemical, physical and biological components for that system. The principles of irreversible and reversible thermodynamics can reveal the extent to which equilibrium has been attained. These principles have been quantitatively applied to an acid mine drainage system in this thesis.

Acid mine drainage is a result of the interaction of the hydrologic cycle with geologic formations aided by the intervention of man and catalyzed by microorganisms. To understand the formation of acid mine waters the integration of hydrology, geology, chemistry, mining methods and microbiology is required.

A multidisciplinary approach has been used in this thesis to describe an environmental system, i.e. a watershed basin severely

affected by acid mine drainage. The description begins with the geologic formation, continues with the mining history, the chemistry of sulfide mineral oxidation, solute-discharge patterns of acid mine waters in the study area, microbial growth in the affected streams and their catalysis of iron oxidation, redox equilibria in acid mine waters and ends with the control of acid mine drainage chemistry by mineral solubility equilibria.

THE SPRING CREEK DRAINAGE AND THE SAMPLING PROGRAM

The main purpose of the present chapter is to introduce the reader to the geographic location of the streams, sampling sites and chief sources of pollution. During the course of this investigation many observations on the distribution of heavy metals and on the general geography were made which could not be further studied because they did not directly relate to the proposed thesis. These observations are discussed in the present chapter, not to detract from the main theme, but rather to bring to the attention of the reader secondary sources of pollutants and information regarding the fate of acid mine waters which leave Spring Creek Reservoir.

The Spring Creek Drainage Basin

Spring Creek lies immediately west of the Sacramento River between the latitudes marked by Shasta Dam and Keswick Dam (fig. 1) in Shasta County, California. The two main tributaries of Spring Creek, Slickrock Creek and Boulder Creek, flow year around, while South Fork Spring Creek, the only other tributary, usually dries up during the summer and fall. Water from Spring Creek and its tributaries collects in Spring Creek Reservoir before discharging into an arm of Keswick Reservoir (formerly the mouth of Spring Creek).

Selected hydrologic characteristics of the Spring Creek Drainage Basin are compiled in table 1. These measurements will become particularly

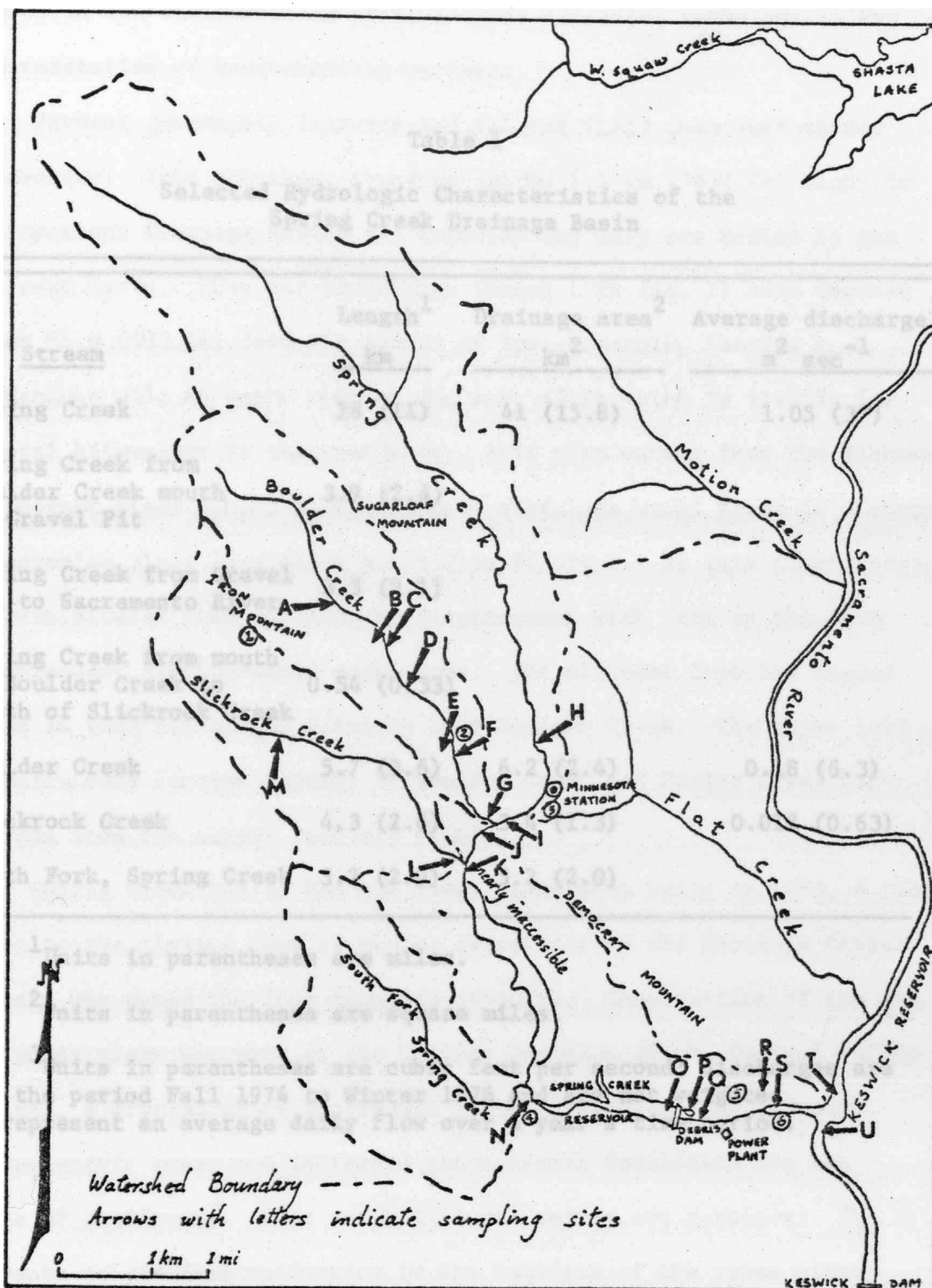


Figure 1. Location of the Spring Creek drainage.

Table 1
Selected Hydrologic Characteristics of the
Spring Creek Drainage Basin

<u>Stream</u>	Length ¹	Drainage area ²	Average discharge ³
	<u>km</u>	<u>km²</u>	<u>m³ sec⁻¹</u>
Spring Creek	18 (11)	41 (15.8)	1.05 (37)
Spring Creek from Boulder Creek mouth to Gravel Pit	3.9 (2.4)		
Spring Creek from Gravel Pit to Sacramento River	3.3 (2.1)		
Spring Creek from mouth of Boulder Creek to mouth of Slickrock Creek	0.54 (0.33)		
Boulder Creek	5.7 (3.6)	6.2 (2.4)	0.18 (6.3)
Slickrock Creek	4.3 (2.6)	3.4 (1.3)	0.018 (0.63)
South Fork, Spring Creek	3.2 (2.0)	5.2 (2.0)	

¹Units in parentheses are miles.

²Units in parentheses are square miles.

³Units in parentheses are cubic feet per second; discharges are for the period Fall 1974 to Winter 1976 and are not weighted to represent an average daily flow over a year's time period.

useful in the determination of downstream oxidation rates and in the interpretation of hydrochemical patterns.

Several geographic features and related field observations are noteworthy. Iron Mountain, standing nearly 1.1 km (3600 ft) high, is an important drainage divide and contains the only ore bodies in the drainage basin. Open pit operations (point 1 in fig. 1) have removed about 91 m (300 ft) from the summit of Iron Mountain, leaving a tremendous pile of waste rock on the west slope which is visible for several kilometers to the southeast. Acid mine waters from the Richmond and Hornet mines (point C) flow down a stainless steel flume to a copper cementation plant located at point 2 in figure 1. At this plant, copper is precipitated from solution by displacement with iron in the form of shredded, alkali-washed steel cans. The effluent from the copper plant is then discharged directly into Boulder Creek. The major load of pollutants (except copper) in Boulder Creek and Spring Creek discharges from the copper recovery plant.

Spring Creek Debris Dam and Power Plant were build in 1963, 4 years prior to the closing down of mining operations by the Mountain Copper Company who owned the Iron Mountain property. Construction of the dam and power plant was part of the Trinity Division of the Central Valley Project, a program which envisioned further flood control, greater hydroelectric power and increased recreational facilities for the State of California. This earth-fill dam serves two purposes: (1) it prevents debris from collecting in the tailrace of the power plant, and (2) it allows regulation of the acid water discharge. Spring Creek Dam is a bottom release structure with a unique block and trashrack design over a single concrete outlet. As sediment builds up to the

trashrack the trashrack is removed, and a concrete block is slid down a track to take its place. The discharge is regulated by a gate, located at the center of the outlet structure in the middle of the dam, which can be controlled from a shaft house on the crest of the dam. Water is released from Spring Creek Reservoir in coordination with Shasta Dam discharges such that if the copper concentration of Spring Creek Reservoir water is known and the discharge out of Shasta Lake is known, the maximum allowable release from Spring Creek can be read from a nomogram. Nomograms were prepared by Lewis (1963) based on 96-hr mortality tests on rainbow trout and king salmon fry, using actual Spring Creek water at different times of the year.

Unfortunately, Lewis' schedule has not always been maintained. In 1969, flash-flood type discharges from the drainage basin caused the reservoir to fill very rapidly, and when full capacity was reached excess water was released from the bottom of the dam rather than simply letting it flow over the spillway. At noon on January 13, 1969, $17.5 \text{ m}^3/\text{sec}$ (620 cfs) of combined bottom release and spillway overflow entered Keswick Reservoir. On January 14, 1620 fish were reported dead in Keswick Reservoir. This particular fish kill can be related to two events: (1) the low releases from Shasta Lake following a dry year and (2) the high releases from Spring Creek, exceeding the criteria set by Lewis (1963). The high discharges from Spring Creek Reservoir were a result of concern by the operators for the safety of Spring Creek Dam. Following this incident an investigation took place leading to closer monitoring and a provision for closing the bottom release and allowing only spillway release when the reservoir overflows.

No fish kills known to the author have occurred in Keswick Reservoir since 1969.

The Spring Creek Power Plant uses water carried through conduits from Whiskeytown Lake, located several miles to the west from Spring Creek. The water from the power plant empties directly into the arm of Keswick Reservoir just below the point where the acid water released from the Spring Creek Dam mixes with Keswick Reservoir. Although the power plant discharges help to mix and further dilute the acid mine drainage, these power plant discharges also have the detrimental effect of keeping the arm of Keswick Reservoir very high in suspended sediment. This turbulence is particularly noticeable when the power plant has just been started up after a period of no flow and no power generation. The turbulence from the tailrace (located below water level and not visible) resuspends fine-grained iron, manganese, aluminum and zinc hydroxides which precipitated at the point of mixing. Resuspended particulates have been observed as a light brown swirling stream being transported down the entire length of the reservoir arm. These particulates have two potentially harmful effects on the fish in Keswick Reservoir: (1) the increased turbidity interferes with their breathing and their feeding (Lloyd, 1965), and (2) the precipitates probably contain large quantities of coprecipitated or adsorbed heavy metals (Jenne, 1968) which are highly toxic (e.g. Cu, Zn and Cd).

Other minor sources of heavy metals being transported into the arm of Keswick Reservoir are (1) metal sulfates being leached from old slag wastes which occur for several hundred feet along the south bank (point 6 in fig. 1), (2) small springs and general runoff which carry dissolved and particulate metals from the old open-air roasting piles

along the southeast slope of Democrat Mountain (point 4 in fig. 1), and possibly (3) drainage from contaminated soils along these same slopes which were exposed to highly noxious smelter fumes when Keswick Smelter was operating (1904-07).

Another interesting field observation is the blue-green pool located at the end of the spillway just north from the bottom release column structure of Spring Creek Dam. This pool is maintained at a near-full capacity all year around, apparently fed by small seeps in the dam. The pool is noteworthy because its chemistry contrasts strikingly with the acid discharges from the dam.

Finally, it should be noted that Flat Creek, a small stream entering Keswick Reservoir to the north of the Spring Creek arm, also contributes acid drainage by seepage from a processed ore tailings pile located at point 3. Preliminary work (Potter, 1976) on the weathering of the sulfides in this tailings pile has begun.

Outline of Sampling Program

A sampling program on Spring Creek was planned so that spatial and temporal variations in dissolved metal concentrations could be measured. Sampling sites were chosen (1) above and below points of confluence, (2) according to accessibility and (3) to define major chemical changes. Sampling sites are shown by the arrows with assigned letter symbols in figure 1. Table 2 contains brief descriptions of the sample sites which are identified by the same letter symbols from figure 1. Samples at site N were collected roughly every 4 weeks (August 1974 to April 1976) in order to study the seasonal variations in the total drainage which reached the reservoir. Additional long-term

Table 2

Description of Reconnaissance and Long-Term Sampling Sites

<u>Site symbol</u>	<u>Name</u>	<u>Location</u>
A	Boulder Creek	Nearly adjacent to gossan outcropping from Hornet mine, above sources of contamination
B	Hornet/Richmond effluent	Acid mine effluent at portal entrance
C	Boulder Creek	Adjacent to Lawson tunnel of Hornet mine
D	Boulder Creek	At road crossing
E	Boulder Creek	Seep through embankment, abundant algal growth
F	Boulder Creek	Just below copper plant discharge
G	Boulder Creek	Mouth
H	Spring Creek	At road crossing
I	Spring Creek	Before confluence w/Boulder Creek
J	Spring Creek	At road crossing \approx 310 ft (94.5 m) from I
K	Spring Creek	100 ft (30.5 m) below Slickrock Creek
L	Slickrock Creek	Near mouth
M	Slickrock Creek	Near old flotation plant
N	Spring Creek	Near old road below gravel pit (point 4)
O	Spring Creek Reservoir	Near center of reservoir \approx 100 ft (30.5 m) away from edge of dam
P	Spring Creek Reservoir	Pool below spillway
Q	Spring Creek Dam	Bottom release
R	Copper Creek	Small spring flowing over old roasting piles
S	Keswick Reservoir	Arm near mixing point
T	Keswick Reservoir	Center of reservoir \approx 200 ft (61 m) north of arm
U	Keswick Reservoir	Center of reservoir \approx 200 ft (61 m) south of arm
V,W,X,Y,Z	Balaklala district	North of Iron Mountain area

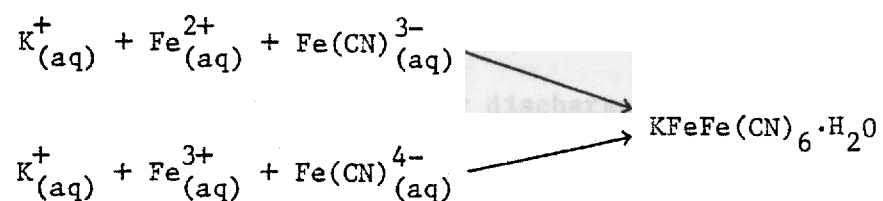
sampling was carried out at sites G and J, an important point of mixing and dilution. The rainstorm sampling was done at sites D, G and J, and the iron oxidation study was done between sites J and N.

Sampling Methods and Discharge Measurements

Collecting water samples requires special attention to filtration and pretreatment procedures in order that chemical changes do not occur during processing and storage. The type of pretreatment varies with the nature of the water sample and the analysis to be performed.

Routine sampling involved on site measurements, filtration and acid pretreatment for cation analysis. Stream temperature, pH, EMF (for Eh), conductivity and dissolved oxygen were measured on site except on a few occasions when conductivity was measured 4 to 6 hrs after sampling. Temperatures were measured with mercury glass thermometers with 1.0°C graduations. pH and EMF were obtained with combination pH electrodes and combination platinum redox electrodes connected to a Sargent-Welch three-rheostat (for slope calibration, intercept calibration and temperature compensation) portable meter. pH was calibrated against pH 4 and 7 buffers at the beginning of each day and rechecked against one buffer at each site. If a buffer check deviated by more than 0.02 of a pH unit, then it was recalibrated. Although the precision of repetitive readings is usually ± 0.02 , the accuracy cannot be considered better than ± 0.05 . pH measurements of the most concentrated acid mine effluent were either quite slow to come to a steady value or, in one instance, were somehow poisoning the electrode and giving spurious readings. Precision on EMF values is approximately ± 5 mv, and the redox electrode was usually checked against ZoBell's reference solution

at the end of the sampling day. It is not advisable to measure the EMF of acid mine waters after an electrode has been placed in ZoBell's solution because just trace amounts of ferrocyanide and ferricyanide ions will react with the ferrous and ferric ions in the acid effluent to form an insoluble blue precipitate which immediately coats the electrode surface and causes erratic EMF readings. The blue compound is the same substance made commercially as Turnbull's blue or Prussian blue which is formed by the addition of ferrous ion to a ferricyanide solution or ferric ion to a ferrocyanide solution (Pauling, 1964):



Conductivities were measured with a Lab-line portable conductivity unit using cells with both 0.1 and 1.0 constants. Reproducibility on a conductivity reading is about ± 2 percent using the temperature compensator. Dissolved oxygen (D.O.) was measured with a YSI meter and probe calibrated on a clean well-mixed stream by a Winkler titration or by assuming saturation with atmospheric oxygen (approximate precision of ± 5 percent). Measurements in the reservoirs were obtained with a Martek combined pH, conductivity, D.O. depth and temperature unit.

Water samples were filtered on site through 0.1 μm membranes held in all-plastic plate filter holders (Kennedy and others, in press). Stream water was transmitted to the filter apparatus through precleaned plastic silicone tubing by means of a portable peristaltic pump. The tubing and filter apparatus were preleached with at least 250 ml of stream water before emptying directly into polyethylene or poly-

propylene sample bottles. Samples collected for cation analysis were acidified with 5 ml of concentrated nitric acid per liter of sample solution. The pH was later adjusted to about 1 by additional quantities of nitric acid (which never exceeded 10 ml of acid per liter of sample solution). Samples collected for ferrous determinations were acidified with 2 ml of concentrated hydrochloric acid per 250 ml of sample solution. Anion analyses were carried out on samples which had been filtered but had no additional pretreatment.

Discharge measurements were usually obtained with a Pygmy current meter, graduated staff and tape measure. The standard Price meter was used for a few high velocity discharges, and stage markers and floating objects were used for special studies (see chapters on Microbiota and Ferrous Iron Oxidation).

ANALYTICAL PROCEDURES

The analyses of water samples in this study included several different techniques, some reliability tests (for accuracy) and analyses for a wide range of elements. Table 3 presents each constituent analyzed and the method used.

Atomic absorption analyses were carried out on a Perkin-Elmer 306 Model spectrophotometer equipped with a 10 cm, three-slot burner head for air-acetylene and a 5 cm single-slot head for nitrous oxide-acetylene. Emission spectrograph analyses were obtained from a Spectra-span Model II (Spectrametrics, Inc.) equipped with a D.C. arc plasma jet which uses argon gas and tungsten electrodes in ceramic sleeves. A photograph of the plasma jet radiation (with no solution pumped in) gave spectral lines for tungsten, sodium and vanadium only. Additional lines were visible, but no more than one line per element could be found. A listing of the analyses is given in Appendix I in chronological order. Standard addition method was tested out on nearly every element, especially where a new technique, to determine the accuracy. Details of analytical problems with acid mine waters will be written as a separate report.

Table 3
Methods of Analysis

<u>Constituent symbol</u>	<u>Constituent name</u>	<u>Analytical method</u>
Ag	Silver	A.A. flame and furnace
Al	Aluminum	A.A. flame, emis. spec.
Au	Gold	Emis. spec.
Ba	Barium	Emis. spec.
B	Boron	Emis. spec.
Ca	Calcium	A.A. flame w/La and HCl
Cd	Cadmium	A.A. flame
Cl	Chloride	Mohr titration
Cu	Copper	A.A. flame
F	Fluorine	Fluoride ion-selective electrode
Fe ²⁺	Ferrous	Spectrophotometric, Ferrozone
Fe (total)	Iron	A.A. flame
Hg	Mercury	Flameless A.A.
K	Potassium	A.A. flame w/Li
Mg	Magnesium	A.A. flame w/La and HCl
Mn	Manganese	A.A. flame
Na	Sodium	A.A. flame w/Li
SO ₄	Sulfate	Spectrophotometric, Thorin
SiO ₂	Silica	Emis. spec.
Zn	Zinc	Emis. spec.

GEOLOGY

The geologic setting of the Spring Creek region provides valuable information for the sequence of physical and chemical processes which occur during weathering. The geologic history, although complex, is kept brief, and geologic facts which bear on the hydrogeochemistry of the area are emphasized.

Geomorphology

The foothills of the Trinity Mountains rise from the Sacramento River and Keswick Reservoir at 179 m (587 ft, spillway elevation) to a fairly uniform altitude of about 1219 m (4000 ft) at the divide separating Spring Creek runoff from Whiskey Creek and Clear Creek runoff. Most of the region has a rugged topography, with steep slopes and V-shaped canyons separated by long ridges. The mountain ridges and peaks are commonly well rounded and are generally accordant in altitude (Kinkel and others, 1956, p. 60-61). A few peaks to the north which rise above this level may be monadnocks, but it should be noted that the peaks in general become progressively higher and have steeper slopes to the north. This remnant of an aged landscape has been called the "old Klamath surface" by Kinkel and others (1956). This landscape surface reflects the topography just prior to late Pliocene-early Pleistocene uplift which caused renewed erosion and formed the deeply dissected valleys. The uplift, in conjunction with erosion from mining activities, induces large amounts of sediment to deposit at the mouth of Spring Creek.

One other prominent feature of the landscape is noteworthy: the occurrence of terraces. A broad flat terrace stands at about 61 m (200 ft) above the Sacramento River, and traces of earlier terraces remain at higher elevations in the mountains. The early terraces are important because they are susceptible to landslides, slumping and solifluction. Most of the Quaternary deposits in the Spring Creek region are of this type.

Tectonic History and Petrogenesis

The sequence of volcanism, sedimentation, igneous intrusion and hydrothermal and regional metamorphism has been documented by Kinkel and others (1956), Irwin (1966), Davis (1966), Burchfiel and Davis (1972, 1975) and Lydon and O'Brien (1974).

According to Burchfiel and Davis (1972) the structural development of the southern Cordilleran orogen may be divided into three periods: (1) late Precambrian through late Paleozoic, (2) early Mesozoic through early Tertiary, and (3) middle Tertiary to Recent. During most of the first period northern California was an ocean floor environment with both marine sediments and mafic lavas forming. Regional metamorphism of these rocks to hornblende and mica schists is evident to the west and southwest of the Spring Creek region. These metamorphics may underlie the oldest rocks (Copley Greenstone) in the region, but no evidence has yet been found to substantiate this. During the Devonian period a Sierran-Klamath island arc began forming above an east-dipping subduction zone. Three formations of roughly Middle Devonian age mark different stages of the island arc development. First a series of underwater mafic flows deposited on the sea floor; later they were

regionally metamorphosed to a greenstone called the Copley Formation. These mafic flows lie conformably below a group of silica-rich flows and pyroclastics which were deposited both above and below sea level, marking the emergence of islands from the ocean floor. These silicic rocks comprise the Balaklala Rhyolite. Conformably overlying the Balaklala are thinly bedded shales and siltstones with occasional layers of more siliceous, calcareous and coarse-grained material making up the third stage, the Kennett Formation. The Kennett sediments reflect erosion and sedimentation from the emerging island arc system. The close of the Paleozoic era is indicated by the Bragdon Formation, a thick, well-bedded sequence of shales and conglomerates. Even though the Bragdon is now in thrust contact with the underlying Kennett and Balaklala Formations, it was probably in conformable contact with the Kennett before thrusting. The Bragdon is of Mississippian age, and signifies a shift in the edge of the continent from the east side of the island arc to just west of it. According to recent plate tectonic arguments, the continental crust which had been moving westerly relative to an east-dipping subduction zone, merged with the island arc. This convergence formed a new continental margin at the western edge of the late Paleozoic volcanics by the time of the Early Triassic.

The second period of structural development was the most eventful. As the continental crust collided with a subducting oceanic crust and welding of the island arc to the continent took place, a northwest-trending volcanic-plutonic mountain chain formed. This orogenesis was similar in many respects to the Andean chain in South America, and it provided the core to what is now the Klamath-Sierra Nevada mountain ranges. Roughly contemporaneous with the volcanism and plutonism,

large-scale low-angle thrusting and regional metamorphism of first period formations occurred. In the Spring Creek region, igneous events are limited to the intrusion of the Mule Mountain granitic stock of Middle Jurassic age and the Shasta Bally dioritic batholith of Late Jurassic-Early Cretaceous age. The date on the latter intrusion has been confirmed by a K-Ar date of 134 m.y. (Curtis and others, 1958). Contact metamorphism, especially in the Copley Greenstone, accompanied the intrusion, with greater intensity near the batholith than the stock. Thrust movements in the Klamaths province are postulated by Irwin (1966) to have occurred along four major fault zones. The most easterly of these bounds the "eastern Klamath plate" wherein lies the Spring Creek region. This thrust fault apparently has a highly contorted branch whose orientation changes from a north-striking, east-dipping direction to a north-striking, west-dipping direction along the contact of the Bragdon with the Kennett Formation. Thrust movement along this fault has probably been sufficient to cover up significant portions of both the Kennett and Balaklala units. Albers (1964) has mapped this as the Spring Creek thrust fault, and Albers (1961) suggested that it predates the intrusive rocks. The geometry of the fault and the igneous intrusions suggest that fault movement occurred after pluton emplacement, placing it in the middle Cretaceous age or younger. The timing on the thrust movement can only be bracketed between Late Triassic and Late Cretaceous until further work is done.

Structural development during the third period centers around the migration of the East Pacific Rise into the continental margin. The Spring Creek region was part of the continental highlands at this time and simply experienced erosion of the Bragdon and younger formations

which now only crop out east of the Sacramento River. No major tectonic events took place except for the late Pliocene-early Pleistocene uplift previously mentioned.

Two other structural trends are noteworthy in the Spring Creek region: (1) east- to northeast-trending high-angle normal faults and (2) a broad anticline reaching from Whiskey Creek through the heart of the West Shasta mining district to some distance north of Behemotosh Mountain. The anticline plunges gently to the north and to the south, cresting near Behemotosh Mountain. Faults are very common and will be briefly mentioned again in the section on ore deposits. Folding is usually gentle and foliations are often parallel to bedding. Where foliation crosscuts bedding, metamorphism is usually so intense that these two surface structures are difficult to distinguish.

Davis (1969), Burchfiel and Davis (1975) and Dickinson (1970) elaborate in much greater detail the tectonic development of this region.

Major Rock Units

The best descriptions of the major rock units in the Spring Creek region are those contained in the works of Hinds (1933), Kinkel and others (1956) and Albers (1964).

Copley Greenstone consists of interlayered mafic flows, tuffs and agglomerate regionally metamorphosed to greenschist facies and locally to higher grades by contact metamorphism. The greenstone is fairly uniform in composition and mineralogy, consisting of keratophyres, spilites and meta-andesites with infrequent diabase sills

and dikes.¹ The lower and middle parts of the Copley are chloritic lava flows and tuff beds of keratophyric composition with a few thin layers of shale. The upper parts are largely amygdaloidal pillow lavas with fine to coarse pyroclastics and some diabase. Albite, augite, olivine, plagioclase and epidote phenocrysts in a groundmass of the same minerals with hornblende and chlorite is the common mineral association. In addition, quartz, zoisite, clinozoisite, montmorillonite, green biotite (resulting from regional metamorphism), are found, and calcite and quartz often fill vesicles. This mineral assemblage gives the rocks a yellowish, grayish or dark-green color on fresh fracture surfaces. Weathered surfaces are usually stained brown to red from oxidation of the ferrous iron in the ferromagnesian minerals.

Identification of the Balaklala caused a curious controversy which has been resolved by Kinkel and others (1956):

The Balaklala Rhyolite was named and first described by Diller (1906, p. 6), who described the Balaklala Rhyolite as a series of siliceous lavas and tuff beds. Graton (1909, p. 81) later studied part of the Shasta copper-zinc district and concluded that the Balaklala Rhyolite of Diller was intrusive into the surrounding rocks and he called it an alaskite porphyry.

An intrusive origin for the rhyolitic rocks was accepted by all the geologists who published information on this area after Graton's work (Averill, 1939, p. 122; Ferguson, 1914, p. 30; Hinds, 1933, p. 107; Seager, 1939, p. 1958-1959), although geologists for some mining companies continued to regard the rocks as flows and pyroclastic rocks. Mapping by the writers has shown that Diller was correct in his belief that the rhyolitic rocks are of volcanic origin, and they have revived Diller's name for the formation.

¹A keratophyre is a soda-rich, feldspar lava (ferromagnesian minerals rarely exceed 20 percent) in which 67 percent or more of the total feldspar is alkali (dominantly albite); a spilite is an altered basalt with unusually high sodium content; an andesite is a feldspar lava in which 67 percent or more of the feldspar is calcic plagioclase; diabase is a medium- to coarse-grained equivalent of a basalt.

The Balaklala Rhyolite is a volcanic pile of hard, light-gray to light-green siliceous lava flows interlayered with sheets and lenses of fine- to coarse-grained pyroclastic and porphyritic material. The composition is chiefly that of quartz keratophyre, and quartz and feldspar phenocrysts are easily recognizable in hand samples. Some of the layers are nonporphyritic but otherwise appear the same. Albite and quartz are the major minerals in the groundmass and the phenocrysts. Regional metamorphism has caused greenschist minerals to form, and faulting plus hydrothermal alteration has formed mica, fine-grained silica and clay minerals. Trace amounts of heavy minerals (magnetite, ilmenite, leucoxene, apatite, pyrite and zircon) are also found in locally altered areas. Though they occur chiefly within the Balaklala Rhyolite, the ore minerals will be mentioned in the section on ore deposits.

The Kennett Formation is a narrow, discontinuous belt of gray to black cherty shale which has a highly contorted character in the Spring Creek region compared to its type locality in Backbone Creek much further to the north. This complex structure is probably a result of thrust movement along Spring Creek fault which borders the Kennett in this area. The shale consists of quartz, mica, clays and carbonaceous material with minor opaques. Limestone is interbedded with the shale.

The Bragdon Formation consists of finer clastics such as shales, siltstones and mudstones in the lower part, grading into 50/50 fine and coarse clastics such as sandstones and conglomerates in the upper part. Finer clastics are usually made of white mica, clay minerals,

carbonaceous material and quartz while coarser clastics include quartz, chert, feldspar clasts and fragments of volcanic rocks.

The roughly elliptical Mule Mountain stock consists of coarse-grained light-colored trondhjemite (quartz-rich, leucocratic quartz diorite with negligible potash feldspar) and albite granite. Since quartz, plagioclase and epidote are the predominant minerals, the rock is often a brilliant white color with occasional greenish patches. Brecciation of the stock and intrusion of aplite dikes is common in a few areas.

The Shasta Bally batholith is a fairly homogeneous leucocratic quartz diorite and granodiorite which has undergone little alteration in contrast to the Mule Mountain stock which is widely silicified and albitized. Significant changes in the texture of biotite and hornblende have allowed Albers (1964) to distinguish different lithologic facies.

Unconsolidated sediments form a somewhat small contribution to the total rock sequence of the Spring Creek region, but they nevertheless have some important features. There is also very little literature on recent deposits or soil development because of the relatively shallow soils and the need for mining information rather than agricultural information. Three types of recent deposits are distinguishable: (1) alluvium, consisting of residual soil and debris mantle material, (2) landslide and (3) sand and gravel deposits in the stream beds. Alluvium and landslide material cover roughly equal areas of land surface and according to the map of Kinkel and others (1956) occur at higher altitudes in the northern part of the region. Their text, however, states that landslide material occurs at higher altitudes, and alluvium is limited to the valleys and low foothills, especially

where the underlying rock is greenstone. My own observations confirm the latter description. There is very little soil development at higher altitudes except near the upper part of the Balaklala Rhyolite which is near the "old Klamath surface." Because of the long exposure of this erosional surface, which is a coarse-grained rhyolite porphyry, a deep mixture of soil and rock debris has developed. This soil is probably the high altitude alluvial cover shown on the map (fig. 2). Since placer gold was found in the sand and gravel deposits of the stream beds, nearly every stream has been dredged at least once, usually by hand. One other point is worth noting: some of the older U.S.G.S. maps show a sand and gravel bar along the banks of the Sacramento River from the mouth of Spring Creek north about 0.5 mi. This suggests debris washed out of Spring Creek and built up in the Sacramento faster than the Sacramento could wash it downstream. This gravel bar is noticeable on Kinkel, Hall and Albers' map which was made after the Shasta Dam was constructed but before Keswick and Spring Creek Dams were constructed. It also shows up on the U.S.G.S. topographic maps before the photorevision of 1969. Since this revision, the Keswick Reservoir has been about 4.6 m (15 ft) higher than before and has just covered this gravel bar, making the Sacramento look much deeper at Spring Creek than it really is.

Summary of Rock Types and Compositions

Subsurface and surface waters within the Spring Creek drainage interact primarily with four rock types: (1) Copley Greenstone, (2) Balaklala Rhyolite, (3) Mule Mountain Granitoid and (4) massive sulfides. Figure 2 shows the principal formations of the drainage in

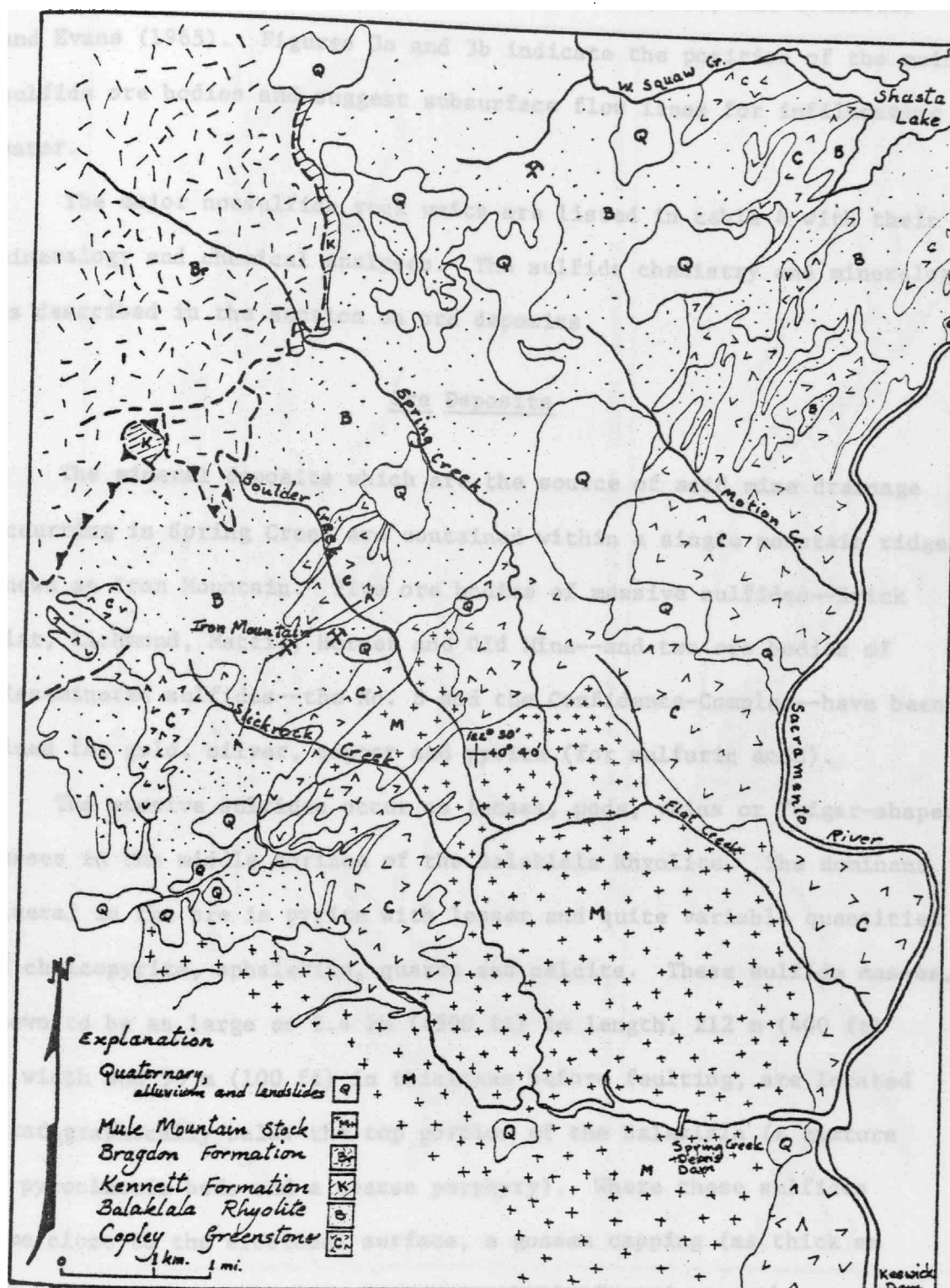


Figure 2. Geologic map of the Spring Creek drainage (modified after Kinkel and others, 1956).

a geologic map modified from Kinkel and others (1956) and Hollister and Evans (1965). Figures 3a and 3b indicate the position of the main sulfide ore bodies and suggest subsurface flow lines for infiltrating water.

The major nonsulfide rock units are listed in table 4 with their mineralogy and chemical analyses. The sulfide chemistry and mineralogy is described in the section on ore deposits.

Ore Deposits

The mineral deposits which are the source of acid mine drainage occurring in Spring Creek are contained within a single mountain ridge known as Iron Mountain. Five ore bodies of massive sulfides--Brick Flat, Richmond, Mattie, Hornet and Old Mine--and two ore bodies of disseminated sulfides--the No. 8 and the Confidence-Complex--have been mined for gold, silver, copper and pyrite (for sulfuric acid).

The massive sulfides occur as lenses, pods, veins or "cigar-shaped" masses in the middle horizon of the Balaklala Rhyolite. The dominant mineral in the ore is pyrite with lesser and quite variable quantities of chalcopyrite, sphalerite, quartz and calcite. These sulfide masses, known to be as large as 2.4 km (4500 ft) in length, 212 m (400 ft) in width and 53 m (100 ft) in thickness before faulting, are located stratigraphically below the top portion of the Balaklala (a mixture of pyroclastic beds and a coarse porphyry). Where these sulfides came close to the erosional surface, a gossan capping (as thick as 200 m) developed. The gossans were probably formed near the top of a fluctuating water table where oxidation of sulfides would readily take place. An early groundwater system corresponding to the beginning

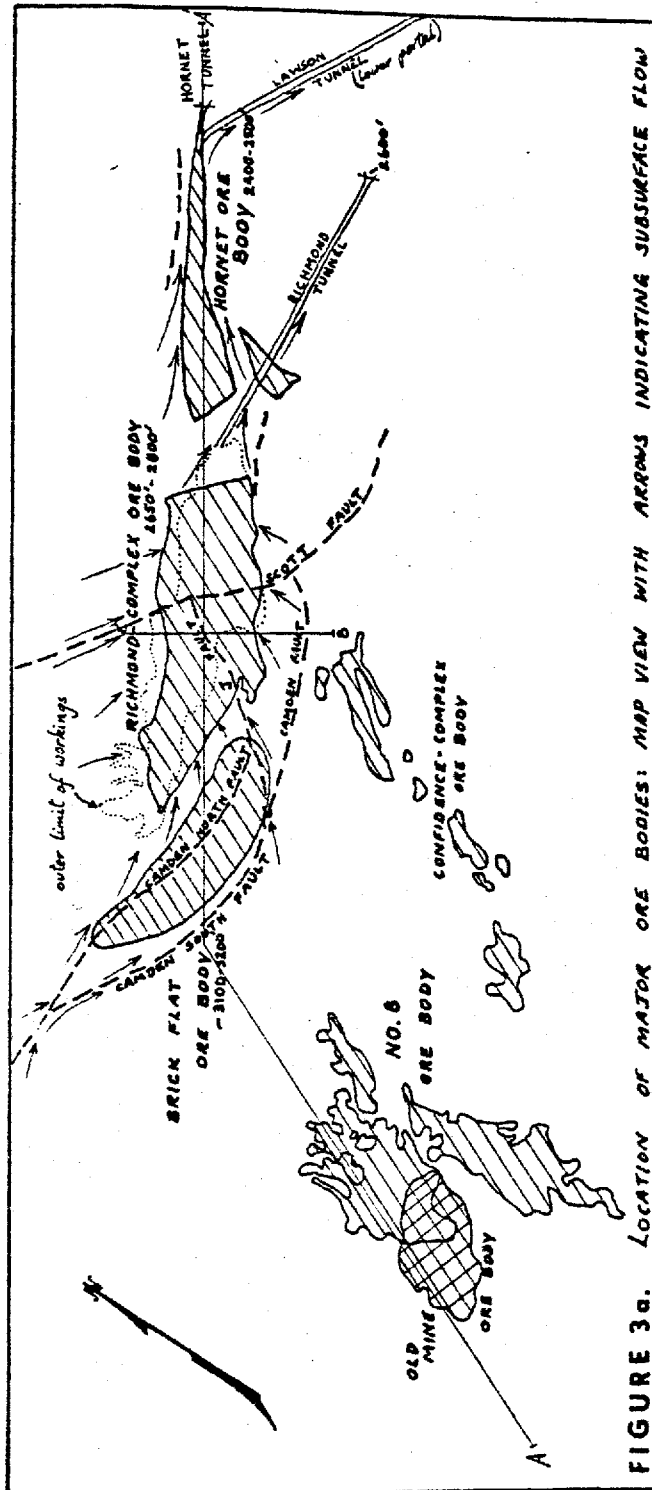


FIGURE 3a. LOCATION OF MAJOR ORE BODIES: MAP VIEW WITH ARROWS INDICATING SUBSURFACE FLOW

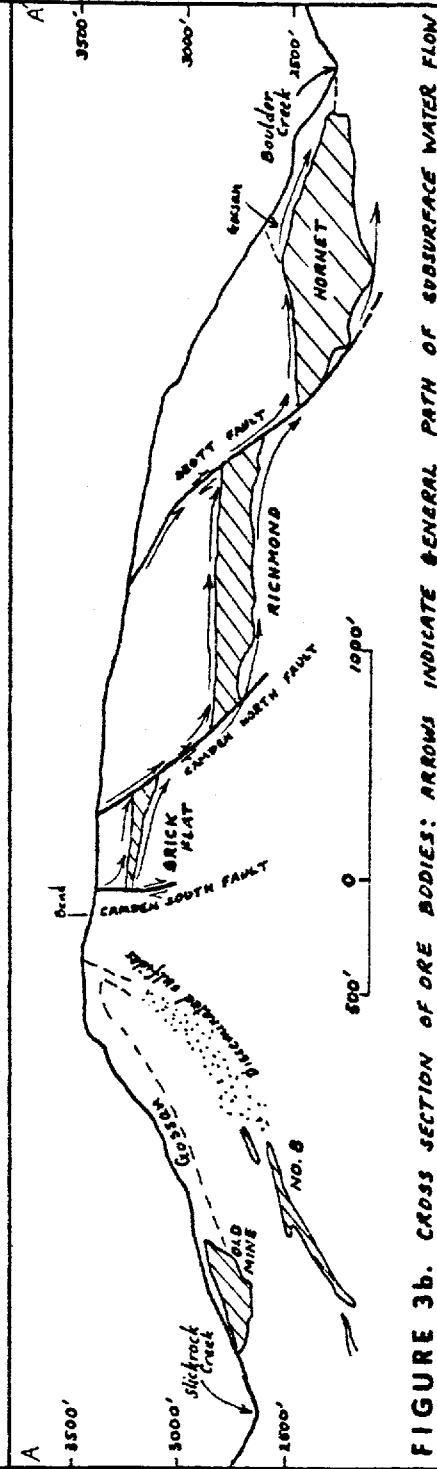


FIGURE 3b. CROSS SECTION OF ORE BODIES: ARROWS INDICATE GENERAL PATH OF SUBSURFACE WATER FLOW

Table 4

Major Rock Units (analyses from Kinkel and others, 1956)

Major minerals	Copley Greenstone ¹		Balaklala Rhyolite ²		Mule Mountain ³ Granitoid	
	Plagioclase (Ab ₉₇ -Ab ₇₈) Chlorite Secondary silica		Quartz Chlorite Albite (Ab ₉₆ -Ab ₉₂)		Quartz Plagioclase (Ab ₉₀ -Ab ₈₆) Green biotite Epidote Chlorite	
Chemical analysis (%)						
SiO ₂	52.56		77.01			72.74
Al ₂ O ₃	17.00		12.04			14.14
Fe ₂ O ₃	0.91		0.67			1.26
FeO	6.12		1.51			1.82
MgO	7.11		1.29			0.63
CaO	5.55		0.86			2.12
Na ₂ O	5.28		4.58			4.12
K ₂ O	0.84		0.59			0.75
TiO ₂	0.40		0.18			0.26
MnO ₂	0.05		0.03			0.05
CO ₂	0.86					
Total	96.68		98.78			97.89

¹ Although most of the Copley is keratophyre, a soda-rich trachyte, only one analysis of a spilite is available.

² The middle and lower units of the Balaklala outcrop in the Spring Creek area and the analysis is for a middle unit sample from the Igo quadrangle. A Na/K ratio for an Iron Mountain sample is 12.9.

³ About 65 percent of the Mule Mountain stock is trondhjemite and this analysis is for a sample from the Whiskeytown quadrangle. Trondhjemite is a quartz-rich quartz diorite where a diorite is the coarse-grained equivalent of andesite.

of the most recent uplift (i.e. late Tertiary to early Quaternary) might explain the distribution of known gossan occurrences. The gossan consists of a dark, reddish-brown cellular mass of limonite with occasional silica "ribs" and isolated nodules of unoxidized sulfide. Gold was enriched in the gossan while silver and copper were leached and enriched in the upper parts of the primary ore body, just below the gossan. Zinc was entirely removed from the primary ore wherever it was oxidized.

The Iron Mountain mines are located near a set of N. 70° E.-striking faults (nearly all normal faults). The sulfide ore replaces the host rhyolite with grain size averaging about 0.5 mm, but locally becoming coarser. The copper and zinc content of the ore is highly variable, and the details of its distribution in the massive sulfides is not well known (Kinkel and others, 1956). Copper ranges from 2 to 7.5 percent and zinc from 0.0 to 21.1 percent. Since large amounts of zinc and unknown amounts of copper were discarded as waste during different periods of the mining operations, it is difficult to estimate the original amounts. Significant amounts of sulfides containing precious metals are scattered among the waste rock today. For example, high concentrations of copper, silver and arsenic are found in the processed residues at the Minnesota tailings pile (Potter, 1976). Gold and silver in the original ore ran 0.02 to 0.06 oz/ton and 1 to 8 oz/ton, respectively.

The following minerals have been reported from the ore deposits in the West Shasta district:

chalcopyrite	CuFeS_2	tennantite- tetrahedrite	$\text{Cu}_{12}(\text{As,Sb})_4\text{S}_{13}$
pyrite	FeS_2	limonite	hydrated ferric oxides

galena	PbS	chlorite	$(\text{Mg}, \text{Fe})_5(\text{Al}, \text{Fe})_2\text{Si}_3\text{O}_{10}(\text{OH})_8$
sphalerite	ZnS	talc	$\text{Mg}_3\text{Si}_4\text{O}_{10}(\text{OH})_2$
greenockite	CdS	muscovite	$\text{KAl}_3\text{Si}_3\text{O}_{10}(\text{OH})_2$
chalcocite	Cu_2S	antlerite	$\text{Cu}_3\text{SO}_4(\text{OH})_4$
covellite	CuS	azurite	$\text{Cu}_3(\text{CO}_3)_2(\text{OH})_2$
pyrrhotite	Fe_{1-n}S	malachite	$\text{Cu}_2\text{CO}_3(\text{OH})_2$
gold	Au	chalcantinite	$\text{CuSO}_4 \cdot 5\text{H}_2\text{O}$
silver	Ag	melanterite	$\text{FeSO}_4 \cdot 7\text{H}_2\text{O}$
copper	Cu	jarosite	$(\text{K}, \text{Na})\text{Fe}_3(\text{SO}_4)_2(\text{OH})_6$
magnetite	Fe_3O_4	copiapite	$(\text{Fe}, \text{Mg})\text{Fe}_4(\text{SO}_4)_6(\text{OH})_2 \cdot 20\text{H}_2\text{O}$
hematite	Fe_2O_3	goslarite	$\text{ZnSO}_4 \cdot 7\text{H}_2\text{O}$
sulfur	S	zoisite	$\text{Ca}_2\text{Al}_3\text{Si}_3\text{O}_{12}(\text{OH})$
cuprite	Cu_2O	wad	hydrated manganic oxides
barite	BaSO_4	smithsonite	ZnCO_3
calcite	CaCO_3	quartz	SiO_2
ilmenite	FeTiO_3	maghemite	Fe_2O_3

Several other observations on the chemistry of the ore minerals are worth mentioning. For example, there is no other mineral which has higher cadmium concentrations than sphalerite. Cadmium is consistently found associated with zinc in nature, and the cadmium content of sphalerites commonly ranges from 0.1 to 1.0 percent (Fleischer, 1955; Wakita, 1970). It is surprising, therefore, that ore from Iron Mountain gave less than detectable cadmium (<0.01 percent) by spectrographic analysis (Kinkel and others, 1956). The samples chosen must also have had a very low zinc content. Samples of zinc-rich ore from the Mammoth mine, north from Iron Mountain, gave 1 percent cadmium, and cadmium was

produced from the electrolytic zinc plant at Kennett during 1917-18. Large quantities of cadmium must have been present in the ore bodies at Iron Mountain associated with the high zinc ores.

Small quantities of arsenic and antimony have been found in the sulfides due to the presence of the tennantite-tetrahedrite group of minerals. These minerals are closely associated with sphalerite, but there is no quantitative data on their distribution. Aubury (1908) reports that the smelted ore from the Iron Mountain was considered high quality because of low arsenic, antimony, and selenium concentrations. However, there are no reliable records on the variations of these metals in the processed ores.

The most plausible theory for the genesis of the West Shasta ores is that proposed by Albers (1966). The ore deposits are (1) found as replacement bodies in the Balaklala Rhyolite at a favorable stratigraphic position; (2) of Late Jurassic to Early Cretaceous age; and (3) controlled by N. 70° E.-trending premineralization faults and secondary foliation. These facts suggest that during intrusion of the two plutonic bodies (Mule Mountain stock and Shasta Bally batholith), groundwater fluids were heated and began circulating through the Copley Formation, extracting heavy metals from it. The Copley contains sufficient metals distributed throughout its known volume to account for the ore deposits. The ore-forming fluids found suitable channels in the Camden and Sugarloaf faults to feed up into the Balaklala at Iron Mountain.

Structural Features at Iron Mountain

The structure of the Balaklala Rhyolite in the vicinity of the ore bodies can be described by three major folds (coincident with regional

metamorphism) and four major faults. Folding produced anticlinal structures on either side of the Brick Flat-Richmond-Hornet ore bodies, so that the massive sulfides sit in the valley of a syncline (fig. 4). This syncline appears to be horizontal even though it is complicated by intersecting faults.

The four major faults are the Camden (North and South sections), the J, the Sugarloaf and the Scott. The study by Kinkel and others (1956) shows that the Brick Flat, Richmond, Complex and Hornet massive sulfide ore bodies were one continuous mass before they were displaced by the Scott and Camden faults. Movement along the Camden fault has displaced the Richmond ore body about 160 m (300 ft) below Brick Flat, and, likewise, the Hornet has dropped about 160 m below the Richmond by movement along the Scott fault (fig. 3b).

All of these faults show postmineral displacement by the sheared, crushed and slickensided sulfide ore found along the contacts. The Camden and the Sugarloaf also may have existed before mineralization and could have been feeder channels for the ore-forming solutions (Kinkel and others, 1956). In addition to these major faults, many small postmineral faults have been identified within the sulfide ore bodies.

Hydrothermal Alteration

The rhyolite volcanics at Iron Mountain have been extensively altered to sericite (very fine-grained muscovite), hydromica (hydrothermal illite), silica, chlorite and pyrite. Sericite and hydromica are widespread and frequently in close association with the ore bodies. This alteration has important consequences for the Na/K content of the

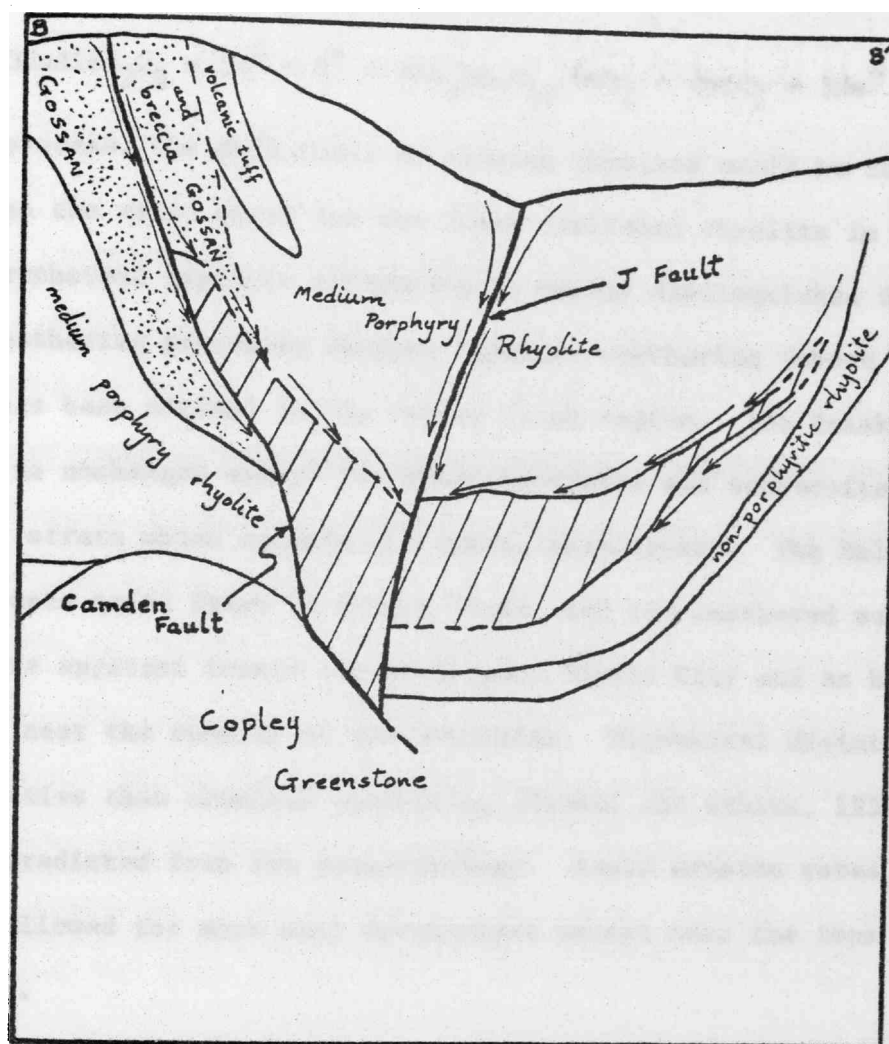
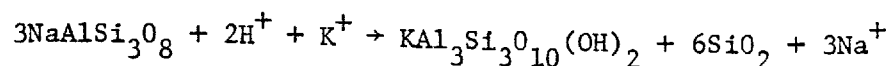


Figure 4. Cross section of Richmond ore body; arrows indicate general path of infiltrating waters.

Balaklala Rhyolite. Sericite and hydromica are potassium micas commonly formed by the reaction of ascending acidic ore-forming solutions and sodic feldspars (Hemley and Jones, 1964):



By this process, the Na/K ratio in altered rhyolite would be considerably lower than the ratio given for the fresh unaltered rhyolite in table 4.

Hydrothermal argillic alteration is easily distinguished from normal weathering processes because chemical weathering (above the ore bodies) has been minimal in the Spring Creek region. The Balaklala Rhyolite is unchanged except for minor kaolinite and nontronite in the uppermost strata which contain the coarse phenocrysts. The Mule Mountain stock appears quite fresh in Spring Creek, and its weathered surfaces become more apparent toward the south near Shasta City and at higher altitudes near the summits of the mountains. Mechanical disintegration is more active than chemical weathering (Kinkel and others, 1956) as might be predicted from the geomorphology. Rapid erosion rates also have not allowed for much soil development except near the tops of the ridges.

Hydrogeology: A Unique Reactor

The unique combination of geologic events, mining history and climatic conditions has created a natural, self-perpetuating reactor which is breaking down sulfide minerals into soluble form as acid sulfate solutions. This process is analogous to dump-leaching operations except that no man-made input is necessary. The structural factors which have produced this reactor are outlined below.

The flow of water through igneous and metamorphic rocks is controlled by major fracture and fault systems and, where mining has occurred, by stoped out areas and drill holes. Porosities are commonly less than 1 percent and permeabilities effectively zero in the solid rock, whereas highly fractured zones may have permeabilities of several hundred darcys (Davis and DeWiest, 1966). In the Balaklala Rhyolite at Iron Mountain, the zones of highest porosity and permeability are in the mines and along the major faults. Of lesser importance in permeability characteristics are the bedding planes of the volcanic strata (along which minor shearing may have occurred during metamorphism) and the fractures which developed after the release of tectonic pressure and grew with weathering.

Figures 3a, 3b and 4 outline the structure of the main sulfide ore bodies, the major faults and the general dip of the strata. Infiltrating waters follow the path of least resistance and would tend to be drawn down toward the Camden, Scott and J faults and into the mined out areas indicated by the dotted boundary line. Nearly all of the Brick Flat ore body has been removed during the open pit operations, and this allows precipitation to infiltrate directly along the Camden and J faults a few hundred meters closer to the remains of the Richmond-Complex ore body. Water which pools in the open pit is presently being drained out to the west into Slickrock Canyon (Leland George, pers. commun.). This pooled water is already acid and enriched in heavy metals by reaction with the remaining sulfides present in dumps and in a small outcrop of the Brick Flat ore body. If this water were allowed to fill in the open pit, it would filter down towards the Richmond mine. The added input of water from the open pit would then increase the

discharge out of the Richmond-Hornet effluent into the copper recovery plant.

Waters drawn into the Richmond and Hornet mines have a highly variable residence time depending on the amount and intensity of rainfall, and on the season of the year. Commonly, there is a 3-day lag following a rainstorm before an increase in discharge occurs in the Richmond-Hornet effluent (Leland George, pers. commun.). The form and structure of the ore bodies and the mine tunnels provide an excellent pathway for a large part of the stored water. After reacting with residual sulfides, either in place or broken up along the tunnels, the water collects toward the lowest point, which happens to be the main portal, in both the Hornet and Richmond mines. Thus, because of the geologic structure and the particular mining methods of the Mountain Copper Co., a unique reactor has been created in which water is pulled toward the sulfides, allowed to react forming acid, metal-rich sulfate solutions and then drawn off through two singular portals.

MINING HISTORY: INITIATING THE REACTOR

This chapter describes the discovery, development and production of the ore deposits at Iron Mountain. The natural weathering of sulfide ores was greatly intensified by man's activities in this region, and a proper study of the sources of acid mine waters should include the historical mining record. Emphasis is placed on the location and duration of mines and processing plants as well as on the various processing methods which were used to recover metals. Production figures, as available, are also included.

Shasta County mining began in 1848 with the gold strike in Clear Creek near Reading Springs (renamed Shasta in 1849). It was not until the early 1860's that William Magee, a United States land surveyor, noticed the enormous gossan capping on the mountain which rose 3300 ft above sea level and 1000 ft above the creek beds between Slickrock and Boulder Creeks. With Charles Camden he secured the property as an iron mine, and until 1879 they held Iron Mountain for its possible future value. In that year, James Sallee discovered silver in an adjoining ledge, and with his partner, Alvin Potter, became one-third owner of the Iron Mountain property.

In the nearly 100 years since the silver discovery, Iron Mountain's story has been one of man's persistent search for valuable ores and his ingenious solutions to transport and processing problems. Silver, gold, copper, zinc and pyrite have been processed from the Iron Mountain ores; numerous processing plants have been built and destroyed; and

copper has been produced by directly smelting ore, from sulfide flotation concentrate, by leaching cinders produced in roasting pyrite and by precipitation from mine water. Only a copper cementation plant continues to operate. The environmental problems which resulted from the vast mining project remain to be solved.

Early mining records seem to be contradictory at times, but a basic outline of events is consistent. According to Aubury (1905), Sallee and Potter transported ore, the surface gossan crust, by pack train and wagon to Redding and from there by rail to reduction works in Denver, Colorado. This enterprise was sufficiently rewarding to merit the construction of a wagon road from the mines to the railroad at Middle Creek (on what was then the main road from Redding to Shasta), a distance of 8 mi. In 1884 John O. Earl and Charles Ellsworth, representing a Honolulu company, paid Magee, Camden and Sallee \$30,000 for the property and built a 20-stamp mill to work the surface gossan ores as a free milling proposition. However, before production began, the property and mill were returned to the original owners, and Sallee successfully operated the works.

Kett (1947) describes the "Washoe" process which was finally used to recover the silver. In this process the mill was equipped with a Brueckner furnace, and the crushed ore was mixed with salt and passed through the furnace to chloridize the silver. The pulp was then transferred in 4-ton batches to pan amalgamators and treated for about 3 hrs, after which sodium amalgam, copper sulfate and about 200 lbs of quick-silver were added and the charge ground for another 5 hrs. Then the batch was washed in a settler, where the silver was recovered in a sodium-mercury amalgam. The mill is said to have had a capacity of

40 tons/24 hrs, but there was always considerable loss of quicksilver due to "flouring." The mill, which operated successfully until 1893, was destroyed by fire in September 1897. According to Sallee's records, between 1889 and 1893, 38,000 tons of gossan, averaging just over 8 oz of silver per ton were treated. The gold content was not determined as there were not means of saving it.

In 1894 apparently unaware of the copper sulfide at depth, Sallee, Camden and Magee's heirs sold the Iron Mountain property for \$300,000. Hugh McDonnell, a Colorado mining engineer, Judge N. F. Cleary of Denver and Alexander Hill, an engineer who had worked in the Rio Tinto mine in Spain, "effected the sale to the Rothschild and Fielding (C. W. Fielding, a British metal broker) people" (Aubury, 1905). Early in 1895 a new company, Mountain Mining Company, Ltd., of London was incorporated with a working capital of \$200,000 to operate the mine. In March of that year Fielding also purchased the Hornet mine from Benjamin N. Bugbey. On January 1, 1897, the property was transferred to Mountain Copper Company, Ltd., of London. Mountain Copper maintained the property until 1967 when it was purchased by Stauffer Chemical Company.

Increased underground diggings had revealed in 1895 the massive copper sulfide deposits carrying 7 percent copper and a couple of dollars per ton in gold and silver (Kett, 1947). This discovery justified the construction of a smelter and a narrow-gauge railway to transport the ore from the mine to the smelter.

M. M. O'Shaughnessy, who was in charge of engineering and construction of the railway, explained that the smelter site, about a mile above the junction of Spring Creek with the Sacramento River, was chosen because it was level, had water available and provided "abundant

dumping ground for slag from furnaces, without interfering with any vested rights in the adjacent lands or streams" (O'Shaughnessy, 1899). The smelter and the town which grew up nearby were named Keswick after the president of Mountain Copper Company, William Keswick, Esquire. The railway, under construction between August 1895 and February 1896, was 11 mi long with a grade of 200 ft/mi. An additional mile of standard track was built from the smelter to the main line of the California and Oregon Railway which ran along the west bank of the Sacramento River.

By March 1896 the first furnace at the Keswick smelter was in operation. By 1897 two large blast furnaces as well as 80 roasting stalls were completed. "Ultimately the smelting plant. . . was increased until at the peak of its operation in 1904 it was treating an average of more than 1,000 tons per day of Iron Mountain sulphide ore, taxing the ability of both the mine and the railway" (Kett, 1947). There were five water jacket blast furnaces with a capacity of 300 tons/day each. The fine ore was roasted in two banks of Wright-McDougal roasters, each 18 ft in diameter with six hearths. Each bank consisted of four roasters with a separate stack. Two briquetting machines were required to compress roasted fines, as well as the crude fines from the mine and the flue dust, before these could be charged into the blast furnaces; and a large oil-burning preheating unit was employed to furnish the hot air essential to the success of the pyritic method of smelting (Kett, 1947).

Prior to 1902 when electric power became available, the necessary power for supplying the smelting plant was furnished by water pressure in the winter and by steam from wood-fired generators in the summer when the water runs short. The 1898 drought caused the construction of

a pumping plant in the Sacramento River, near the Spring Creek railroad bridge.

Both O'Shaughnessy (1899) and Kett (1947) report that the method of reducing the ore caused much trouble, necessitating numerous experiments. The problems of furnace design and the high zinc content in the ore were eventually overcome by the use of the preheated air blast method of pyritic smelting. Another problem in the early years was the high sulfur content of the ore. First several tiers of roasting kilns were constructed on the hillside above the smelter to burn off the sulfur before the ore was processed. The kilns were all connected with a big smoke stack leading up the side of the mountain to carry away the sulfur fumes. The concentration of smoke from all the kilns proved so annoying to the workmen that the simpler process of burning the ores in various heaps, distributed at isolated and suitable points along the narrow-gauge railway, was put into practice. The ore was received in bunkers from the mine cars, and piled on the ground around flues made of wood. After the piles were shaped and a draft provided for, the wood was ignited, and the piles burned slowly for 60 days. Then the ore, less the excess sulfur, was again loaded on the railway cars and conveyed to the smelter (O'Shaughnessy, 1899).

At the mine, Alexander Hill, mine superintendent 1895-97, had introduced a simple mining method of replacing quarry rock from the surface of the adjacent ground in cavities formed by the extraction of ore, thus reducing the cost of timbering to a minimum and preventing any caves in the surface ground. However, this method resulted in spontaneous combustion fires when the refilled areas had been sealed off, and it was impossible to get water to these fires. A large fan

was installed at the mine entrance, thus reducing the temperature and holding the gases back. Men were then able to fight the face of the fires with water and to cool the high-grade ore enough to extract it.

Despite the processing problems and the fires, Mountain Copper Company, and therefore the state of California, enjoyed a turn-of-the-century copper boom. In 1901 the state produced 34,931,985 lbs of copper worth \$5,501,782 and ranked as the fourth copper producing state in the Union (after Montana, Michigan and Arizona). Iron Mountain "soon took high rank among the great copper mines of the world," exceeded by six in the United States and a total of eight in the world (Aubury, 1905). In fact 1901 marked the peak of copper production for Shasta County, 30,990,781 lbs worth \$4,881,048 (Aubury, 1905), and for California. The Iron Mountain mines produced 197,951,738 lbs of copper by the end of 1919 from direct smelting ore (Kinkel and others, 1956). After 1919, the principal periods of copper production from Iron Mountain ore were in 1925, 1928-30 and 1943-47.

Even though copper production was at an all time high, Mountain Copper Company had its share of problems. Between 1902 and 1908, several law suits for damages were brought against the company by private property owners and the U. S. Forest Reserve for destruction of vegetation. The effects of the sulfur fumes had been a topic of concern in the area from the time the smelters started operation. The January 2, 1897, weekly edition of the Shasta Courier reported:

The smelter smoke question is fuming and promises to become a burning one before long. Shasta is fortunate for once. The air currents and topography of the country almost entirely exempts her from objectionable odors and her citizens can breathe God's pure, free air without tax or permission granted by any corporation foreign or domestic.

A week later the paper reported that a man was found "insensible in his cabin" in Keswick, and the physician who treated him considered that the smelter fumes were "the cause of the trouble."

An injunction against the roasting of ores was eventually served. Roasting in heaps and stalls was abandoned, and by 1907 the Keswick smelter was completely shut down. While there is some suggestion in Aubury's 1908 account that the company planned to resume operations at Keswick as soon as legal problems were solved, much of the Keswick equipment had already been moved to their new processing plant in Martinez. It should be noted that by Kett's account, the closing of the Keswick smelter was purely a matter of convenience and economy.

As early as 1900 Mountain Copper Company had contracted with Pacific Coast Oil Company (now Standard of California) for the production of sulfuric acid at Pacific's Richmond refinery. The sulfides were returned to Keswick after roasting at Richmond, so that the calcines could be smelted for copper, silver and gold. Mountain Copper's Martinez plant simplified the procedure; it was complete with copper smelter, an acid plant, and a factory for manufacturing commercial fertilizers. Between 1904 and 1907 several blast furnaces were retained at Keswick and used for production of copper matte which was refined in Baltimore by the electrolyte method.

In 1907 as the high-grade copper ore in the original ore body (Old mine) was nearing exhaustion, diamond drilling revealed large masses of siliceous, chalcopyrite ore below the Old mine. This siliceous ore was needed in the Martinez smelter as flux, and beginning in 1909 regular shipments of No. 8 ore, with about a 5 percent copper content, were made. The No. 8 mine produced close to a million tons of ore and

was not exhausted when mining was discontinued in 1919. In 1914 and 1915 a mill for treating the No. 8 ore was built in two parts. Primary crushing was done at the mine portal, and secondary crushing and flotation was done at Minnesota on the Iron Mountain Railway. The Minnesota Mill, designed by Gelasio Caetani, was the first flotation plant in California. The mill site was adjacent to Spring Creek, its water source. An adjoining flat area was available for tailings disposal. The plant's operation is described by Kett (1905, p. 122-123).

Trial runs indicated the need for a mechanical filter to obtain a flotation concentration that was dry enough to ship. A Dorr thickener and an Oliver filter solved this problem, and the mill ran from April 1915 to March 1917 when it was shut down for modification to an "all flotation" plant with a capacity of 550 to 600 tons/day. The plant then operated from May 1917 to March 1919 when the low price of copper caused it to close.

The No. 2 mill at Minnesota operated briefly in 1919 to treat the Old mine filling, estimated from 150,000 to 500,000 tons, containing 1.6 to 2 percent copper and some gold and silver. Because of the drop in the price of copper and numerous mechanical and metallurgical defects, the plant was short lived.

In 1928 when the price of copper indicated profitable operation was again possible, the Minnesota mill was re-erected at a site just below the No. 8 mine portal. The narrow gauge railway operations had been suspended in 1921; therefore it had become more economical to pump the Spring Creek water up Iron Mountain to the plant than to take the ore down the mountain to be processed. This plant was simpler than the previous one, and the mechanical and metallurgical problems were

solved. However, there were other problems. Tailings disposal in the steep canyon proved to be difficult. Tailings dams were built in Slick-rock Creek, but they were a constant source of trouble and resulted in numerous complaints from the California Fish and Game Commission. Also the production from the mine was low and erratic, and in 1930 the price of copper began to fall once again. The operation continued for a little over a year, 1929-30, and was operated occasionally until 1933.

Mountain Copper Company developed the No. 8 mine concurrently with the Hornet mine, located on the east side of Iron Mountain. The original discovery of the Hornet consisted of a limited showing of mineralized material that projected into Boulder Creek and had been exposed by erosion. In 1885 C. W. Fielding had been fascinated by the massive pyrite deposit, and despite the fact that there was no immediate market for pyrite and only nominal amounts of copper in the ore, he had purchased the mine and surrounding land. As West Coast oil refining grew so did the demand for the pyrite with its 50 percent sulfur content, necessary for the manufacture of strong sulfur used in oil refining. The mine was in operation continuously from 1907 to 1963 and produced 2 million tons of pyrite ore (L. George, pers. commun.), averaging 50 percent sulfur, nominal copper, and practically no gold or silver (Kett, 1947).

Originally sulfuric acid manufacturers used lump pyrite, 1.5 to 2 in. in size. From 1900 to 1907 the lumps were supplied from the Old mine. Beginning in 1907 they were supplied by the Hornet. Production of these lumps involved screening out the fines; these fines were put into storage near Boulder Creek. In 1920 the manufacturers abandoned lumps in favor of fines. The fines in storage were sold immediately, and a new crushing and screening plant was installed and put into operation

in October 1920. This plant replaced the crushing operations at Keswick and was built near the mine. It operated until 1943.

To transport the ore and pyrites after the railway shut down an aerial tramway was completed late in 1921, and it ran until 1963. The tram had 2.5 mi of ropeway and transported 75 to 100 tons/hr; it ran from a point close by the Hornet to Matheson, a few miles north of Keswick on the Southern Pacific railroad line. To support the tram and the crushing plant, a machine shop and warehouse were constructed in the old bed of Boulder Creek. The creek had been diverted by a tunnel, and the bed had been filled with jig tailings. At the same time headquarters was transferred from the Iron Mountain camp to the Hornet. A road was blasted out of the left bank of Boulder Creek to permit easy access to the Hornet tunnel.

The gossan outcrop at Iron Mountain attracted continual attention from the mining engineers. Supergene enrichment occurred in the Old mine ore body, and residual concentrations of silver and gold were left in this oxidation zone. In 1928 J. M. Basham completed pilot-plant cyanide-leaching tests, and the results warranted construction of a 250 ton/day plant. The cyanidation plant operated between December 1929 and February 1942, and the gossan was extracted by the open-pit method. Kett (1947) explains the plant operation. As an example, in June 1938 the cyanide plant treated 22,434 tons of ore which averaged 0.054 oz of gold and 0.1434 oz of silver per ton (O'Brien, 1957). Tailings storage was in Hogtown Gulch, a deep, narrow ravine cutting across the course of Slickrock Creek almost at right angles. Ultimately, Hogtown Gulch held a million tons. At first the tailings had an iron

content of 50 to 55 percent; later the content was as low as 30 to 35 percent (Kett, 1947).

In the early days of the open-pit mining, very little overburden had to be removed to get to the gossan. Later as much as 10 tons of overburden had to be removed to obtain 1 ton of gossan. It was dumped in the Slickrock Creek bed and eventually made a fill across the gulch. 2.6 million tons of gossan were mined during the 13 years of operation (Lydon and O'Brien, 1974).

As the gossan operations were ending in 1942, mining at the Mattie and Richmond Extension ore bodies was begun. Exploration of these ore bodies had revealed ore containing 2.25 percent copper and 3.5 to 4 percent zinc. The war-inflated prices offered for these metals encouraged the building of a selective flotation plant at the portal of the Richmond adit. This plant began operations in July 1943 and ran until June 1947, and has been dismantled (Lydon and O'Brien, 1974). Lydon and O'Brien (1974, p. 38) describe the plant operations. When plant construction was completed, all of the company's surface facilities--shops, warehouses and garages--were transferred to the site. Crushing operations continued at the same location until 1963. About 3 million tons of ore were mined from the Richmond and Mattie ore bodies (L. George, pers. commun.).

By 1950, more than 6 million tons of massive sulfide ore had been mined at Iron Mountain, and at least 3.6 million tons of pyrite were mined (Kinkel and others, 1956). After 1950, the mining operations were limited to the open-pit mining of the Brick Flat ore body and the operation of a copper cementation plant. Underground mining ceased at the Richmond ore body by 1956. In 1955-56, the crushing plant was

modernized, and an extension was built on the tram. Two copper recovery plants have operated. The one currently in operation was built in 1958 at the Iron Mountain access road. It operates by electrolytically displacing copper from solution with scrap iron. The mineralized water of the Richmond and Hornet mines passes through three pairs of double-ended, concrete tanks filled with the scrap metal. Annual recovery amounts of 75 to 150 tons of cement containing 65 to 80 percent copper (Lydon and O'Brien, 1974).

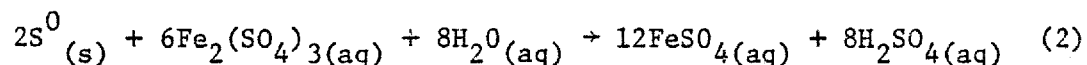
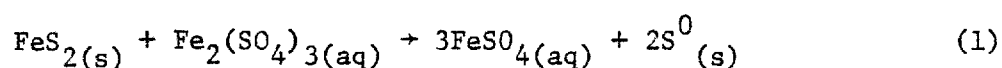
Open-pit mining at the Brick Flat ore body was in progress between 1955 and July 1962. After 2.5 million tons of overburden had been stripped, the first pyrite was mined in January 1956. Production from the Brick Flat ore body amounted to about 600,000 tons of pyrite, and 9.5 million tons of waste were removed (Lydon and O'Brien, 1974).

All mining operations at Iron Mountain were discontinued in 1963. The amount of ore remaining in place in the Hornet, Richmond and Brick Flat ore bodies is approximately 12.5 million tons (L. George, pers. commun.).

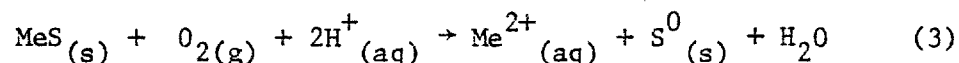
THE AQUEOUS OXIDATION OF SULFIDE ORES

The mechanism by which sulfide minerals break down to form acid mine drainage has been studied by several investigators, and the process is now well characterized. The important equilibrium and rate-determining parameters include temperature, pH, particle size, rate of oxygen transport, concentration of dissolved oxygen, rate of electron transfer, concentration of oxidants other than oxygen, concentration and types of organic complexes, concentration and types of anions, presence and concentration of microorganisms and changes in these variables in space and time for a flowing system.

Stokes (1901) reminds us that the chemistry of pyrite oxidation has been studied since at least the late 1800's when publications from Europe described the effect of ferric sulfate solutions on the oxidation rate. Stokes formulated the breakdown of pyrite in a two-step process:

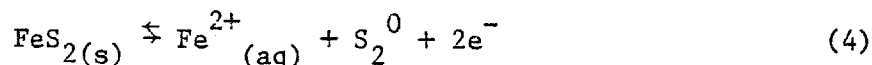


where ferric iron is the oxidant. Experimentation in hydrometallurgy has shown that the leaching of metallic sulfides with sulfuric acid solutions yields sulfur and the dissolved form of the corresponding metal:



(Burkin, 1966; Peters and Majima, 1968; Majima, 1971; Wadsworth, 1973).

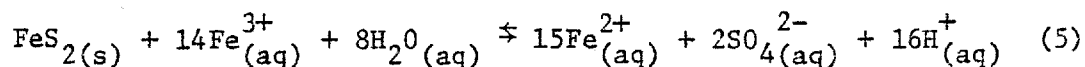
Sato (1960) clearly defined the initial step in the oxidation of pyrite as:



by measuring the electrode potential of pyrite in acid solutions and comparing the observed emf with that calculated from thermodynamic data. Likewise, the initial oxidation step of chalcocite, covellite, galena and sphalerite implied the production of sulfur and the soluble form of the corresponding metal. At near neutral pH values (4 to 10) the reaction is followed by hydrolysis of the metal and formation of the metal hydroxide. The presence of iron hydroxide as a reaction product has been observed by Mossbauer spectrometry (Baker, 1972). This initial oxidation step has been confirmed by Garrels and Thompson (1960) and Smith and others (1968) for pyrite.

The rate of pyrite oxidation in the presence of oxygen as the only oxidant is proportional to the partial pressure of oxygen, and oxygen diffusion is the rate-limiting factor (Burkin, 1966; Smith and Shumate, 1970).

Pyrite oxidizes most rapidly in the presence of ferric iron, and experiments by Garrels and Thompson (1960) and Smith and others (1968) have confirmed the stoichiometry of the reaction:



in acid sulfate solutions and in the absence of oxygen. These investigations also show that the oxidation of sulfide sulfur is so rapid that it is found only as sulfate in the reaction products. This observation confirms Sato's (1960) statement that the sulfur dimers released by pyrite are very unstable and can be easily oxidized.

Sulfur has been observed as a weathering product by the author in mine workings of some mineral deposits (other than Iron Mountain) and probably results from the lack of available ferric iron. If the chemical environment (lack of oxygen, high temperature, toxic solutions) prohibits the existence of ferrous-oxidizing catalysts, then there may not be sufficient ferric iron available to complete the oxidation of sulfur. These conditions might exist in deep underground workings, in high temperature mines, in mines where no pyrite occurred, or in coal mines where organics may maintain a reducing environment.

The next step is the oxidation of ferrous iron to ferric:

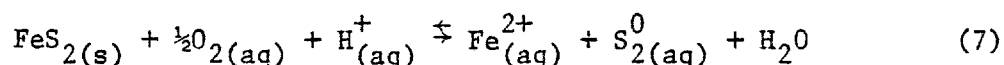


which is quite slow at pH values less than 4.0 and has been properly called the "rate-determining step" in the formation of acid mine drainage (Singer and Stumm, 1970). The mechanism behind this pH dependence of the rate constant has not been examined, but there is evidence to suggest that an electron is transferred from the ferrous ion through its hydration sphere to an oxidant, producing a hydrated ferric hydroxide which would be more stable in neutral to alkaline solutions (Jayson and others, 1972). In acid solutions, the hydroxide complex is inhibited, and the electron would have greater difficulty in transferring. This hypothesis is substantiated by the hydrolysis constants for ferric iron. The pK values for iron hydrolysis begin to show dominance at about pH values of 3, the same region where the oxidation rate begins to increase.

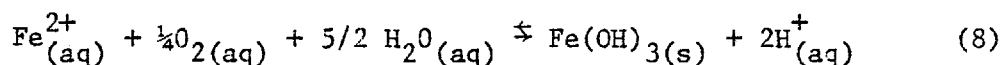
Finally, the ferric iron hydrolysis products may form various iron hydroxide precipitates depending on the pH and iron content. On the basis of thermodynamic calculations Brown (1971) has shown that in iron-

and sulfate-rich waters, goethite is the stable phase for pH values greater than about 2. Below this pH, jarosite $[\text{KFe}_3(\text{SO}_4)_2(\text{OH})_6]$ is stable as long as the Eh is 600 mv or higher and sufficient potassium is present. Other forms of jarosite such as natrojarosite and hydronium jarosite are also found; in fact, pure jarosite is practically never found in nature. Hematite, lepidocrocite and amorphous iron hydroxides will also appear depending on the amount of aging, the chemical potential of water and the temperature.

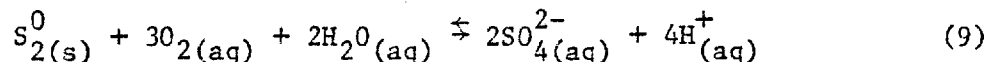
Based on experimental and field evidence, the sequence of reactions which describe the decomposition of pyrite and similar sulfides in natural surface environments is as follows. Initially, pyrite is oxidized to ferrous iron and sulfur by the action of oxygen dissolved in water:



Since ferrous ions are rapidly oxidized and hydrolyzed at these initially neutral pH values, the next reaction:

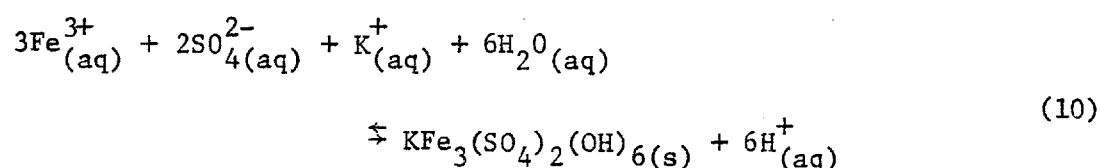


takes place, balancing the pH shift from reaction (7). The sulfur in reaction (7) is also oxidized to sulfate, and it is this process which lowers the pH:

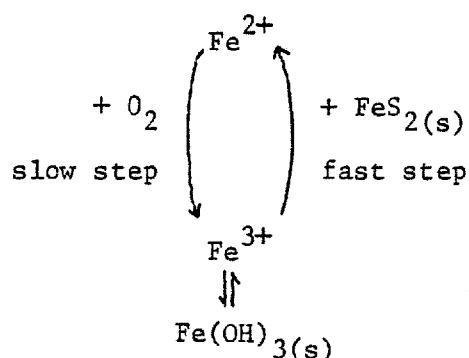


As the pH drops, less and less ferric iron is hydrolyzed, and the activity of ferric iron is increased so that it becomes more and more important as an oxidant. At pH values less than 3, ferric ions are the dominant oxidant as shown in reaction (5), and nearly all the acidity

is due to the sulfur oxidizing to sulfate. Reaction (5) would quickly come to a halt, however, if there were not acidophilic iron-oxidizing bacteria which speed up the ferrous to ferric oxidation rate by several orders of magnitude over the abiotic rate (Lacey and Lawson, 1970; Singer and Stumm, 1970). These bacteria grow deep inside mines in the absence of light. Oxidation of iron in waters with pH values around 2 or less leads to the formation of jarosite:

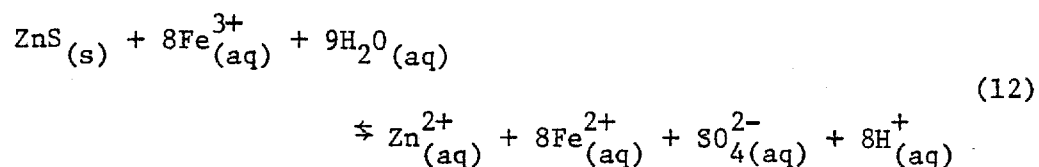
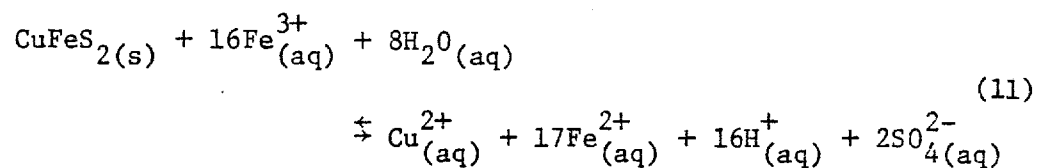


The oxidation of pyrite has been modeled by Singer and Stumm (1970) as a cyclical process wherein dissolved iron is rapidly reduced by pyrite but slowly oxidized by oxygen:



With microbial catalysis the slow reaction is speeded up many times, so that the production of acid mine drainage is a rapid, self-perpetuating process which continues as long as there is water and pyrite available.

The oxidation of other nonferrous sulfides is probably caused by the ferric iron from pyrite oxidation rather than direct microbial attack. Chalcopyrite and sphalerite, two common ore minerals, would be expected to break down at the expense of ferric iron as follows:



forming more acid sulfate.

To summarize, pyrite is oxidized primarily by ferric iron to acid ferrous sulfate solutions. The ferric iron is rapidly regenerated by iron-oxidizing bacteria making acid mine water production a natural, self-perpetuating process. Most of the acid is released during the oxidation of the sulfide sulfur to sulfate with a minor amount produced by the hydrolysis of ferric iron. Either iron hydroxides or jarosites may precipitate from acid mine waters depending on the pH. The reactions presented in this chapter provide a stoichiometry for testing the reaction products in the acid mine waters issuing directly from mines in the field area.

MICROBIOTA AND THEIR EFFECT ON FERROUS IRON OXIDATION IN ACID MINE WATERS

Microorganisms are extremely important in maintaining the balance of life on earth and are found in nearly every part of the natural environment. Bacteria and algae have been found in ice, on snow (*Rhodophyta*), in halite crystals, in boiling hot springs (*Sulfolobus* and *Cyanidium*), in the absence of oxygen, in fully oxygenated systems, in strongly acid waters, in alkaline waters, and in doubly distilled water. The widespread occurrence, activity and rapid genetic adaptability of microorganisms enable them to catalyze many biochemical and geochemical processes. This catalytic influence is responsible for keeping such elements as carbon, sulfur, nitrogen and silicon distributed in proportions best utilized by higher order organisms.

Acid mine drainage provides an example of an extreme environment habitable only by microorganisms. Both acid-tolerant and acidophilic¹ species of microorganisms have been found in acid waters, and the high concentrations of heavy metals which occur in acid mine drainage seem to have no deleterious effect on the survival of these species.

¹The distinction between acid-tolerant and acidophilic is based simply on the pH range over which the species can survive. Acidophilic species can only survive when the pH of the water is below 4 or 5, whereas acid-tolerant species have been able to adapt to acid conditions but also grow in neutral to alkaline waters. Commonly, acid-tolerant species are those which grow optimally under neutral conditions but have developed strains which can grow quite comfortably in acid waters.

This chapter introduces the ecology of microorganisms living in acid mine waters, identifies known species and outlines their role in chemical oxidation processes. With this background, field observations of microorganisms in the Spring Creek drainage basin are presented, and the isolation of an iron-oxidizing bacterium is described. Finally, on-site and laboratory measurements of iron oxidation by bacteria are discussed.

Microbial Ecology of Acid Mine Waters: Literature Review

Both eucaryotes (definitive and complex cellular structure with true nuclei) and procaryotes (primitive cell structure with no nuclei) have been found in acid mine waters. Joseph (1953) found gram-positive and gram-negative bacilli and cocci, fungi, green algae, diatoms and actinomyces in several acid streams, ponds and soils in West Virginia and Pennsylvania. Ehrlich (1963b) found yeasts, flagellates, protozoa and amoebae in acid mine waters coming from a copper mine in the southwestern United States. Dugan and others (1970a, b) have found gram-negative and gram-positive bacilli, yeasts and fungi in bacterial slime collected from an acid drainage, and they note that Lackey (1938) observed flagellates, rhizopods, ciliates and green algae in 62 West Virginia streams.

Two general groups of microorganisms are commonly reported in acid mine waters from different parts of the world: procaryotic bacilli and eucaryotic green algae (*Chlorophyta*). *Cyanophyta* or blue-green algae (a procaryote) are not found in waters where the pH is less than 4 or 5 (Brock, 1973), although they are common in neutral to alkaline polluted waters, especially those with high phosphate content. Acid-

tolerant algae have not been as extensively studied as have several strains of bacilli (i.e. genus *Thiobacillus*), yet a few species consistently occur in the acid mine drainage environment. Bennet (1969) made a survey of algae in mine waters of the Appalachians and found that three species--*Euglene mutablis*, *Eunotica tenelle* and *Pinnularia braunii*--were the most abundant, although a wide variety existed. Fott and others (1964) described five flagellates from acid peat waters: (1) *Chlamydomonas acidophila* (pH = 1 to 2), (2) *Euglena mutablis* (pH = 1 to 5), (3) *Lepocinclis teres* (pH = 2 to 5), (4) *Carteria turfosa* (pH = 3 to 5), and (5) *Carteria acidocola* (pH = 3.5 to 5). They also noted *E. mutablis* has been observed the world over where acid waters occur as iron seeps. Laskin and Lechevalier (1973) reported *E. mutablis* as common in extremely acid waters. Ferguson and Bubella (1974) used a species of filamentous *Ulothrix* from a bloom growing in an acid seep to measure the uptake of copper, zinc and lead. Lackey (1938) as cited by Dugan and others (1970a) reported *Ulothrix zonata* and *Euglena mutablis* in acid streams of West Virginia. Other algae which have been noted in acid waters (but not necessarily mine drainage) include *Cyanidium caldarium* (Doemel and Brock, 1971), *Zygogonium* sp. (Lynn and Brock, 1969) and *Chlorella* sp. (Kessler, 1967). Darland and others (1970) have also isolated the first thermophilic, acidophilic mycoplasma (procaryote with no cell wall) from self-heating coal refuse piles. The mycoplasma *Thermoplasma acidophilum*, grows optimally at pH values of 1 to 2 and temperatures near 59°C (Belly and others, 1973) on many heated coal refuse piles and their drainage (Bohloul and Brock, 1974).

Bacillus bacteria seem ubiquitous in acid waters, regardless of whether they come from mine drainage (Dugan and others, 1970a, b) or

from hot springs (Belly and Brock, 1974).² Two divisions of bacilli are known, the gram-negative acidophilic chemolithotrophic genus *Thiobacillus* and the endospore-forming chemoorganotroph (heterotroph) genus *Bacillus* which is usually gram-positive and part of the family *Bacillaceae* (Buchanan and Gibbon, 1974). Whereas yeasts, fungi, algae and possibly even some *Bacilli* may be acid-tolerant and are known to grow optimally in the acid media of laboratory preparations because the competition is minimized (Brock, 1974; Alexander, 1961), *Thiobacillus thiooxidans* and *Thiobacillus ferrooxidans* are strictly acidophilic. These two species, the only two known to have a widespread occurrence in acid mine drainage, cannot survive at pH values greater than about 4.

The genus *Thiobacillus* was first isolated in 1902 by Nathanson and obtained in pure culture two years later by Beijerinck (see Sokolova and Karavaiko, 1968). These bacteria are described as nonmotile and motile rods about 0.5 by 1 μm , often showing polyhedral inclusion bodies of unknown function. Although this genus is usually considered to be obligate chemolithotropic, some facultative heterotrophy has been demonstrated (Lundgren and others, 1974). Only those aspects of *Thiobacillus* which relate to chemical reactions in acid mine drainage will be discussed here. Adequate reviews of their physiology and biochemistry are available (Sokolova and Karavaiko, 1968; Laskin and Lechevalier, 1973; Tuttle, 1969).

Species of the genus *Thiobacillus* have been differentiated by their physiological characteristics using two different methods: (1) numerical

²Thus far, bacilli have been used to describe bacteria of a characteristic morphology (i.e. rods), not a taxonomic division.

taxonomy (Hutchinson and others, 1966, 1969) and (2) analysis of DNA base composition (Jackson and others, 1968). The results of these two approaches are in excellent agreement and have helped to clarify misnomers due to slight differences in strain variability. Only two species, *T. ferrooxidans*, which oxidizes both iron and sulfur and *T. thiooxidans*, which oxidizes sulfur and not iron, have been isolated from acid mine drainage. *Ferrobacillus ferrooxidans*, isolated by Leathen and others (1956), has been shown to be identical to *T. ferrooxidans* by morphology and nutritional requirements (Unz and Lundgren, 1961) and by numerical taxonomy (Hutchinson and others, 1966). For the same reasons *Ferrobacillus sulfooxidans* has been found to be redundant and is renamed *T. ferrooxidans*.

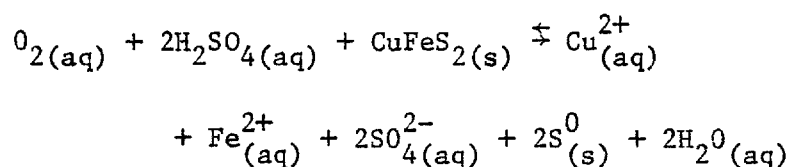
T. ferrooxidans was the first chemolithotrophic bacterium whose chief energy source was clearly derived from the oxidation of iron (Colmer and Hinkle, 1947; Colmer and others, 1950; Temple and Colmer, 1951). This microbe clearly catalyzes the aqueous oxidation of dissolved ferrous iron to ferric iron (Lundgren and others, 1964; Schnaitman and others, 1969), but the catalysis of pyrite oxidation is not clearly understood. Bacterial oxidation of sulfide minerals can occur by two mechanisms (Silverman, 1967): (1) direct contact mechanism--bacteria adsorb onto the mineral surface and directly oxidize the solid; (2) indirect mechanism--bacteria simply oxidize solubilized ferrous iron to ferric, and then the ferric ions oxidize the solid mineral.

The indirect mechanism is generally believed to be correct because: (1) dissolved ferric iron is a strong oxidizing agent even at low pH values (Garrels and Thompson, 1960), (2) the presence of *T. ferrooxidans* increases the rate of ferrous to ferric oxidation by about six orders

of magnitude over the inorganic rate (Lacey and Lawson, 1970; Singer and Stumm, 1970), and (3) bacteria utilize soluble material for energy and there is no known mechanism by which they can attack solid surfaces. Several studies have attempted to show that the direct contact mechanism is operative (Bryner and Jameson, 1958; Silverman, 1967; Beck and Brown, 1968; Beck and Hatch, 1969), but the results can be interpreted just as well by the indirect mechanism. Although there is no sufficient evidence demonstrating that direct contact is important, there are several facts which relate to this question and may explain what is happening. First, bacteria are readily adsorbed onto solid surfaces especially at low nutrient levels (Daniels, 1972; L. Young, 1976, pers. commun.). Therefore, regardless of the biological oxidation mechanism, the microbes should always be found closely attached to the mineral surface and usually in higher numbers than in the solution. In addition, solution at the surface of pyrite would be expected to have a greater concentration of ferrous iron than in the bulk at some distance, and this would attract microbes using ferrous iron as an energy source. In the comprehensive review by Tuovinen and Kelly (1972), attachment to sulfur and sulfide mineral surfaces is cited as being necessary. Surfactants in low concentrations increase the oxidation rate of sulfur and sulfide minerals which, presumably, increases the adsorption of thiobacilli. It is not known why surfactants have this effect on thiobacilli. Tuovinen and Kelly (1972) also cite investigators who have found thiobacilli to excrete phospholipid wetting agents. These phospholipids provide a means for the microbes to attach to the sulfide surfaces, but it is doubtful that by bonding directly to the solid substrate iron is withdrawn by an organic complex and oxidized to ferric

without prior chemical solubilization. The direct contact mechanism would also seem unlikely in light of the sulfate requirement for oxidation by *T. ferrooxidans* (Lazaroff, 1963). Thiobacilli incubated in ferrous chloride or ferrous nitrate solutions do not oxidize ferrous iron, and sulfate solutions are needed for the microbial oxidation of pyrite.

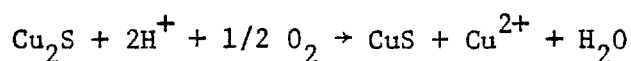
T. ferrooxidans oxidizes sulfur at about the same rate as *T. thiooxidans*. *T. ferrooxidans*, however, is able to oxidize iron at a faster rate than sulfur (Tuovinen and Kelly, 1972); therefore, iron sulfide minerals are more rapidly oxidized by *T. ferrooxidans* than by *T. thiooxidans*. The sulfur in other sulfide minerals is likewise oxidized by these microbes, and this oxidation process may be a major factor in the breakdown of nonferrous sulfides as well as contributing to the sulfuric acid production from ferrous-containing sulfides. The action of acid reagents on any sulfide tends to solubilize the metals and form free sulfur, e.g.



The sulfur thus formed would then be in a form readily available for oxidation by *T. ferrooxidans* and *T. thiooxidans*. There is some indication (Silver, 1970; Silver and Torma, 1974) that the oxidation rate of nonferrous sulfide minerals is comparable to that of elemental sulfur, but no one seems to have directly determined this possibility. If oxidation rates are found to be the same, then it would appear that all nonferrous sulfide minerals break down by the same mechanism which oxidizes sulfur and that the metals present simply dissolve into solution. Duncan and Walden (1972) present data on the oxidation of sphalerite

in concentrated ferric sulfate solutions which show that considerably more zinc is released into solution when *T. ferrooxidans* are present. The same high zinc levels are attained with the bacteria in the absence of ferric sulfate, and this suggests that ferric iron is not as good an oxidant as oxygen in the presence of iron-oxidizing bacteria.

The oxidation of chalcocite by *T. ferrooxidans* resulted in an increase in pH, an increase in soluble copper, and the formation of digenite and covellite (Nielson and Beck, 1972) which supports the proposed reaction:



The possible utilization of the Cu(I)/Cu(II) redox couple as an energy source for *T. ferrooxidans* was further demonstrated by Silver and Torma (1974), who also found antlerite, $\text{Cu}_3\text{SO}_4(\text{OH})_4$, and metallic copper with digenite and covellite. The starting material is highly reactive (Silver and Torma used -400 mesh chalcocite ground in a ball mill), and since the oxygen uptake was almost negligible the reaction may have been purely an inorganic disproportionation (with minor oxidation) reaction rather than a biologically mediated reaction. The same criticism can be made about the other substrates that Silver and Torma (1974) tried because they had no sterile controls.

Nearly every common sulfide mineral has been subject to attack by *T. ferrooxidans*, and these data are compiled in table 5. It must be reemphasized that although metal concentrations increased during the incubation period in these experiments there is not always evidence available that the microorganisms were obtaining energy from oxidation of the sulfide substrates.

Table 5
Sulfide Minerals Used as Substrates for *T. ferrooxidans*³

<u>Mineral formula</u>	<u>Mineral name</u>	<u>Reference</u>
S; FeS ₂	elemental sulfur; pyrite	Bryner and Jones (1965), Silver (1970), and see reviews by Kuznetsov and others (1963), Sokolova and Karavaiko (1968), Roy and Trudinger (1970) and Tuovinen and Kelly (1972)
FeS ₂	marcasite	Silverman and others (1961)
Fe _{1-x} S	pyrrhotite	Duncan and others (1964)
CuFeS ₂	chalcopyrite	Bryner and others (1954), Bryner and Jameson (1958), Corrick and Sutton (1961), Sutton and Corrick (1961), Sutton and Corrick (1963), DeCuyper (1964), Duncan and Trussell (1964), Duncan and others (1964), Corrick and Sutton (1965), Duncan and Walden (1972), Silver and Torma (1974)
ZnS	sphalerite, mimetite	Ivanov and others (1962), Duncan and Walden (1972)
Cu ₂ S	chalcocite	Bryner and others (1954), Bryner and Anderson (1957), Duncan and Walden (1972), Nielson and Beck (1972), Silver and Torma (1974)
CuS	covellite (digenite?)	Duncan and Walden (1972)
MoS ₂	molybdenite	Bryner and others (1954), Bryner and Anderson (1957), Bryner and Jameson (1958)

³For general reference, see Zajic (1969) and Silverman and Ehrlich (1964).

Table 5 (cont'd.)

<u>Mineral formula</u>	<u>Mineral name</u>	<u>Reference</u>
CoS	synthetic and selected ores	Sutton and Corrick (1961), DeCuyper (1964), Torma (1971), Silver and Torma (1974)
(Fe,Ni)S; NiS	pentlandite, millerite and synthetic	Razzell and Trussell (1963), Torma (1971), Silver and Torma (1974)
PbS, CdS, Sb ₂ S ₃	galena and synthetic	Silver and Torma (1974)
HgS	cinnabar and synthetic	J. Burkstaller, pers. commun. (1975), Silver and Torma (1974)
As ₂ S ₃	orpiment	Ehrlich (1963a)
FeAsS, Cu ₃ AsS ₄	arsenopyrite, enargite	Ehrlich (1964)
Cu ₅ FeS ₄	bornite	Bryner and others (1954), Ivanov and others (1962), Sutton and Corrick (1963), Razzell and Trussell (1963)
Cu ₁₂ Sb ₄ S ₁₃	tetrahedrite	Bryner and others (1954)

In this review I have attempted to summarize the ecology of microorganisms living in acid mine waters and their role in catalyzing inorganic oxidation processes. Obviously, iron and sulfur oxidation rates are greatly accelerated by the presence of *Thiobacillus* but several questions remain unsatisfactorily answered:

(1) What effect, other than proximity, does the direct contact of thiobacilli to a sulfide surface have on the oxidation mechanism? Can adsorption experiments be applied to determine whether the direct or indirect contact mechanism is most applicable? Is it not possible that a direct contact, indirect oxidation most clearly describes the process?

(2) Of what relative importance is the oxidation of the sulfur in sulfides by thiobacilli? Do the microbes react with soluble or solid sulfur?

(3) Do thiobacilli oxidize nonferrous sulfides? And if so, how.

(4) Is reaction stoichiometry conserved during microbial mediation of sulfide oxidation? Do pH, Eh, metal concentrations, sulfate concentrations and sulfur oxidation states, mineral weight loss and oxygen and CO₂ uptake fit into an appropriate mass balance?

(5) What effect does the presence of a semiconductor like pyrite have on the microbial oxidation of chalcopyrite or sphalerite or chalcocite?

Microbial Ecology of Acid Mine Waters: Field Observations

The Spring Creek drainage contains abundant and diverse acidophilic and acid-tolerant microorganisms. To determine fully the interactions of the microbiota with the ore deposits and the mine effluent would require several research projects which are clearly outside of the limitations of this thesis. The field observations in this section reveal that these organisms play an integral role in the aquatic geochemistry of the drainage basin.

In the open pit at the top of Iron Mountain (fig. 2), microbial activity may be observed nearly all year round in a seep which begins near the main road and drains down into the bottom-most pool. Loose debris, broken-off boulders and smaller, unsorted massive sulfide ore lie in the seep and provide the necessary minerals to produce acid drainage. On October 2, 1975, near the origin of the seep, great blooms of green, filamentous algae were growing intermixed with a white to yellow powdery microorganism presumed to be a fungus. The alga fits the description of *Ulothrix* because of its colonial, filamentous habit and known association with acid waters. The mixture of green algae, fungi and precipitating iron oxides formed a striking color pattern as seen in plate 1. Although this seep was about 50 m in length, the population of microorganisms died out at about 20 to 30 m, and no sign of microbial life was visible in the red pool at the bottom. Along this reach the pH decreased from 3.20 in the algal pool to 2.48 in the red pool, while the Eh increased from 0.611 v to 0.737 v, implying that significant amounts of ferrous iron had oxidized. Hydrolysis of the ferric iron presumably caused the decrease in measured pH.



Plate 1. Green filamentous algae (*Ulothrix?*) growing in acid spring in the open pit at Iron Mountain. Spring is about 1 m in width diagonally across photo.

On January 18, 1976, the site was revisited, and the same microorganisms appeared to be there, but their general appearance had changed with an apparent increase in the fungi.

The most concentrated acid mine water flows from the Hornet and Richmond mines into a stainless steel flume (site B in fig. 1). This water has a nearly constant pH of 1.0 throughout the year and contains 10 to 12 g/l of iron (with about 80 percent as ferrous iron), 10 g/l of zinc, 200 to 300 mg/l of copper, 10 g/l of aluminum and 30 to 50 g/l of sulfate. A distinctively foul organic odor which might result from decomposing bacteria can always be detected in this effluent. At several points along the flume, slime streamers of microbial colonies are visible. These slime colonies contain two distinct types: a green alga growing as small spotted aggregates and the slime itself which appears as off-white gelatinous streamers similar to *Sphaerotilus* in gross appearance without any iron oxide coatings. *Sphaerotilus* is ruled out as a possibility, however, since it cannot survive in water having a pH less than about 6, and it is filamentous rather than gelatinous (Brock, 1974).

The same slime growths can be found growing in the trough where the Richmond-Hornet effluent exits the copper cementation plant. Again, in Boulder Creek about 1 km downstream from the copper plant discharge, the bacterial slime reappears, and the slime population density gradually increases downstream. On November 6, 1974, at least the last 100 m of the Boulder Creek gravel bed was completely covered with a grayish-yellow layer of slime streamers. (The green color in plate 2 is an unfortunate result of the reproduction and it is not true color.) These streamers are shown in plate 2 and fit very closely the description



Plate 2. "Acid slime streamers" covering bottom of Boulder Creek as seen through about 5 to 10 cm of water. Boulder at upper right of photo is about 0.5 m across.

given by Dugan and others (1970a) of "acid-streamers" discovered in an acid coal mine drainage in Ohio.

On closer examination the streamers were found to have a surface coating of a finely powdered, grayish mineral substance which was causing the gray color. Upstream the gray particles increased slightly in grain size and had the luster, color and hardness of pyrite. The gray particles were finally traced upstream to an old, partially buried tailings pile located on the steeply eroded west slope of Boulder Creek just below the mineral processing plant near the Richmond mine entrance. During rainstorms, these tailings are washed into Boulder Creek and are found in the lower reaches of Spring Creek. The sulfide particles easily get caught in the outer gel-like layers of the bacterial slime giving the slime a grayish tint.

Underneath the sulfide coating, strands of white gelatinous fibers were observed, and inside some of these fibers a core of a sulfur-yellow substance had formed. By X-ray diffractometry this yellow material was identified as jarosite $[\text{KFe}_3(\text{SO}_4)_2(\text{OH})_6]$. The jarosite was found inside the gelatinous streamers and underneath the attached bacterial slime on the surface of stream gravels and boulders. This close association indicates that microorganisms in the slime are promoting the precipitation of jarosite, and it strongly suggests the presence of *Thiobacillus ferrooxidans*. The *Thiobacilli* oxidize the iron and thereby bring the water closer to saturation with respect to jarosite. The active precipitation of jarosite during the microbial leaching of sulfide ores has been observed in laboratory investigations by Duncan and Walden (1972). Although *T. ferrooxidans* has been isolated from acid sulfate soils and pyrite-rich rocks containing jarosite (Bloomfield, 1972; Ivarson,

1973), this is the first known occurrence of active jarosite precipitation in a mountainous stream by iron-oxidizing bacteria. Occasionally the slime streamers grow in Spring Creek, beginning at the Boulder Creek confluence and gradually decreasing in density downstream. At some point below site K but above site N in figure 1, the bacterial slime does out, and no slime has ever been observed at site N. This spatial change in bacterial population density correlates very well with the increased oxidation state of dissolved iron as one proceeds downstream (see the last section in this chapter).

Slime streamers still covered the bottom of Boulder Creek on November 18 but by December 20, 1974, enough precipitation and high flow had occurred to wash out all of the bacteria, and no further slime growth was observed until May 12, 1975. Then the growth began again, reaching the same dimensions as the preceeding year by the end of the summer of 1975. The cyclic growth of the bacterial slime has a profound effect upon the foaming characteristics of the streams and the oxidation potential of the dissolved iron (discussed later). During the first few rains of the fall and winter, a great deal of stable foam floats downstream. After several major rains have washed away the microbiota, the foaming capability significantly decreases, indicating that the presence of the bacteria is needed to produce the surfactant. Surfactants are generally molecules with a hydrophobic and a hydrophilic part. Decay of the microbiota could produce long-chained hydrocarbons which would hydrolyze and sulfonate in the acid sulfate waters thereby forming a surfactant with the hydrocarbon as the hydrophobic part and the sulfonate as the hydrophilic part. Organic sulfates made from hydrolyzed fatty acids have been used effectively as soaps for acid solutions,

and these sulfates do not form insoluble residues in the presence of calcium and magnesium or other divalent cations. These sulfates have been made commercially for some time and may be similar in composition to the surfactants in Spring Creek.

Several occurrences of filamentous green algae, probably *Ulothrix* spp., have been observed in Boulder Creek and in Spring Creek. These occurrences have one characteristic in common: they always form at the source of a seep from the creek rather than in the main flow of water. The largest growth of algae has been observed adjacent to the copper cementation plant at the base of a large embankment on Boulder Creek. A very small flow of water seeps out at the base of this embankment and spreads out nearly 2 m in width over a bright green filamentous algal blanket. Under the algae is a thick layer of precipitated iron oxides. A water analysis of this seep is given in table 6 along with an analysis of Boulder Creek before it infiltrates the embankment. The infiltration apparently reduces the amount of total iron and zinc, while it increases ferrous iron, pH, manganese, aluminum, silica, calcium, magnesium and sulfate. Some of these changes could have occurred before infiltration, since sample 75WA136 was collected a few hundred meters upstream from the embankment. These analyses shed little light on why the algae prefer to grow here, and it is most likely that growth is dependent upon a physical quality of the environs rather than a chemical quality, i.e. the algae need a slow-moving but continuous supply of water and nutrients. The higher and inconsistent velocities in the main stream beds are too strong for continued attachment and stable growth. Plate 3 shows a typical growth of filamentous green algae at the edge of Spring Creek.

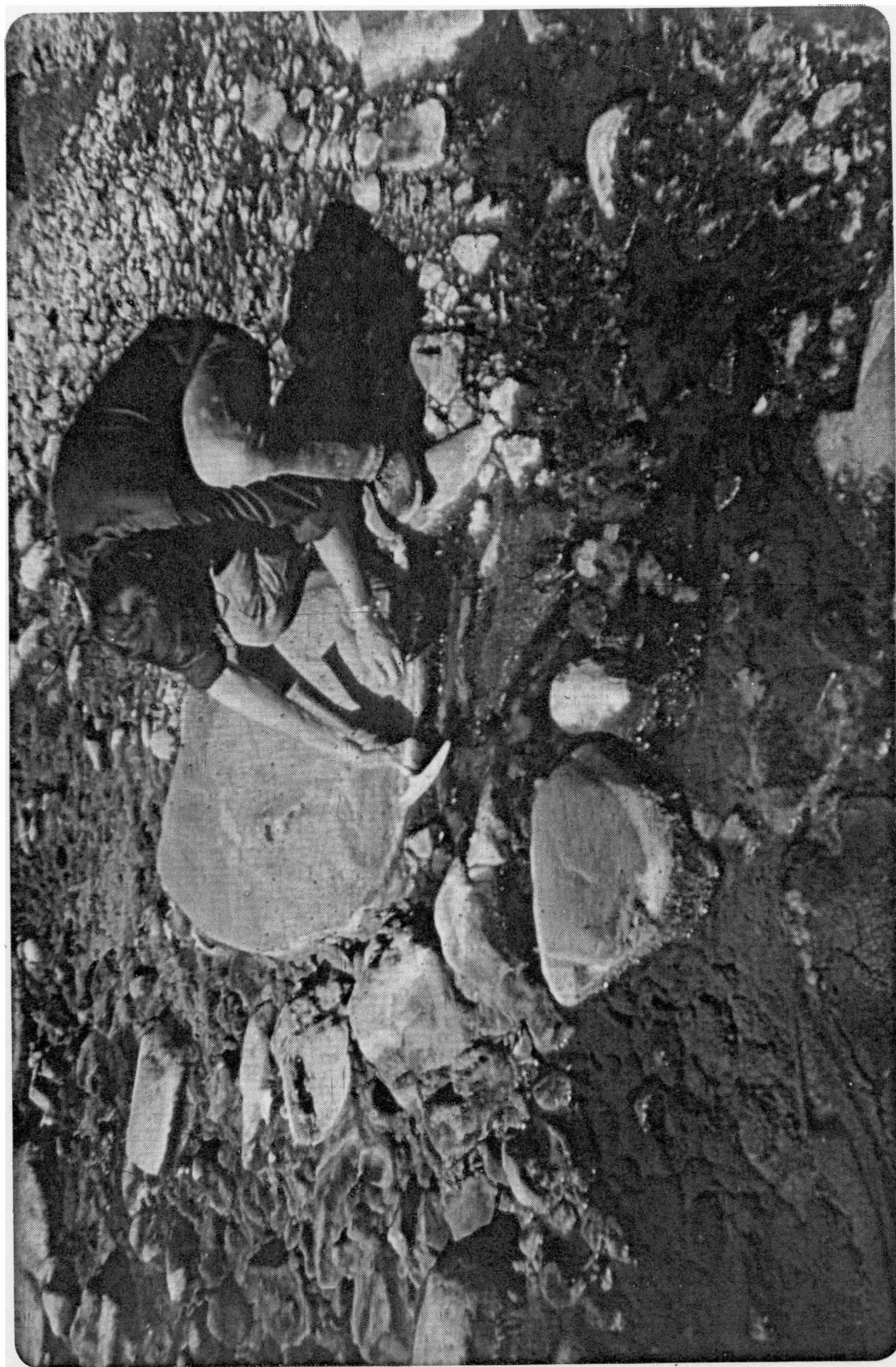


Plate 3. Green filamentous algal (*Ulothrix*?) growth along the banks of Spring Creek.

Table 6

Water Analysis of Boulder Creek Before and After Infiltrating
an Embankment (concentrations in mg/l)

	Sample 75WA136 (filtered) (above embankment)	Sample 75WA137 (unfiltered) (embankment seep)
T(°C)	8.5	14
pH	3.02	3.68
Eh (v)	0.725	0.532
Conductivity (µS)	460	1040
Fe ²⁺	3.48	66
Total Fe	660	100
Cu	1.28	1.48
Zn	63	15
Cd	0.05	0.08
Mn	1.45	3.55
Al	11	33
SiO ₂	28	84
Na	2.9	5.8
K	0.22	0.70
Ca	3.0	30
Mg	8.0	35.5
SO ₄	180	650

Orange-colored microorganisms have been found growing in a stagnant side pool of Spring Creek. The same microbes have been cultured on nutrient agar from samples of oxidized Richmond-Hornet effluent and from their macroscopic and microscopic features appear to be a yeastlike growth.

One other type of alga enjoys the acid waters of Spring Creek, a green alga which grows as colonies in botryoidal mosslike clumps up to 10 to 15 cm in diameter. The alga is commonly found in the waters issuing from the base of the Spring Creek Dam as shown in plate 4. The iron oxide precipitates are often so thick that the algae are completely covered and not distinguishable. The same microorganisms have sometimes been found in smaller quantities in Spring Creek near site J (fig. 1). This alga is a nonfilamentous colonial chlorophyte which cannot be associated with any of the free-swimming species described in the previous section.

The bacteria and algae serve an interesting function: they provide a surface for the precipitation of iron oxides. In every location where algae and bacteria have been found, there is an associated precipitate of either jarosite or some form of an iron oxyhydroxide. The iron precipitates are always thickest where the most abundant microbial growth occurs, and the porous, cellular structure of some of the thicker precipitates are patterned after the gross morphology of the microorganisms.

Isolation of the Iron-Oxidizing Bacterium: *Thiobacillus ferrooxidans*

Identification of a particular species of microorganism requires selective enrichment in an appropriate medium and evidence of morphological

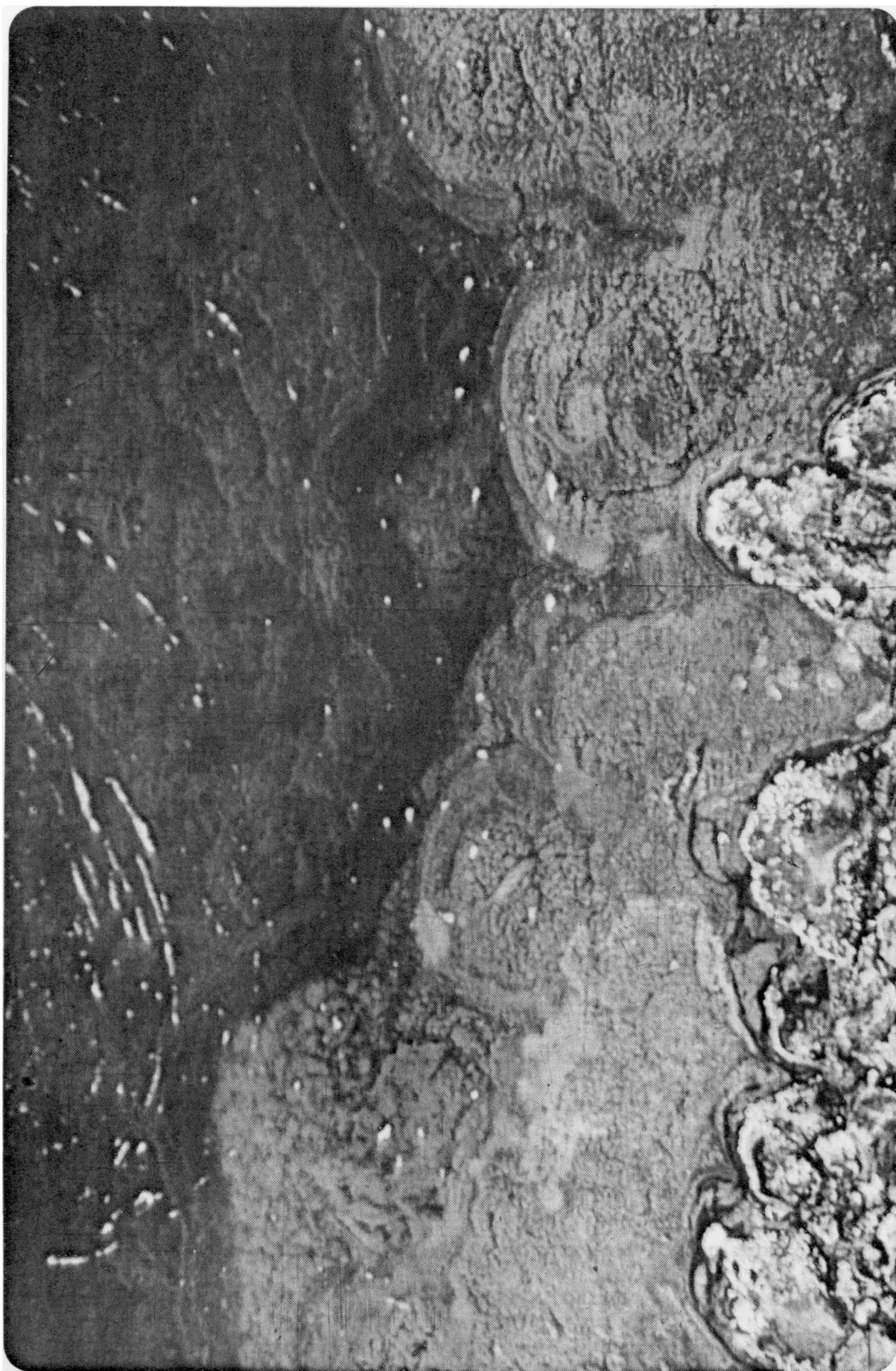


Plate 4. Mosslike clumps of green algae growing at base of Spring Creek Dam outlet; clumps are 10 to 15 cm in diameter.

and physiological characteristics comparable to the known characteristics for that species. The chemoautotrophic iron bacterium, *Thiobacillus ferrooxidans*, is the only bacterium known to oxidize ferrous iron to ferric at pH values less than 3.5 and can be readily enriched in the widely used 9 K medium developed by Silverman and Lundgren (1959). The composition of 9 K medium is given in table 7.

Slime streamers from Boulder Creek were collected in sterile containers and stored in a chilled icebox. About 20 ml of the slime were split between two 250 ml erlenmeyer flasks, and 125 ml of 9 K was added to each. The flasks were capped with cotton gauze and the solutions allowed to oxidize for one week in a gyratory shaker at ambient temperature. The solutions turned red brown, and microscopic examination revealed the presence of numerous rods about 0.5 by 1 to 3 μm fitting the description of *T. ferrooxidans*. Before inoculation, the slime itself showed the presence of thousands of rod-shaped cells of the same size and shape as *T. ferrooxidans*, but only a few were obviously motile. The bacilli were held in a fibrous network of extracellular material fitting very closely the description of the acid polysaccharide exopolymer fibrils mentioned by Dugan and others (1970b). This fibrous network clearly makes up the bulk of the slime and is probably excreted by a gram-positive heterotrophic *Bacillus* sp. (Dugan and others, 1970b), possibly *Bacillus cereus* (P. Dugan, pers. commun., quoted to G. Ehrlich). Several forms of diatoms and some filamentous fungi were also observed in the slime.

Five 250 ml erlenmeyer flasks were prepared for an iron oxidation rate study of the microbes in 9 K medium. Flasks A and B were kept as sterile controls; flask A contained 9 K medium only and flask B

Table 7
Composition of 9 K Medium

<u>Reagent</u>	<u>Amount (g)</u>
$(\text{NH}_4)_2\text{SO}_4$ or	3
$\text{Fe}(\text{NH}_4)_2(\text{SO}_4)_2 \cdot 6\text{H}_2\text{O}$	6.86
KCl	0.1
$\text{K}_2\text{HPO}_4 \cdot 3\text{H}_2\text{O}$	0.65
$\text{MgSO}_4 \cdot 7\text{H}_2\text{O}$	0.5
$\text{Ca}(\text{NO}_3)_2$	0.01
deion. H_2O	to 700 ml
36 N H_2SO_4	added dropwise to approximate pH
$\text{FeSO}_4 \cdot 7\text{H}_2\text{O}$	45
deion. H_2O	to 1 l

contained 9 K inoculated with 2 ml of the autoclaved enrichment. The next three flasks, C, D and E, were inoculated with 2, 2 and 10 ml, respectively, of the previous enrichment. Flasks C and D were adjusted to pH values of 2.0 and 2.7. All flasks contained 100 ml of 9 K, were placed in a gyratory shaker in a constant temperature water bath at 25°C, and were monitored by measuring pH, Eh and ferrous iron. pH was measured with a combination electrode on a Sargent-Welch three rheostat pH meter, Eh was measured with an Orion combination platinum electrode, and ferrous iron was determined using the orthophenanthroline method as written in *Standard Methods of Water and Wastewater Analysis* (1971). Ferrous values below 500 mg/l were determined by the modified Ferrozine method (Nelson and others, 1976, in prep.).

The results, shown in figure 5, follow the expected exponential rate curve for bacterial catalysis of iron oxidation. The rate of change of ferrous iron concentration is not a function of the ferrous iron concentration but rather of the concentration of bacterial cells. Sterile control flasks A and B showed no significant changes in ferrous iron during the period of the study. Silverman and Lundgren (1959) and Lundgren and others (1964) have shown that the growth rate of cells parallels the increase in ferric iron concentration. In figure 6, I have plotted the data points from Lundgren and others (1964) to show the linear dependence of the ferric iron concentration on the \log_{10} cells/ml. The discrepancy at low cell count may be due to the increased inaccuracy of the Petroff-Hausser counting technique as the detection limit of 1×10^6 cells/ml is approached. From this type of a plot, an estimate of the bacterial growth rate can be made. Unlike Silverman and Lundgren (1959) I did not autoclave the ferrous sulfate solution

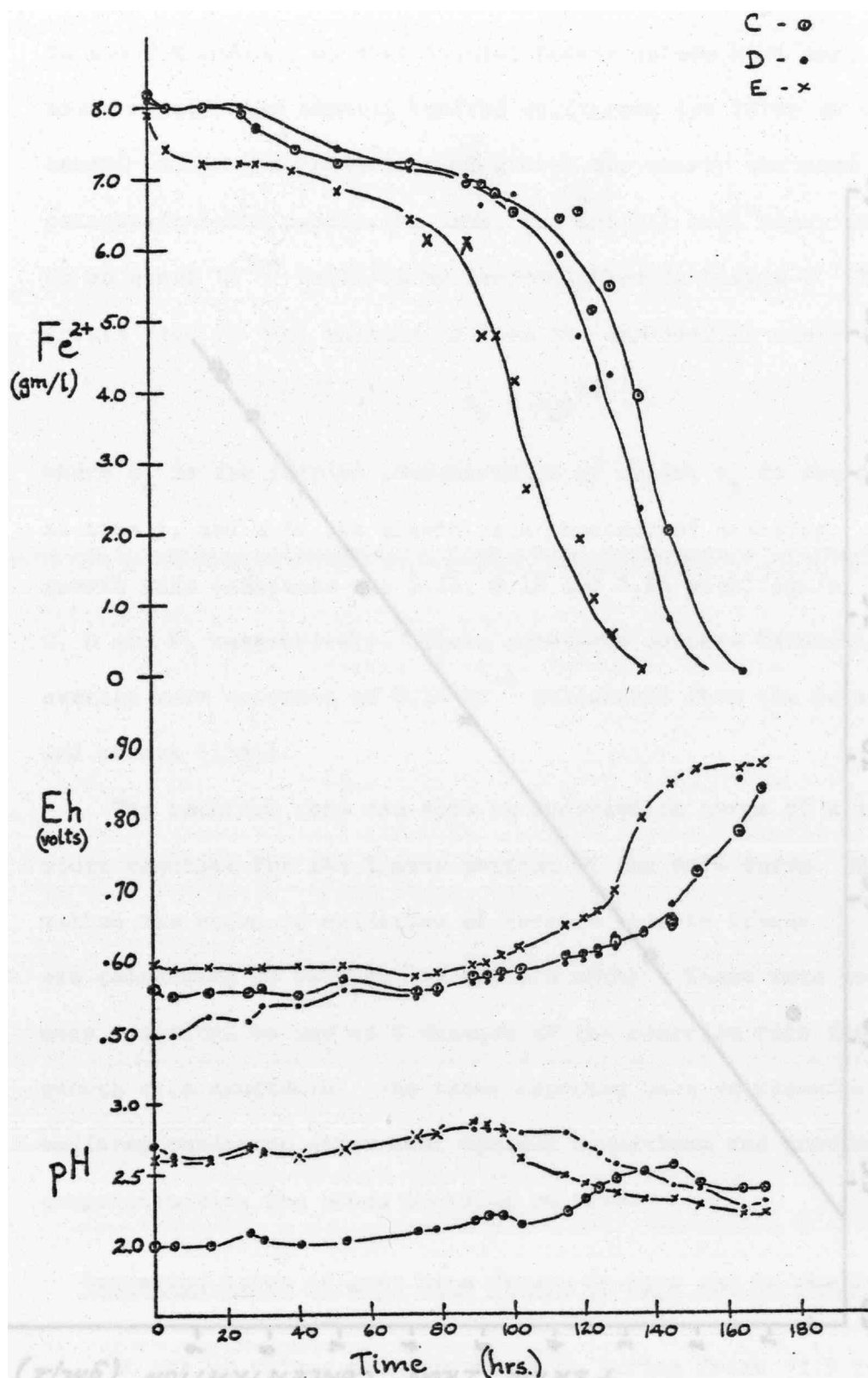


Figure 5. Change in ferrous iron, Eh and pH during oxidation of 9 K culture media by *T. ferrooxidans*.

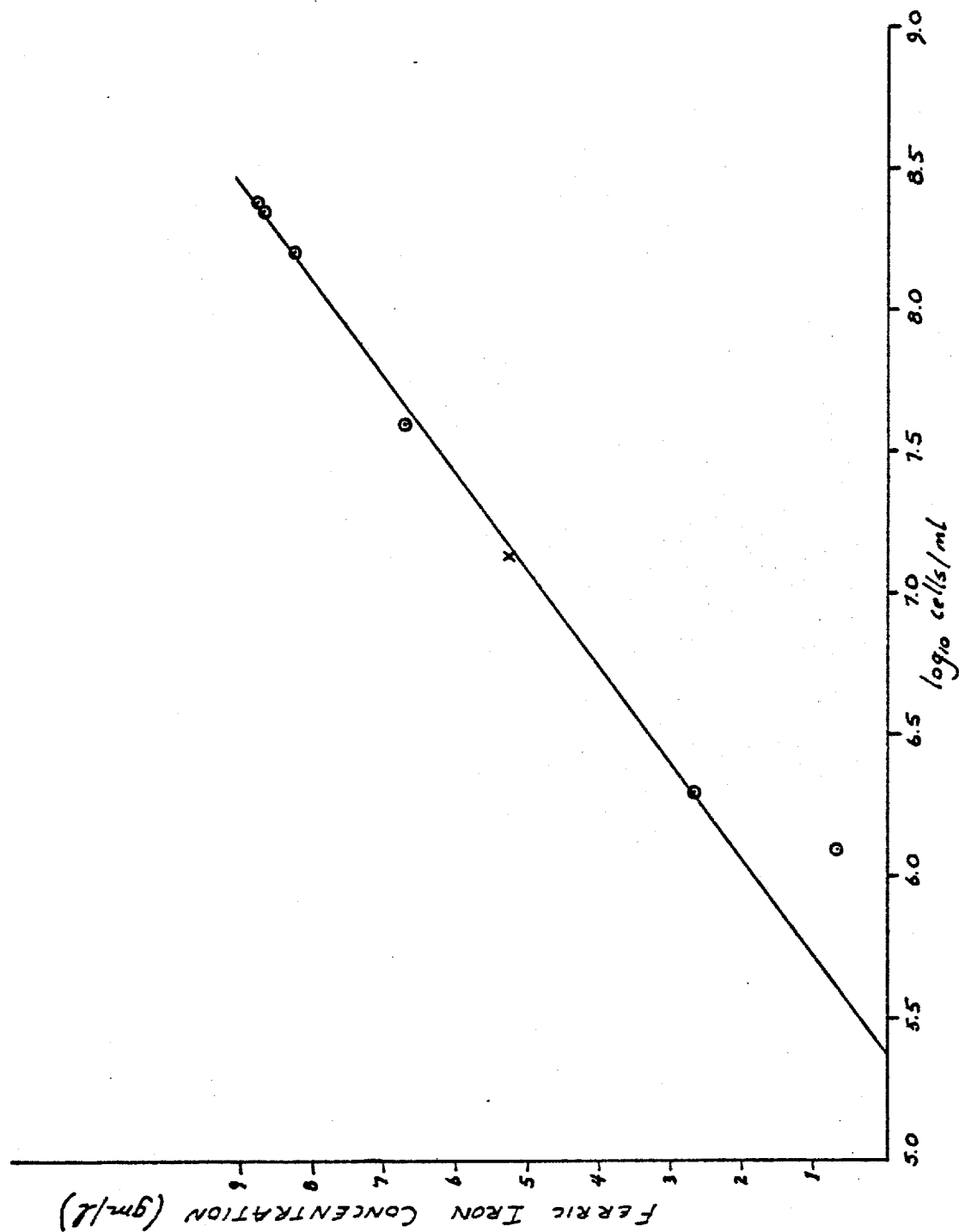


Figure 6. Dependence of ferric iron concentration on bacterial cell count. Circles plotted from data of Lundgren and others (1964); x is a point taken from the fitted curves of the same reference.

in the 9 K medium, so that initial ferric values were zero in this study rather than several hundred milligrams per liter as in their study. Since the conditions of growth are nearly the same and the percent inoculum nearly the same, the initial cell count is assumed to be about $10^{5.4}$ cells/ml by extrapolation in figure 6. The average growth rate is then calculated from the exponential expression:

$$x_t = x_0 e^{kt}$$

where x_0 is the initial concentration of cells, x_t is the concentration at time t , and k is the growth rate constant of doubling. The average growth rate constants are 0.18, 0.18 and 0.14 doublings/hr for samples C, D and E, respectively. These constants compare favorably with an average rate constant of 0.14 hr^{-1} calculated from the data of Lundgren and others (1964).

The reaction rate can also be analyzed in terms of a simple zero order reaction for the linear portion of the rate curve. By this method the rates of oxidation of ferrous iron in flasks C, D and E are calculated to be 3.4, 2.9 and 2.5 mM/hr. These rate constants are more practical to use as a measure of the reaction rate than the growth rate constants. The rates reported here represent bacterially mediated oxidation under near optimal conditions and provide a valuable comparison with the rates measured on site.

Oxidation Rates of Acid Mine Waters on Site and in the Laboratory

At the pH values normally found in Spring Creek (2.5 to 3.0, below the Boulder Creek confluence), the rate of ferrous iron oxidation has been measured at 1.4×10^{-5} mM/hr at 25°C in the absence of bacteria

(Singer and Stumm, 1970). The iron-oxidizing bacterium, *T. ferrooxidans*, catalyzes this reaction by five to six orders of magnitude. Lundgren and others (1964) present data on the growth of *T. ferrooxidans* in 9 K medium which indicates a rate constant of 3 mM/hr, more than five orders of magnitude greater than the inorganic rate. There are numerous reports testifying to the presence of iron-oxidizing bacteria in acid mine drainage, but no one has measured the *actual* oxidation rate on site. The purpose of the present study is to determine the rate constant for acid mine waters *in the stream environment* and to compare this rate with the optimal rate measured in batch culture using 9 K medium.

During the dry season (June to November), Spring Creek develops a strong rust-red appearance due to the high ferric iron concentrations (see pl. 5). Proceeding from site J downstream to site K, an increase in color intensity may often be observed. As an example of the amount of iron oxidation taking place, the ferrous iron decreased from 670 mg/l at site J to 6.1 mg/l at site N (3.9 km downstream) on August 15, 1975. This color change also correlates with the decrease in bacterial population, implying that ferrous iron is essential for the growth of these microbiota.

To determine on-site oxidation rates, seven sample sites were chosen from J to K at approximately equal intervals. The sites were labeled J1, J2, J3, J4, J5, K and N, and their locations are identified in figure 7. Samples were collected in the routine manner for all major constituents. Ten days after the samples had been collected, a mild rainstorm occurred, diluting the solute concentrations and washing out a major portion of the bacteria. The sampling was



Plate 5. Intense red-brown color of Spring Creek between sites J and K caused by the oxidation and hydrolysis of high dissolved iron concentrations.

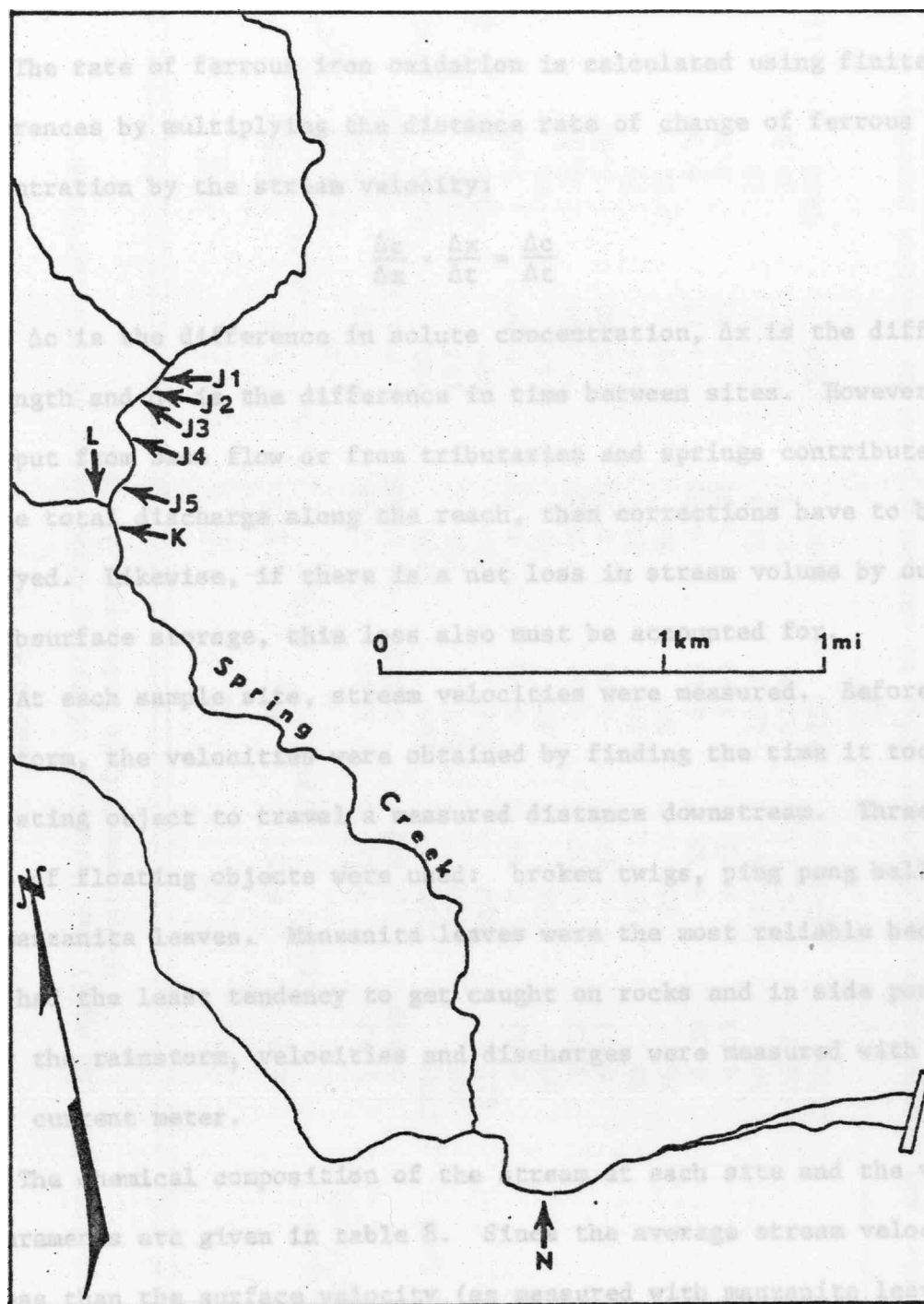


Figure 7. Location of sample sites for iron oxidation study (drawn from a high altitude aerial photo).

repeated to determine the effects of dilution and decreased bacterial activity.

The rate of ferrous iron oxidation is calculated using finite differences by multiplying the distance rate of change of ferrous iron concentration by the stream velocity:

$$\frac{\Delta c}{\Delta x} \cdot \frac{\Delta x}{\Delta t} = \frac{\Delta c}{\Delta t} \quad (1)$$

where Δc is the difference in solute concentration, Δx is the difference in length and Δt is the difference in time between sites. However, if input from base flow or from tributaries and springs contributes to the total discharge along the reach, then corrections have to be employed. Likewise, if there is a net loss in stream volume by outflow to subsurface storage, this loss also must be accounted for.

At each sample site, stream velocities were measured. Before the rainstorm, the velocities were obtained by finding the time it took a floating object to travel a measured distance downstream. Three types of floating objects were used: broken twigs, ping pong balls and manzanita leaves. Manzanita leaves were the most reliable because they had the least tendency to get caught on rocks and in side pools. After the rainstorm, velocities and discharges were measured with a Pygmy current meter.

The chemical composition of the stream at each site and the velocity measurements are given in table 8. Since the average stream velocity is less than the surface velocity (as measured with manzanita leaves) a correction factor had to be used. For streams having very high width to depth ratios, like Spring Creek, the average velocity would generally be 80 to 90 percent of the surface velocity near the stream's

Table 8a

Composition (in mg/l) and Velocity¹ of Spring Creek Water at Selected Sites
Downstream Before Rainstorm, 11/26/75

	<u>J1</u>	<u>J2</u>	<u>J3</u>	<u>J4</u>	<u>J5</u>	<u>K</u>	<u>N</u>
T(°C)	8.3	8.2	8.4	9.5	6.8	6.5	7.0
Velocity (ft/sec)	0.64	0.30	0.70	0.71	0.55	1.0	
Discharge (ft ³ /sec)					(4)	(4.2)	(5.4)
pH	2.40	2.45	2.46	2.48	2.53	2.62	2.61
Eh (v)	0.639	0.647	0.650	0.661	0.673	0.693	0.774
Conductivity (μS)	3350	3230	3140	2970	2720	2670	2080
Fe ²⁺	300	278	267	234	182	140	4.9
Total Fe	412	400	396	392	386	360	252
Cu	0.80	0.75	0.75	0.75	0.80	5.57	4.80
Zn	50	50	50	49	48	46	37
Cd	0.37	0.37	0.37	0.37	0.37	0.33	0.28
Mn	0.97	0.97	0.96	0.95	0.96	1.56	1.35
Al	50	50	50	49	49	70	57
SiO ₂	26	26	26	26	26	32	33
Na	6.30	6.30	6.15	6.15	6.15	6.30	6.68
K	4.05	4.01	3.94	3.95	3.88	3.35	2.90
Ca	19	18.5	18.3	18.3	18.3	22	21
Mg	28.7	28.1	27.8	27.5	27.6	39.5	34.2
SO ₄	1420	1440	1410	1400	1390	1400	1260

¹Velocities and discharges in parentheses refer to estimates based on previous records.

Table 8b

Composition (in mg/l) and Velocity¹ of Spring Creek Water at Selected Sites
Downstream After Rainstorm, 6/12/75

	<u>J1</u>	<u>J2</u>	<u>J4</u>	<u>J5</u>	<u>K</u>	<u>N</u>
T(°C)	9.5	(1.0)	9.5	9.0	9.0	9.5
Velocity (ft/sec)			1.0		1.8	
Discharge (ft ³ /sec)						
pH	2.90	15	18	18	20	19
Eh (v)	0.663	2.90	2.90	2.90	2.90	2.88
Conductivity (μS)	0.661	0.661	0.668	0.669	0.676	0.689
Fe ²⁺	1148	1148	1102	1040	1038	1040
Total Fe	55	52	49	42	31	18
Cu	100	102	100	93	84	77
Zn	0.68	0.70	0.72	0.67	2.25	1.95
Cd	12	12	12	11	10	10
Mn	0.084	0.084	0.084	0.084	0.083	0.078
Al	0.37	0.37	0.37	0.36	0.53	0.50
SiO ₂	17	17	17	17	22	21
Na	16	16	16	16	18	18
K	3.30	3.30	3.30	3.30	3.48	4.05
Ca	1.06	1.05	1.10	1.09	1.05	0.88
Mg	8.5	8.5	8.5	8.5	10	10
SO ₄	9.5	9.5	9.5	9.0	13	12
	431	431	443	414	447	437

center (Morisawa, 1968). The manzanita leaves would probably give a slightly lower velocity than the true surface value because of their surface tension, wind resistance, and tendency to catch on rocks or floating debris. Thus, the average velocity was taken as 90 percent of the measured surface velocity.

Discharge measurements along the reach from J1 to K show that at different times of the year there is no detectable change in volume flow except from J5 to K, which is due to the input from Slickrock Creek. Solute concentrations (except iron) are also constant, within analytical error, between J1 and J5 as shown in table 8. Ferrous iron decreases from oxidation, and total iron decreases due to hydrolysis and precipitation of ferric iron. Changes in discharge and solute concentrations between J5 and K may be balanced by considering the input from L by the equation:

$$C_K Q_K = C_{J5} Q_{J5} + C_L Q_L \quad (2)$$

where C_K , C_{J5} and C_L are the solute concentrations at sites K, J5 and L, respectively, and Q_K , Q_{J5} and Q_L are the respective discharges. By subtracting the mass rate of ferrous iron flow at Slickrock from the total at site K, the true change in ferrous iron between J5 and K can be obtained. A small amount of oxidation of ferrous iron from L also occurs before sampling at K. This additional oxidation was calculated by assuming the same rate as measured between sites J4 and J5. As a sample calculation, on December 6, 1975, 7 mg/l of ferrous iron oxidized over a distance of 730 ft between J4 and J5. The average velocity for this section of the reach was 1.0 ft/sec giving an oxidation rate of:

$$\frac{\Delta c}{\Delta x} \cdot \frac{\Delta x}{\Delta t} = \frac{(7 \text{ mg/l})(1.0 \text{ ft/sec})(3600 \text{ sec/hr})}{(730 \text{ ft})(56 \text{ mg/mole})} = 0.62 \text{ mM/hr}$$

The oxidation rates for sites J1 through J5, shown in table 9, were calculated by this method. Assuming 0.62 mM/hr is a reasonable rate for the change in ferrous iron coming from site L to site K (a distance of 120 ft) and using 0.53 ft/sec as the average velocity (as measured at K), the expected ferrous iron would be:

$$C_L - \frac{\Delta c}{\Delta t} \cdot \frac{\Delta x}{v} = \frac{(9.48 \text{ mg/l})}{(56 \text{ mg/mole})} - \frac{(0.62 \text{ mM/hr})(120 \text{ ft})}{(0.53 \text{ ft/sec})(3600 \text{ sec/hr})}$$

$$= 0.130 \text{ mM or } 7.38 \text{ mg/l.}$$

Since the total ferrous iron at K is 31 mg/l, the amount carried through from J5 should be:

$$\frac{C_K Q_K - C_L Q_L}{Q_{J5}} = \frac{(31 \text{ mg/l})(20 \text{ ft/sec}) - (7.28 \text{ mg/l})(1.54 \text{ ft/sec})}{18.5 \text{ ft/sec}}$$

$$= 33 \text{ mg/l}$$

so that the actual decrease in ferrous iron from J5 to K is 9 mg/l rather than 11 mg/l. Solutes normally present as trace elements (copper, zinc, cadmium, manganese and aluminum) all show a slight decrease in concentration between sites K and N. The ferrous iron was assumed to be diluted by the same amount, so that for purposes of calculating rate constants, values of 6 mg/l on November 26, 1975, and 20 mg/l on December 6, 1975, were used. This dilution results from the input of South Fork Spring Creek, a relatively clean stream with a small flow in the dry season.

The results in table 9 show several interesting features. First there is a marked contrast in rate constants before and after a rain-storm. Although the oxidation rates after the rains are still greater than those predicted from laboratory studies of inorganic rates, the

Table 9
On-Site Ferrous Iron Oxidation Rates Before
and After a Rainstorm

<u>Site intervals</u>	<u>$\Delta c/\Delta x$ (mg/l/ft)</u>	<u>$\Delta x/\Delta t$ (ft/sec)</u>	<u>$\Delta c/\Delta t$ (mM/hr)</u>
11-26-75			
J1-J2	0.073	0.64	3.02
J2-J3	0.055	0.30	1.03
J3-J4	0.078	0.70	3.54
J4-J5	0.071	0.71	3.21
J5-K	0.146	0.55	5.14
K-N	0.013	0.013	<u>0.84</u>
Average			2.80
12-6-75			
J1-J2	0.010	1.0	0.64
J2-J4	0.0046	0.88	0.26
J4-J5	0.0096	1.0	0.62
J5-K	0.038	0.76	1.86
K-N	0.001	1.8	<u>0.12</u>
Average			0.70

average rate is only one-fourth the magnitude of the average rate before the washout. Precipitation of greater intensity would decrease the rate even more dramatically. Microbial mediation of iron oxidation would never halt, however, as long as the Richmond-Hornet effluent continued to discharge into Boulder Creek. This effluent is probably the largest single source of iron-oxidizing bacteria.

The average rate of oxidation before the rainstorm, 2.8 mM/hr, is comparable to the average rate of 2.9 mM/hr measured in 9 K medium. Physicochemical conditions of growth appear to be near optimal for *T. ferrooxidans*. The only other published report on iron oxidation rates measured on site is contained in Singer and Stumm (1970); they did not measure stream velocities but did estimate a doubling time of 0.11 hr^{-1} from the decrease in ferrous iron vs. time in water samples collected from the Mercer seam near Elkins, West Virginia. This doubling rate is only slightly less than those measured by Silverman and Lundgren (1959), Lundgren and others (1964) and in this study.

It is interesting to note that near site J, both before and after the rainstorm, there is a marked decrease in the oxidation rate while there is an increase between sites J5 and K. The decrease seen between sites K and N is due to the decrease in the ferrous iron available to the microorganisms and the observed absence of macroscopic signs of slime growth near site N. The decrease in oxidation rate near site J is not so easily explained. Just upstream from site J is a thick growth of oak trees whose limbs and leaves crowd over, into and above the stream. In fact, the stream is always completely shaded there, unlike the rest of Spring Creek. Since oak bark and leaves are noted for their production of tannin which is water soluble (Tannin, 1911;

Tannin, 1958) and for their reduction of ferric iron (Morgan and Stumm, 1965), it is proposed that the leaching of tannin at this point in the stream complexes with and fixes a portion of the ferrous iron, thereby slowing down its oxidation rate. Hem (1960) has demonstrated the ability of tannic acid to complex with ferrous iron and slow down its oxidation rate. In Boulder Creek, the leached oak tannin drips on stream boulders and reacts with the dissolved iron in the stream to form a dark pigment causing black streaks. The same reaction occurs when fresh oak leaves are vigorously mixed with acid mine drainage from Boulder Creek, and even the stream water becomes blackened at certain times of the year from iron-tannin complexes. Hem (1960) found a similar black pigment when he mixed ferric iron with tannic acid and he described the precipitate as a ferric tannate. Tannin is composed chiefly of tannic and gallic acids which form dark and colored pigments when mixed with soluble ferrous and ferric salts (Tannin, 1958).

The increase in oxidation rate between J5 and K may be due to the greater growth rate of bacteria in the slower moving waters at site K (stream velocity is about 0.53 ft/sec and may be a maximum value).

Attempts to sample Spring Creek and allow the sample to oxidize in the lab were unsuccessful because even with chilled storage the samples did not have sufficient ferrous iron left for an appropriate study. Effluent from the Richmond and Hornet mines was successfully stored, and figure 8 portrays the rate of oxidation in a laboratory where ambient air temperatures were kept constant at 25°C. Flasks A and B were unfiltered samples collected on January 18, 1976, and stored

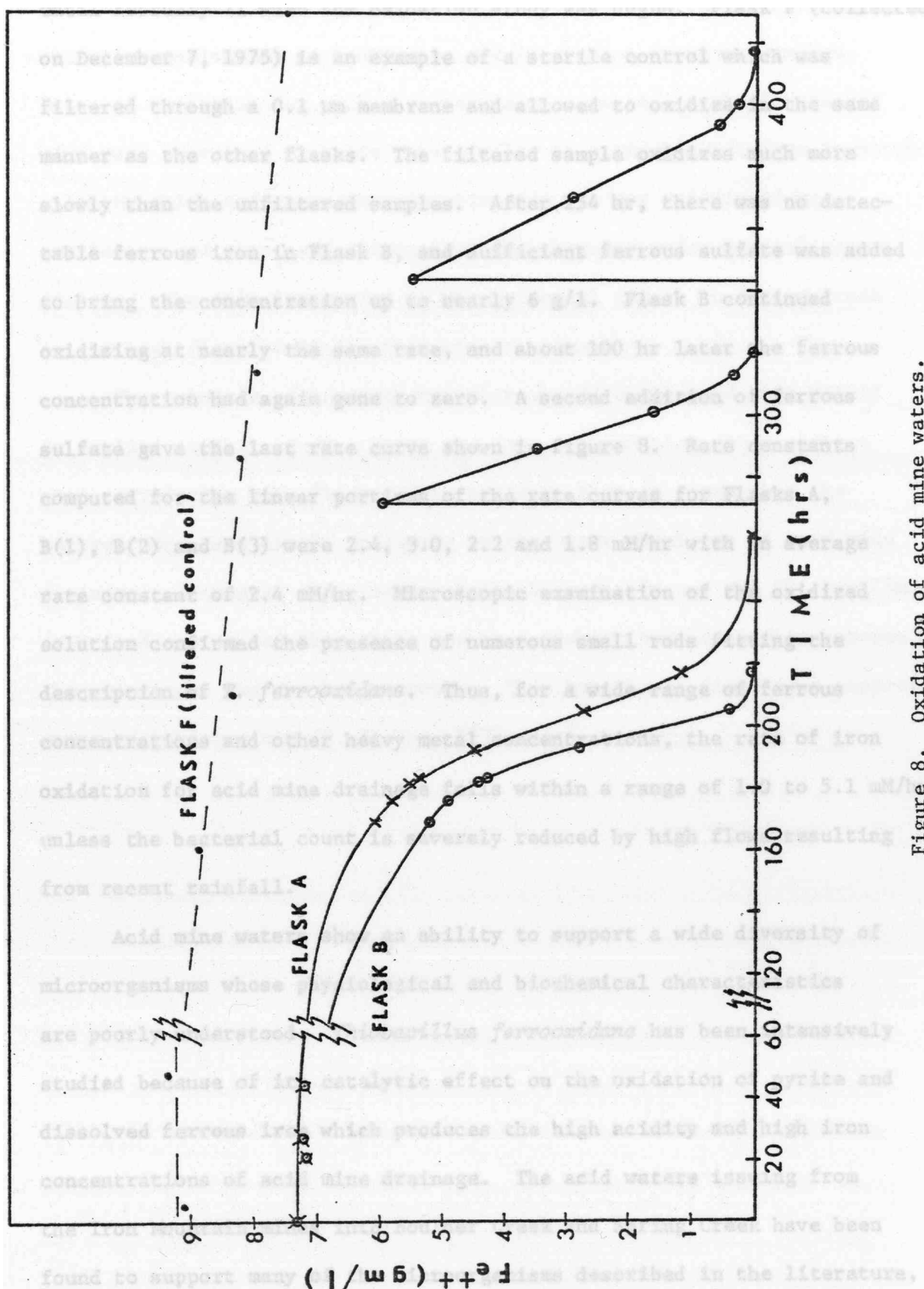


Figure 8. Oxidation of acid mine waters.

until February 21 when the oxidation study was begun. Flask F (collected on December 7, 1975) is an example of a sterile control which was filtered through a 0.1 μ m membrane and allowed to oxidize in the same manner as the other flasks. The filtered sample oxidizes much more slowly than the unfiltered samples. After 254 hr, there was no detectable ferrous iron in Flask B, and sufficient ferrous sulfate was added to bring the concentration up to nearly 6 g/l. Flask B continued oxidizing at nearly the same rate, and about 100 hr later the ferrous concentration had again gone to zero. A second addition of ferrous sulfate gave the last rate curve shown in figure 8. Rate constants computed for the linear portions of the rate curves for Flasks A, B(1), B(2) and B(3) were 2.4, 3.0, 2.2 and 1.8 mM/hr with an average rate constant of 2.4 mM/hr. Microscopic examination of the oxidized solution confirmed the presence of numerous small rods fitting the description of *T. ferrooxidans*. Thus, for a wide range of ferrous concentrations and other heavy metal concentrations, the rate of iron oxidation for acid mine drainage falls within a range of 1.0 to 5.1 mM/hr unless the bacterial count is severely reduced by high flows resulting from recent rainfall.

Acid mine waters show an ability to support a wide diversity of microorganisms whose physiological and biochemical characteristics are poorly understood. *Thiobacillus ferrooxidans* has been intensively studied because of its catalytic effect on the oxidation of pyrite and dissolved ferrous iron which produces the high acidity and high iron concentrations of acid mine drainage. The acid waters issuing from the Iron Mountain mines into Boulder Creek and Spring Creek have been found to support many of the microorganisms described in the literature,

and *Thiobacillus ferrooxidans* has been isolated from the drainage by selective enrichment in 9 K medium and incubation in water samples. Rates of oxidation for acid mine waters on site and in the laboratory give rate constants that are very similar to optimal conditions in batch culture, which indicates that the bacteria are not restricted by nutrients, and they maintain optimal growth rates under natural conditions. The only limitation to the bacterial growth in Spring Creek is the high flows resulting from winter rains.

The presence of numerous heterotrophs in these acid mine waters is implied in this study. Since the data on oxidation rates shows a good correlation with *Thiobacillus* activity then it seems that the heterotrophs have little influence on the water chemistry of acid mine drainage. I suggest that the heterotrophs probably use the *Thiobacillus* as a food source and that there may be a symbiotic relationship between the autotrophs and the heterotrophs. This hypothesis finds some support among microbiologists (R. F. Unz, 1976, pers. commun.).

OXIDATION-REDUCTION EQUILIBRIA IN ACID MINE WATERS

Eh Measurements in Natural Waters: Equilibria or Disequilibria?

The measured potential, or Eh, of natural waters has been used (1) qualitatively, as an operational parameter, and (2) quantitatively, as an indication of a dominant redox couple. The qualitative use of Eh was originally advocated by ZoBell (1946) and has resulted in a great many measurements (see Baas-Becking and others, 1960). As a quantitative tool, the use of Eh has not enjoyed a widespread success. Several criteria must be met before the Eh can be properly related to a redox couple: (1) the net exchange current at the electrode-solution interface must be zero (an equilibrium criterion required for the application of the Nernst equation), (2) a single redox couple must be dominant in the system so that "mixed potentials" are not measured, (3) the electrode surface should be free of electroactive impurities, (4) no redox-controlling reactions must be allowed between the electrode surface and the sample solution, and (5) ionic strength and complex formation must be accounted for. These criteria are difficult to meet and have led to the skeptical outlook that most Eh measurements are not amenable to quantitative interpretation (Stumm, 1966; Morris and Stumm, 1967; Stumm and Morgan, 1970). Contamination of platinum electrode surfaces by oxygen and sulfur has been considered in a thermodynamic treatment by Whitfield (1974) as likely to cause deviations from expected values for both oxidizing and reducing environments. Furthermore, natural waters are often thought to contain concentrations of redox species too

low for reliable measurements. It is interesting to note, however, that no one has ever correctly compared an Eh measurement with an analyzed redox couple from an aquatic environment by computing the activity ratios of redox species *after taking the ionic strength and complex formation into account.*

Although a general pessimism pervades the study of Eh measurements in natural waters, several investigators have found good agreement between measured and calculated Eh values. Sato (1960) could relate the measured Eh and pH values of subsurface waters near oxidizing ore bodies to the oxygen-peroxide redox couple. Berner (1963) found that Eh measurements in anoxic marine sediments obeyed the Nernstian relationship:

$$Eh = -0.475 - 0.0295 \log a_{S^{2-}} \quad (1)$$

for the reaction



which demonstrated an equilibrium control of Eh in strongly reduced sediments. This redox control has been further substantiated by Skopintsev and others (1966) and Whitfield (1969). Doyle (1968) demonstrated the control of Nernstian potential by the ferrous-ferric oxide couple under certain conditions. Thorstenson (1970) found good agreement between the redox couples of sulfur and nitrogen species for five reducing marine environments, implying that a dominant couple is imposed on these systems and mixed potentials are not a significant problem. Natarajan and Iwasaki (1974) obtained meaningful Nernstian relationships of measured Eh with dissolved oxygen and with dissolved ferrous-ferric ratios in laboratory experiments which further suggests

there may be some control by oxygen of measured Eh values in natural oxidizing waters. Some support for this has been found in the observed trend of increasing Eh with increasing dissolved oxygen in hot spring overflows (E. A. Jenne, pers. commun.). Thus, amid the skepticism about Eh measurements, the evidence strongly suggests that redox equilibria are not only measureable but have quantitative, thermodynamic significance in several aquatic environments.

Acid mine drainage is a type of water that should be well suited to quantitative Eh interpretation. The dominant redox couple is ferrous-ferric iron with both oxidation states present in relatively high concentrations, and the low pH values help to stabilize the system and prevent surface coatings of ferric oxide or other possible contaminants on the electrodes (e.g. Doyle, 1968).

Experimental Method

Potential measurements were made in the field with an Orion combination redox electrode connected to a Sargent-Welch portable pH meter. Millivolt readings could be estimated to the nearest millivolt, but precision is no better than ± 2.5 mv. The accuracy is no better than ± 5 mv based on potential measurements in ZoBell's solution. Ferrous iron was analyzed by a modified Ferrozine method (Nelson and others, 1976) on samples which were filtered through $0.1 \mu\text{m}$ membranes and acidified with concentrated HCl in the field. Precision errors for this method are less than 5 percent. Total iron was determined by atomic absorption spectrometry using standard flame techniques on a Perkin-Elmer Model 306. Samples collected for total iron were similarly filtered and acidified. Ferric iron was obtained by difference.

Eh values were obtained by adding the potential of the field measurements to the half-cell potential for the Orion reference electrode. Since Orion did not specify the half-cell potential of their electrodes, an investigation was made to determine this potential. The measurements were made by using ZoBell's solution (ZoBell, 1946) and, as an aside, the redox chemistry of ZoBell's solution was determined.

The Redox Chemistry of ZoBell's Solution

The oxidation-reduction equilibria of ZoBell's solution, a stable aqueous solution of potassium ferro-ferricyanide, was investigated during the determination of the Orion half-cell reference potential. The reference electrode was built into the Orion combination redox electrode, and no direct information on its properties was available. Instead of attempting to substitute a reference electrode of known properties for the built-in electrode, measurements were made in ZoBell's solution (ZoBell, 1946) using the Orion electrode and a separate platinum/silver, silver chloride cell. The solution of ZoBell was chosen because (1) the Eh of 430 mv at 25°C has been carefully determined (ZoBell, 1946), (2) it is a very stable redox solution due to strong complex formation, (3) it has been in popular use to check the performance of redox electrodes (Garrels and Christ, 1965) and (4) although Garrels (1960) and Langmuir (1971) both report temperature dependent equations for the Eh of ZoBell's solution no sources of data are given. Thus, measurements of this system may be of use to others as well.

The temperature dependence of the Eh for ZoBell's solution (0.0033 M $K_4Fe(CN)_6$, 0.0033 M $K_3Fe(CN)_6$ and 0.1 M KCl) was measured

with a Radiometer platinum electrode and a sat. KCl Ag/AgCl reference electrode. Two Orion combination electrodes accompanied the Pt and Ag/AgCl electrodes in a 400 ml beaker fitted with a polypropylene lid. The lid contained holes just large enough to allow the electrodes and a platinum resistance thermometer to fit in it. The beaker was filled with nearly 300 ml of freshly prepared ZoBell's solution and a teflon stirring bar was placed in the bottom. The beaker-electrode assembly was placed on a magnetic stirrer in an insulated water bath. The water bath contained a cooling coil regulated by a Polytemp Unit and a Tecam heating and stirring unit which, together, provided temperature regulation for the range 8° to 85°C. Temperatures could be read to the nearest hundredth part of a degree centigrade with a N.B.S. calibrated platinum resistance thermometer. The average error in the temperature measurement is estimated at $\pm 0.02^\circ\text{C}$. Potentials were measured with a Keithley 190 Digital Multimeter which could be read to a hundredth of a millivolt.

At the beginning of each day of measurements, the ferro-ferricyanide solution was replenished with a fresh solution because slight oxidation had been observed in chilled solutions which were stored for several weeks. Since temperatures of 84°C were reached in this investigation, it was considered necessary to start with fresh solutions each day. Replicate temperatures reached on different days were found to give potential readings that agreed to 0.5 mv.

The emf of ZoBells' solution as measured by the three electrode pairs is plotted as a function of temperature in figure 9 (the data is given in Appendix II). The potentials are linear up to about 60°C and since most measurements of cell potentials by other investigators

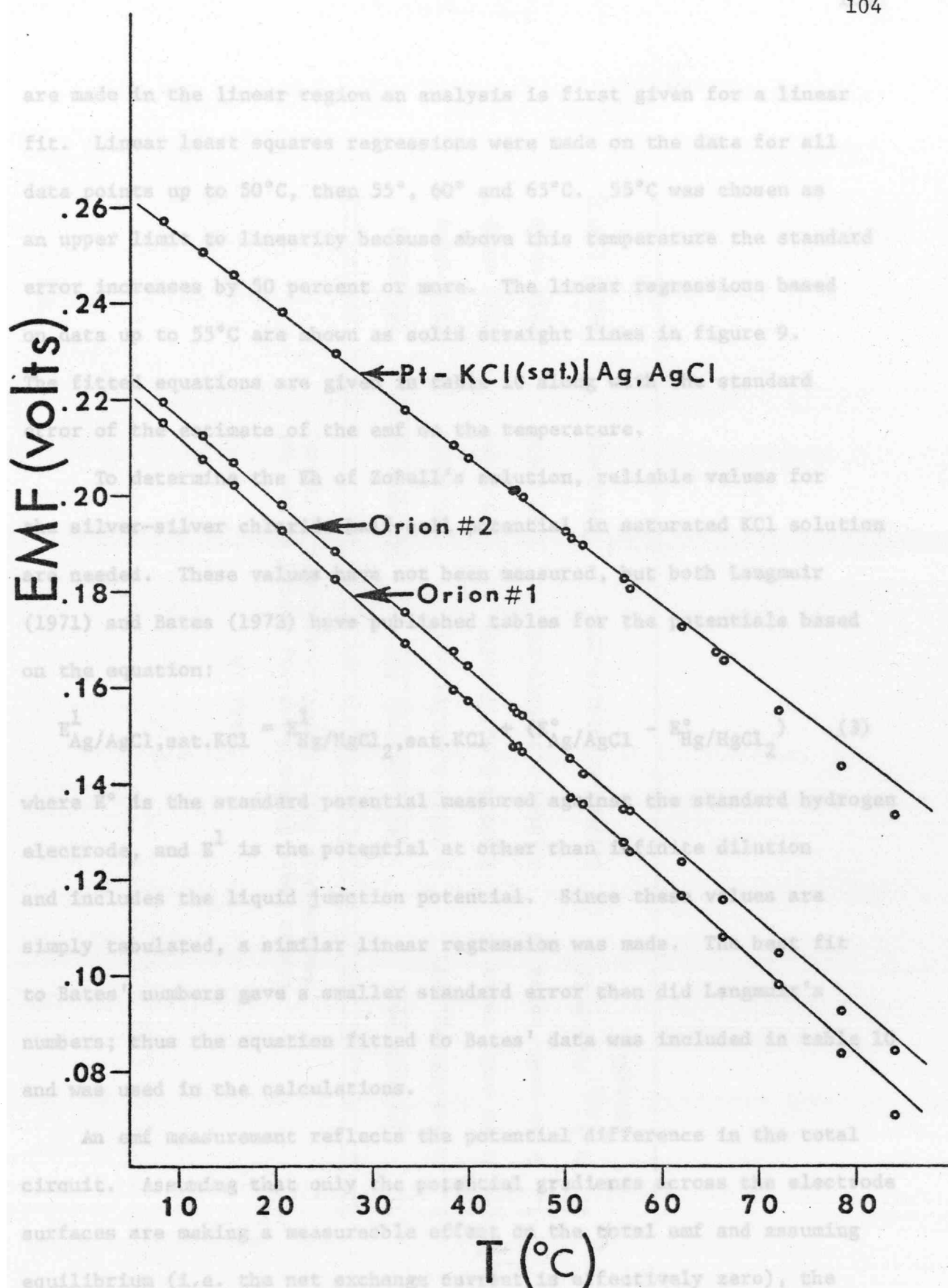


Figure 9. Measured potentials of ZoBell's solution.

are made in the linear region an analysis is first given for a linear fit. Linear least squares regressions were made on the data for all data points up to 50°C, then 55°, 60° and 65°C. 55°C was chosen as an upper limit to linearity because above this temperature the standard error increases by 50 percent or more. The linear regressions based on data up to 55°C are shown as solid straight lines in figure 9. The fitted equations are given in table 10 along with the standard error of the estimate of the emf on the temperature.

To determine the Eh of ZoBell's solution, reliable values for the silver-silver chloride half-cell potential in saturated KCl solution are needed. These values have not been measured, but both Langmuir (1971) and Bates (1973) have published tables for the potentials based on the equation:

$$E_{\text{Ag/AgCl, sat.KCl}}^1 = E_{\text{Hg/HgCl}_2, \text{sat.KCl}}^1 + (E_{\text{Ag/AgCl}}^\circ - E_{\text{Hg/HgCl}_2}^\circ) \quad (3)$$

where E° is the standard potential measured against the standard hydrogen electrode, and E^1 is the potential at other than infinite dilution and includes the liquid junction potential. Since these values are simply tabulated, a similar linear regression was made. The best fit to Bates' numbers gave a smaller standard error than did Langmuir's numbers; thus the equation fitted to Bates' data was included in table 10 and was used in the calculations.

An emf measurement reflects the potential difference in the total circuit. Assuming that only the potential gradients across the electrode surfaces are making a measureable effect on the total emf and assuming equilibrium (i.e. the net exchange current is effectively zero), the emf is the sum of the half-cell potentials:

Table 10

Linear Least Square Equations Fitted to the Emf
Measurements for $T < 55^{\circ}\text{C}$ (potentials in volts)

<u>Electrode pair</u>	<u>Emf, analytic fit</u>	<u>Standard error</u>	<u>Reference</u>
1. Pt/sat.KCl/Ag,AgCl	$0.23112 - 0.00156(T-25)$	± 0.00034	this study
2. Orion comb. redox #1	$0.19026 - 0.00177(T-25)$	± 0.00041	this study
3. Orion comb. redox #2	$0.18441 - 0.00185(T-25)$	± 0.00028	this study
4. Pt, $\text{H}_2(\text{g})$ /sat.KCl/ Ag,AgCl	$0.19881 - 0.00101(T-25)$	± 0.00014	Bates (1973)

$$E_{\text{total}} = E_{\text{solution/Pt}} + E_{\text{Ag/AgCl,sat.KCl}} \quad (4)$$

The Eh of ZoBell's solution is then obtained by subtracting the Ag/AgCl half-cell potential from the total measured emf. However, the sign must be changed on the reference half-cell potential, so that the potentials are consistent with the direction of electron flow in the circuit:

$$E_{\text{ZoBell}} = E_{\text{solution/Pt}} = E_{\text{total}} - (-E_{\text{Ag/AgCl,sat.KCl}}) \quad (5)$$

Thus the Eh is obtained by adding equations (1) and (4) in table 10 yielding:

$$E_{\text{ZoBell}} = 0.42993 - 0.00257 (T - 25) \quad (6)$$

where T is the temperature in degrees centigrade and the potential is in volts. At 25°C, this value is in excellent agreement with the value of 430 mv obtained by ZoBell (1946).

From equation (6), the half-cell potential for the two Orion electrodes can be calculated. This time the calculation is simply reversed:

$$E_{\text{Orion reference}} = E_{\text{ZoBell}} - E_{\text{total, Orion}} \quad (7)$$

The Orion combination redox electrode #1 gives a reference potential of:

$$E = 0.23967 - 0.00080 (T - 25) \quad (8)$$

and the Orion combination redox electrode #2 gives a reference potential of:

$$E = 0.24552 - 0.00072 (T - 25) \quad (9)$$

These two electrodes, although similar in construction, differ by about 6 mv. Two other Orion redox electrodes, one of which was brand new, were tested alongside these two at 21°C and gave potential readings

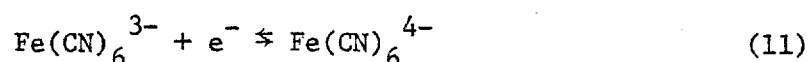
within 1 mv of the #2 electrode. From this comparison I suggest that the #1 electrode is slightly contaminated and that the #2 electrode more accurately represents the half-cell potential.

These half-cell potentials can now be used to calculate the correct Eh of water samples at the on-site temperature.

$$E_{\text{sample}} = E_{\text{Orion, field measurement}} + E_{\text{Orion, reference}} \quad (10)$$

The Eh of ZoBell's solution is determined by the activity ratio of the redox solute species, the aqueous ferrocyanide and ferricyanide ions. As a check on the accuracy of these Eh measurements, the Eh is calculated theoretically from a knowledge of the standard potential, complex formation and activity coefficient corrections.

The controlling redox equilibrium in ZoBell's solution is:



The standard electrode potential for this reaction at 25°C was first determined by the careful measurements of Kolthoff and Tomsicek (1935). Their value of 0.3560 v agrees quite well with the more recent determinations of Hanania and others (1967), who report 0.355 ± 0.001 v at 25°C. The latter investigators are further supported by the good agreement between Debye-Hückel calculations (including ion association) and their measured values for varying ionic strengths. Several other investigators have determined different values for the same couple (see Charlot, 1971). The most divergent values from those reported above are the potentials determined by Rock (1966) of 0.3704 ± 0.005 v and Murray and Rock (1968) of 0.3610 ± 0.005 v. The latter value was obtained by using cells without liquid junction potentials and is considered more accurate than the former value. Since the range of

standard potentials is only 6 mv, an average value of 0.358 v will be used. This value is further validated by the good agreement between the calculated and the measured E_h .

The Nernst equilibrium equation for the ferro-ferricyanide reaction is:

$$E_h = E^\circ (T, 1 \text{ atm}) - 2.303 \frac{RT}{F} \log \frac{[\text{Fe(CN)}_6^{4-}]}{[\text{Fe(CN)}_6^{3-}]} \quad (12)$$

where E_h is the measured electromotive force of the half-cell potential relative to the standard hydrogen electrode, E° is the standard potential at a reference temperature, T , and 1 atm pressure, R is the ideal gas constant, F is the faraday, and square brackets denote activities.

Equation (12) can be rewritten:

$$E_h = E^\circ - 0.059 \log \frac{(\text{Fe(CN)}_6^{4-})}{(\text{Fe(CN)}_6^{3-})} - 0.059 \log \frac{\gamma_2}{\gamma_1} \quad (13)$$

for $T = 25^\circ\text{C}$ where parentheses contain molar concentrations, γ_2 is the activity coefficient for the ferrocyanide ion and γ_1 is the activity coefficient for the ferricyanide ion. It is first assumed that in an equimolar potassium ferro-ferricyanide solution the concentration of the trivalent ferricyanide ion is equal to the concentration of tetravalent ferrocyanide ion. This assumption is equivalent to saying that ion association can be neglected and that the measured potential is strictly dependent upon the ionic strength. Equation (13) then becomes:

$$E_h = 0.358 - 0.059 \log \frac{\gamma_2}{\gamma_1} \quad (14)$$

Since the ionic strength of ZoBell's solution is slightly greater than 10^{-1} M, the Davies equation should be more reliable than the extended Debye-Huckel equation (Butler, 1964; Stumm and Morgan, 1970). Using the revised Davies equation:

$$\log \gamma = -Az^2 \left(\frac{I^{\frac{1}{2}}}{1 + I^{\frac{1}{2}}} - 0.3I \right) \quad (15)$$

$$\gamma_1 = 0.084 \text{ and } \gamma_2 = 0.012 \text{ for } 25^\circ\text{C},$$

where $A = 0.5085$, $I = 0.1528$ and z is the charge on the ion. Substituting these values into equation (14) gives:

$$E_h = 0.358 + 0.050 = 0.408.$$

This E_h value is 22 mv short of the measured potential, and it seems reasonable to assume that taking into account the small amount of complexing could make the agreement even better. Ferrocyanide ion is more strongly complexed than the ferricyanide ion, and this complexing would tend to decrease the ratio of the activities, thereby increasing the resultant potential.

Complex association reactions which can occur in the aqueous potassium ferro-ferricyanide system are given in table 11. Fortunately, the first and last pairs of reactions (K_1 , K_2 , K_5 and K_6) can be ignored because the equilibrium constants show that protonization is weak and that ferro- and ferricyanide ions are very strong complexes. Hanania and others (1967) also demonstrated that protonization is unimportant until the pH drops below 6. Thus, ferro- and ferricyanide will be present in only two dominant forms, as the free ion and as the potassium complex. The mass balance equations are:

$$\text{Fe(II)}_{\text{total}} = \frac{[\text{Fe(CN)}_6^{4-}]_{\text{free}}}{\gamma_2} + \frac{[\text{KFe(CN)}_6^{3-}]}{\gamma_4} \quad (17)$$

Table 11
Complex Association in the Aqueous Potassium Ferro-Ferricyanide System at 25°C

<u>Reaction</u>	<u>Symbol</u>	<u>log K</u>	<u>Reference</u>
$\text{H}^+ + \text{Fe}(\text{CN})_6^{4-} \rightleftharpoons \text{HFe}(\text{CN})_6^{3-}$	K_1	-4.28	Eaton and others (1967)
$\text{H}^+ + \text{HFe}(\text{CN})_6^{3-} \rightleftharpoons \text{H}_2\text{Fe}(\text{CN})_6^{2-}$	K_2	-2.3	Eaton and others (1967)
$\text{K}^+ + \text{Fe}(\text{CN})_6^{3-} \rightleftharpoons \text{KFe}(\text{CN})_6^{2-}$	K_3	1.46	Eaton and others (1967)
$\text{K}^+ + \text{Fe}(\text{CN})_6^{4-} \rightleftharpoons \text{KFe}(\text{CN})_6^{3-}$	K_4	2.35	Eaton and others (1967)
$\text{Fe}^{2+} + 6\text{CN}^- \rightleftharpoons \text{Fe}(\text{CN})_6^{4-}$	K_5	35.4	Christensen and others (1975)
$\text{Fe}^{3+} + 6\text{CN}^- \rightleftharpoons \text{Fe}(\text{CN})_6^{3-}$	K_6	43.6	Christensen and others (1975)

$$\text{Fe(III)}_{\text{total}} = \frac{[\text{Fe(CN)}_6^{3-}]_{\text{free}}}{\gamma_1} + \frac{[\text{KFe(CN)}_6^{2-}]}{\gamma_3} \quad (18)$$

where γ_3 and γ_4 represent activity coefficients for the ferricyanide and ferrocyanide complexes of potassium, respectively.

Substituting in the appropriate stability constants from table 11 and rearranging equations (17) and (18), we have:

$$[\text{Fe(CN)}_6^{4-}] = \frac{\gamma_2 \cdot \text{Fe(II)}_T}{1 + \frac{[\text{K}^+]\gamma_2 K_4}{\gamma_4}} \quad (19)$$

and,

$$[\text{Fe(CN)}_6^{4-}] = \frac{\gamma_1 \cdot \text{Fe(III)}_T}{1 + \frac{[\text{K}^+]\gamma_1 K_3}{\gamma_3}} \quad (20)$$

yielding:

$$\frac{[\text{Fe(CN)}_6^{4-}]}{[\text{Fe(CN)}_6^{3-}]} = \frac{\gamma_2 \gamma_4 (\gamma_3 + \gamma_1 [\text{K}^+] K_3)}{\gamma_1 \gamma_3 (\gamma_4 + \gamma_2 [\text{K}^+] K_4)} \quad (21)$$

The total iron concentrations disappear because the solution is equimolar in ferrocyanide and ferricyanide. Using the Davies equation $\gamma_3 = 0.332$, $\gamma_4 = 0.084$ and $[\text{K}^+] = 0.093$.

Substituting these values into equation (21) results in

$$\frac{[\text{Fe(CN)}_6^{4-}]}{[\text{Fe(CN)}_6^{3-}]} = 0.06034.$$

Substituting into equation (12) gives:

$$\text{Eh} = 0.358 - 0.095 \log (0.06034) = 0.4299$$

which agrees perfectly with the measured value.

The temperature dependence of the Eh for ZoBell's solution requires a standard enthalpy value and knowledge of the heat capacity change, ΔC_p° , for reaction (11). The heat capacity change should be close to zero for temperatures of practical interest. The reaction involves a simple one-electron transfer between two complexes of similar size, geometry and composition. If the heat capacity is zero then the enthalpy of reaction is a constant, independent of temperature, and the expression for the Eh of ZoBell's solution becomes a linear function of the temperature:

$$Eh(T) = E^\circ (25^\circ\text{C}, 1 \text{ atm}) + T \left[\frac{\partial E}{\partial T} \right] - \frac{2.303RT}{F} \log \frac{[\gamma_2 \gamma_4 (\gamma_3 + \gamma_1 [K^+] K^3)]}{[\gamma_1 \gamma_3 (\gamma_4 + \gamma_2 [K^+] K^4)]} \quad (22)$$

where the temperature coefficient is derived from the Gibbs-Helmholtz equation (Lewis and Randall, 1961, p. 165):

$$\frac{\partial E}{\partial T} = \frac{1}{T} \left[E + \frac{\Delta H}{nF} \right] \quad (23)$$

If the ratio of the terms in the log function of equation (22) is independent of temperature then this equation can be expanded in terms of the multiplier $\Delta T = (T - 25)$ to:

$$Eh(T) = E^\circ(25^\circ\text{C}, 1 \text{ atm}) + (T - 25) \frac{\partial E}{\partial T} - \frac{2.303R(298)}{F} \log (0.06034) + \frac{(T - 25)2.303R}{F} \log (0.06034) \quad (24)$$

or:

$$Eh(T) = E^\circ(25^\circ\text{C}, 1 \text{ atm}) - \frac{2.303R(298)}{F} \log (0.06034) + (T - 25) \frac{\partial E}{\partial T} - \frac{2.303R}{F} \log (0.06034) \quad (25)$$

Using the enthalpy values listed in Wagman and others (1969), the standard enthalpy of reaction (11) is -24.4 kcal/mole. Substituting

this value into equation (23) gives a temperature coefficient of -2.35×10^{-3} v/°K. Thus, equation (25) becomes:

$$E_h(T) = 0.430 + 0.0021 (25 - T) \quad (26)$$

which compares well with the measured value (eq. (13)). The greater slope in equation (6) suggests the enthalpy of reaction measured in this experiment is more negative than the values compiled in Wagman and others (1969).

Another estimate of the reaction enthalpy, which suggests a more negative value, can be obtained by applying Hess' rule to the enthalpies for the dissociation of the ferrocyanide and ferricyanide ions and the ferrous to ferric oxidation couple:

	ΔH_R° (kcal/mole)	Reference
$\text{Fe}(\text{CN})_6^{3-} \rightarrow \text{Fe}^{3+} + 6\text{CN}^-$	-87.77	Christensen and others (1975)
$\text{Fe}^{2+} + 6\text{CN}^- \rightarrow \text{Fe}(\text{CN})_6^{4-}$	70.14	"
$\text{Fe}^{3+} + e^- \rightarrow \text{Fe}^{2+}$	-9.62	de Bethune and Loud (1964)
$\text{Fe}(\text{CN})_6^{3-} + e^- \rightarrow \text{Fe}(\text{CN})_6^{4-}$	-27.25	

The temperature coefficient calculated from this reaction enthalpy is -2.76×10^{-3} v/°K. Based on the measurements in this investigation, the temperature coefficient is -2.81×10^{-3} v/°K and the reaction enthalpy is -27.58 kcal/mole at an ionic strength of 0.1528. Carrying through the standard error of the estimate of the emf on the temperature from table 10, the error in the reaction enthalpy is only ± 50 cal/mole. The magnitude of the error in the final enthalpy function is difficult to assess because of the unknown uncertainties in the calculation of

the saturated silver-silver chloride half-cell potential. Further discussion of the results will be considered below.

Potential values of ZoBell's solution can be analytically expressed with a second order equation for the entire temperature range. Unfortunately, the absence of potential data on the saturated KCl calomel electrode above 50°C and the saturated KCl silver-silver chloride electrode at any temperature prevents reliable calculation of E_h values for ZoBell's solution and of the Orion half-cell potential above 55°C. It is possible, by making some assumptions, to estimate the necessary potentials and arrive at an approximate equation for the Orion reference potential which should suffice for field use at high temperatures provided that probable errors of at least ± 5 mv are not a severe handicap.

Cell potentials for the saturated KCl calomel electrode up to 70°C have been calculated by Chateau (1954) from data obtained by Pouradier and Chateau (1953) and by Harned and Ehlers (see Harned and Owen, 1958, p. 456). This method of calculation overlooked differences between HCl and KCl reference solutions and assumed chloride is the only electrolyte affecting the cell potential. More importantly, this method cancels out liquid-junction potentials which are needed for the present study. Alner and others (as cited by Covington, 1969) carefully measured the saturated calomel half-cell potential up to 50°C which included the liquid junction potential as part of the measurement. An estimate of the liquid-junction potential is obtained when the values of Chateau (1954) are subtracted from those of Alner and others and have been extrapolated to 90°C by a linear equation fitted to the 0° to 50° data. The estimated liquid junction potentials were then added

on to Chateau's values up to 70°C. Extrapolations were made to obtain values at 80° and 90°C.

The standard state potentials for the silver-silver chloride and calomel electrodes have been evaluated with the "third-law" method by Ahluwalia and Cobble (1964). Combining the extrapolated potentials for the saturated calomel with the difference between the standard state potentials using equation (3) gives the desired half-cell potentials for the saturated silver-silver chloride electrode from 0° to 90°C. These potentials are listed in table 12 and were fitted to a second order equation:

$$E = 0.22259 - 9.160 \times 10^{-4} T - 1.553 \times 10^{-6} T^2. \quad (27)$$

Adding equation (27) to the second order fit of the measured potentials yields the Eh of ZoBell's solution:

$$E_h = 0.49080 - 2.326 \times 10^{-3} T - 3.798 \times 10^{-6} T^2 \quad (28)$$

or

$$E_h = 0.43028 - 2.326 \times 10^{-3} (T - 25) - 3.798 \times 10^{-6} (T - 25)^2 \quad (29)$$

where T is in degrees centigrade. Subtracting the second order equation for the Orion combination redox electrode #1 from equation (28) yields:

$$0.23983 - 0.6212 \times 10^{-3} (T - 25) - 2.690 \times 10^{-6} (T - 25)^2 \quad (30)$$

and for electrode #2:

$$0.24552 - 0.6045 \times 10^{-3} (T - 25) - 2.035 \times 10^{-6} (T - 25)^2 \quad (31)$$

These potentials are also listed in table 12. Using the standard thermodynamic equations for the temperature dependence of the cell potential (Lewis and Randall, 1961, p. 165), estimates of the enthalpy, entropy and heat capacity for reaction (11) were derived. These values are given in table 13 along with comparative data from other investigators.

Table 12

Half-Cell Potentials for the Saturated KCl Silver-Silver Chloride
and Orion Combination Redox Reference Electrodes

<u>T(°C)</u>	<u>sat. Ag/AgCl (volts)</u>	<u>Orion #1 (volts)</u>	<u>Orion #2 (volts)</u>
0	0.22264	0.25368	0.25936
10	0.21313	0.24854	0.25413
20	0.20362	0.24287	0.24849
25	0.19877	0.23983	0.24552
30	0.19382	0.23666	0.24245
40	0.18351	0.22991	0.23599
50	0.17301	0.22262	0.22914
60	0.16200	0.21479	0.22187
70	0.15050	0.20643	0.21420
80	0.13959	0.19753	0.20612
90	0.12758	0.18809	0.19763

Table 13a
Thermodynamic Values for Equimolar Potassium Ferro-Ferricyanide Solutions at 25°C

Property	Value	Ionic strength	Method	Reference
$\Delta H^\circ (\text{kcal mole}^{-1})$	-27.58	0.1528	potentiometric	this study ¹
	-26.7	0.064	potentiometric	Hanania and others (1967)
	-24.4	0		Wagman and others (1969)
	-27.6		potentiometric	Lin and Breck (1965)
	-25.25	0	calculation	this study
$\Delta S^\circ (\text{cal deg}^{-1} \text{mole}^{-1})$	-26.8		calorimetric	Heppler and others (1960)
	-58	0.1528	potentiometric	this study
$\Delta C_p^\circ (\text{cal deg}^{-1} \text{mole}^{-1})$	-62.1	0.064	potentiometric	Hanania and others (1967)
	-52	0.1528	potentiometric	this study

¹This enthalpy value is derived from the more reliable linear fit.

Table 13b
Temperature Dependent Equations for the Thermodynamic Functions

$$\begin{aligned}\Delta H &= -19435 - 0.08759T^2 \text{ cal mole}^{-1} \\ \Delta S &= -5.818 - 0.175T \text{ cal deg}^{-1} \text{ mole}^{-1} \\ \Delta C_p &= -0.175T \text{ cal deg}^{-1} \text{ mole}^{-1}\end{aligned}$$

where T is in degrees absolute and the values are
considered meaningful only for the interval 273°
to 373°K

The advantage of the present study is the greater number of cell measurements over a much larger temperature range than had been previously reported. This larger temperature range permits an estimate of the heat capacity for the ferro-ferricyanide redox couple which is reported here for the first time. All of the literature data compares quite well with the results from this study and the discrepancies can be attributed to differences in ionic strength.

The half-cell reference potentials for two Orion combination redox electrodes have been determined from 8° to 84°C for Eh corrections of field measurements. In addition, the thermodynamic properties of ZoBell's solution have been investigated resulting in values for the enthalpy, entropy and heat capacity of the ferro-ferricyanide redox reaction.

Correlation of Measured Eh with the Ferrous-Ferric Redox Couple

The thermodynamic relationship of the ferrous-ferric redox couple to the Eh is found in the Nernst equation:

$$E_h = E^\circ - 2.303 \frac{RT}{F} \log \frac{[Fe^{2+}]}{[Fe^{3+}]} \quad (32)$$

where square brackets denote activities, and the E° is the standard state potential. To determine the activities of ferrous and ferric ions the ionic strength and the amount of complex formation must be known. The iron-complexing ligands in acid mine drainage are primarily sulfate and hydroxide. These stability constants for the iron complexes have been evaluated and placed into the computer program WATEQ2 for calculation of chemical equilibrium. Evaluation procedures and description of the computer program will be described in a later chapter.

It is sufficient to mention that the ionic strength and the complexation were calculated by an iterative approach based on the method of Garrels and Thompson (1962). All complexing between major cations and anions is simultaneously considered by this method, and the computations have been especially adapted for high concentrations of sulfate and heavy metals.

The output from the equilibrium computations includes a value for the Eh based on equation (32). This computed Eh uses analyses of ferrous and total iron as well as pH, temperature and all of the major solute species. These values are compared to the field measurements of Eh in figure 10. The comparison shows that the general trend in slope is similar, but the calculated Eh values are higher than measured by about 25 mv. This consistency in slopes is quite encouraging when the difficulty of obtaining reliable field measurements and of making the calculations is considered. The shift of the intercept in figure 10 may be due to the assumption that ferric iron is equal to the total analyzed iron minus the analyzed ferrous iron. Some of the "dissolved" ferric iron could be present as polymers containing more than three iron atoms per molecule. WATEQ2 only considers polymeric hydrolysis up to $\text{Fe}_3(\text{OH})_4^{5+}$ and would distribute any higher polymers among Fe^{3+} and the other complexes. The presence of higher polymers would therefore increase the calculated Eh over the measured values. Such polymers might be identified by analyzing for ferric iron with orthophenanthroline and ferrous iron with Ferrozone and comparing the sum of these two with total iron by atomic absorption methods. A consistently higher value (of 10 percent or more) by atomic absorption over the sum should indicate the existence of high molecular weight iron polymers. Another

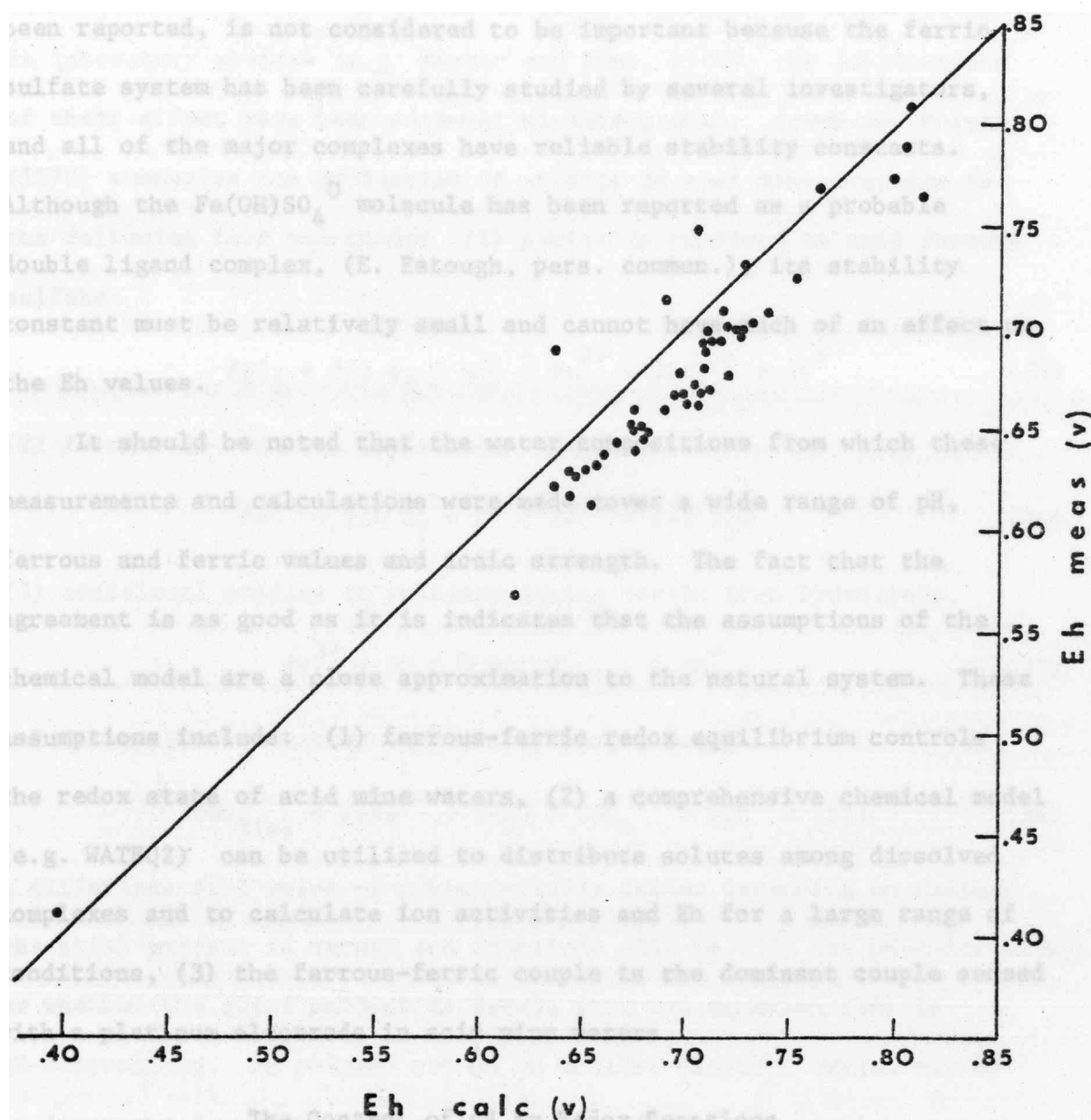


Figure 10. Comparison of calculated with measured Eh values.

possible explanation for the Eh discrepancy would be the existence of a complex not accounted for. A complex likely to occur in this system, such as $\text{Fe}(\text{OH})\text{SO}_4^0$, for which a stability constant has not been reported, is not considered to be important because the ferric sulfate system has been carefully studied by several investigators, and all of the major complexes have reliable stability constants. Although the $\text{Fe}(\text{OH})\text{SO}_4^0$ molecule has been reported as a probable double ligand complex, (E. Eatough, pers. commun.), its stability constant must be relatively small and cannot have much of an effect on the Eh values.

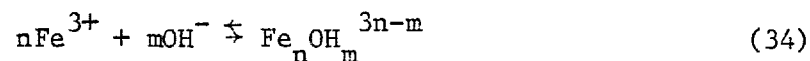
It should be noted that the water compositions from which these measurements and calculations were made cover a wide range of pH, ferrous and ferric values and ionic strength. The fact that the agreement is as good as it is indicates that the assumptions of the chemical model are a close approximation to the natural system. These assumptions include: (1) ferrous-ferric redox equilibrium controls the redox state of acid mine waters, (2) a comprehensive chemical model (e.g. WATEQ2) can be utilized to distribute solutes among dissolved complexes and to calculate ion activities and Eh for a large range of conditions, (3) the ferrous-ferric couple is the dominant couple sensed with a platinum electrode in acid mine waters.

The Control of pH by Redox Reactions

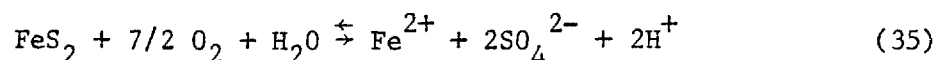
The oxidation of dissolved ferrous iron is commonly written as a sequence of two important reactions: (1) the oxidation of ferrous to ferric iron,



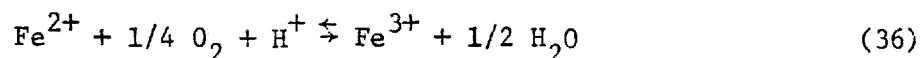
and (2) the hydrolysis of ferric iron,



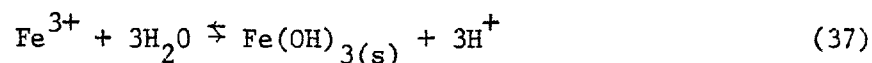
Although the chemical equilibria of these reactions are well documented in laboratory studies (e.g. Mesmer and Baes, 1975), the implications of their effect have been somewhat misinterpreted. Stumm and Morgan (1970) summarize the production of acidity in coal mine drainage in the following four reactions: (1) pyrite is oxidized to acid ferrous sulfate:



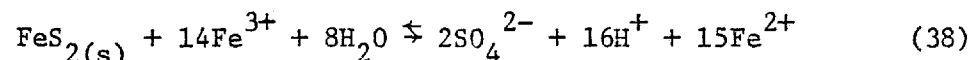
(2) ferrous is oxidized to ferric,



(3) additional acidity is released during ferric iron hydrolysis,



and (4) pyrite is further oxidized by ferric ions,



A difference of 9 moles of proton acidity arises depending on whether the chief oxidant is oxygen and equations (35) to (37) are pH-controlling, or whether the chief oxidant is ferric iron and equation (38) is pH-controlling. As pointed out in an earlier chapter, oxygen may be an important factor in the initial stages of pyrite oxidation, but the acidity is primarily due to the oxidation of sulfide sulfur to sulfate because of the formation of 16 protons required by the transfer of 16 electrons from the sulfide sulfur as shown in reaction (38). Once the pH is below 3.5 to 4.0, smaller quantities of ferric hydroxide will

precipitate, the ferric ion activity increases and ferric iron becomes a more important oxidant. When ferric iron is the chief oxidant, reaction (38) becomes dominant and 16 moles of proton acidity are produced. In this reaction all of the protons come from the oxidation of the sulfur and the iron plays no role in the acidity. To regenerate ferric ions, however, protons are consumed by reaction (36) which would actually *reduce* the acidity from that predicted by reaction (38).

The important point here is that the statement, "The decomposition of iron pyrite is among the most acidic of all weathering reactions because of the great insolubility of Fe(III)" (Stumm and Morgan, 1970), is a bit misleading. The oxidation of sulfur has the potential for being a much greater force in decreasing the pH than does iron. The following chemical interpretation of data from other sections of this thesis substantiates this hypothesis, demonstrates an effective pH buffering mechanism during iron oxidation and confirms the validity of reactions (33) and (34) in acid mine drainage.

During the study of iron oxidation by *Thiobacillus ferrooxidans* the pH was measured along with the ferrous concentration. All of the pH measurements are plotted vs. time in figure 11 and show a very striking convergence to a pH of 2.1 to 2.4. This indicates that when the initial pH is greater than 2.5 the acidity from ferric hydrolysis is greater than the acidity consumed when ferrous is oxidized to ferric iron and the pH decreases. When the initial pH is below 2.0, negligible hydrolysis occurs and protons are consumed during oxidation thereby raising the pH. For pH values below 2.0 the bisulfate-sulfate equilibrium buffers against an increase in pH from iron oxidation by the reaction:



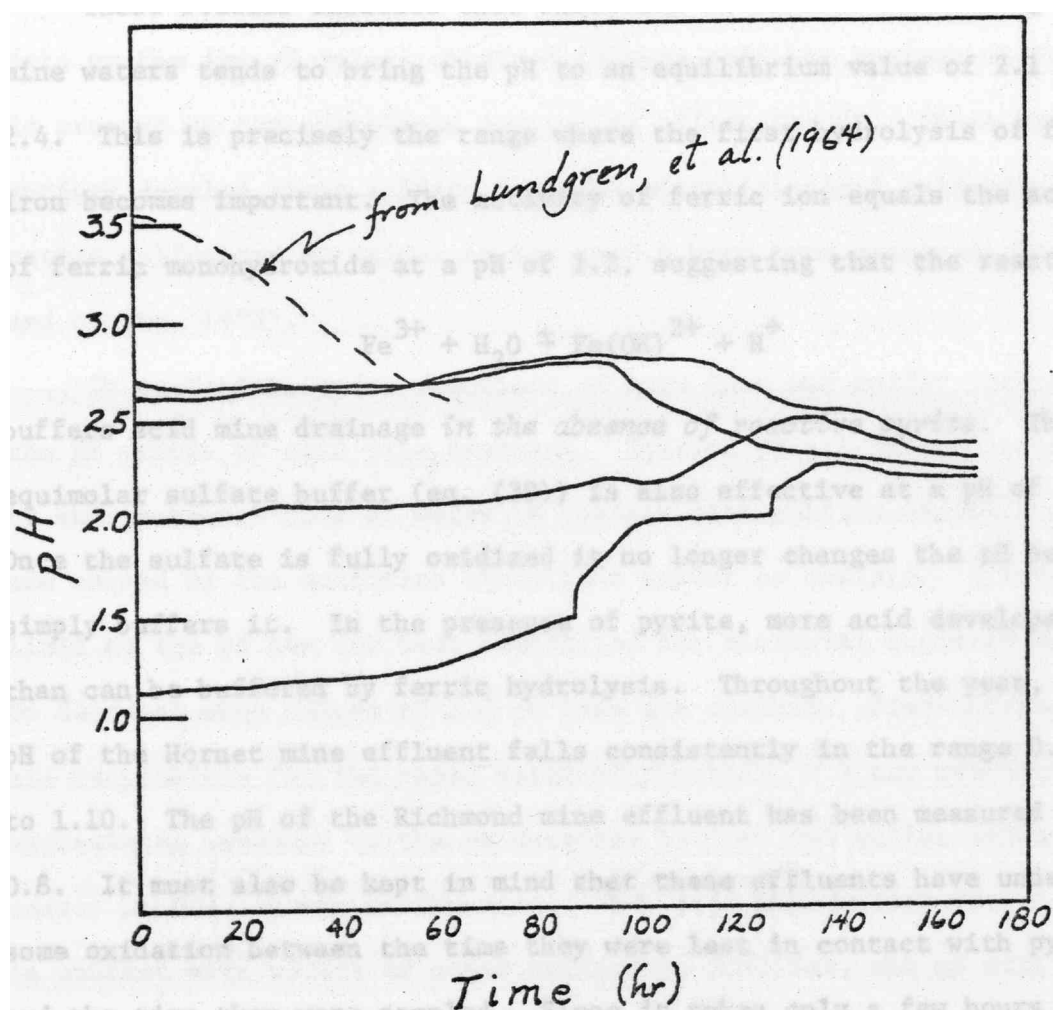
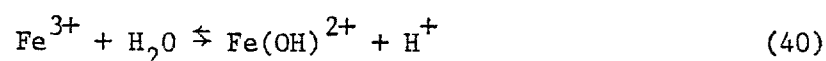


Figure 11. pH convergence of oxidizing mine waters and 9 K media.

The amount of bisulfate buffering is complicated by the formation of several metal sulfate complexes and makes the resultant change in pH difficult to predict.

These studies indicate that oxidation of ferrous-containing acid mine waters tends to bring the pH to an equilibrium value of 2.1 to 2.4. This is precisely the range where the first hydrolysis of ferric iron becomes important. The activity of ferric ion equals the activity of ferric monohydroxide at a pH of 2.2, suggesting that the reaction



buffers acid mine drainage *in the absence of reactive pyrite*. The equimolar sulfate buffer (eq. (39)) is also effective at a pH of 2.0. Once the sulfate is fully oxidized it no longer changes the pH but simply buffers it. In the presence of pyrite, more acid develops than can be buffered by ferric hydrolysis. Throughout the year, the pH of the Hornet mine effluent falls consistently in the range 0.9 to 1.10. The pH of the Richmond mine effluent has been measured at 0.8. It must also be kept in mind that these effluents have undergone some oxidation between the time they were last in contact with pyrite and the time they were sampled. Since it takes only a few hours for the pH of these samples to increase a few tenths of a pH unit, these measurements should be considered maximum pH values. Iron oxidation in solution *increases* the pH when the initial pH is below 2.0; therefore it must be the oxidation of the sulfide sulfur from pyrite which produces these initially low pH values. The main reason why acid mine drainage is the most acidic of all weathering reactions is the high concentration of protons produced when sulfur is oxidized from the

S_2^{2-} to the S^{6+} oxidation state. This conclusion is supported by studies on the oxidation of elemental sulfur to sulfuric acid by *T. thiooxidans* and *T. ferrooxidans* where the pH decreases to 1.0 by the production of sulfuric acid (Bryner and Jones, 1965). Further support comes from data on the low pH values obtained in some acid hot springs where iron is present in concentrations too low to affect the pH. These hot springs develop their acidity from the microbiological oxidation of native sulfur and pH values as low as 0.9 have been measured (Brock and others, 1972).

To summarize, redox reactions of both iron and sulfur influence the pH values of acid mine drainage. Initial pH values are determined by the residence time of water in contact with sulfide minerals and are caused by the oxidation of sulfide sulfur to sulfate. A lower limit to the pH has not been identified but microbial activity appears to decrease when values of 1.0 or less are reached. Since microorganisms are responsible for the rapid rates of reaction, 0.5 may represent an approximate boundary to the pH decrease by iron and sulfur redox processes in the aquatic environment. When acid mine waters are no longer in contact with pyrite or other oxidizable sulfides, the pH will tend to decrease or increase toward 2.2 until all of the ferrous iron is oxidized. If the initial pH is about 1.0, the pH increases to only 1.5 upon oxidation of all the iron because some of the protons consumed are buffered by the bisulfate-sulfate equilibria. Both sulfate and ferric iron act as buffering agents in acid mine waters which, in the absence of other strong neutralizing agents such as carbonate minerals, tend to keep the pH of acid mine waters in the region of 2.0 to 2.5.

HYDROCHEMICAL PATTERNS

Climate

The climate of the Spring Creek drainage basin and the surrounding region varies considerably over short distances and during the year because of the rapid changes in elevation and the swiftly moving storm fronts originating off the Pacific Coast. At Redding on the Central Valley floor, summertime temperatures can reach 43°C (110°F) while 10 mi away at Whiskeytown Lake the temperature may be as low as 24°C (75°F). I have observed moderate rainfall at Iron Mountain while no rainfall occurred in Redding. Similarly, the snowfall at Iron Mountain is greater and stays much longer than in Redding.

A rainfall gaging station is maintained at Minnesota Station (courtesy of Leland George, Stauffer Chemical Co.) at an altitude of 488 m (1600 ft). Minnesota is located near the confluence of Boulder Creek with Spring Creek, a favorable site to collect precipitation data representative of the whole drainage basin. From past records at Iron Mountain (762 m, 2500 ft), Leland George has found that the average annual rainfall is about 20 percent higher at Iron Mountain than at Minnesota and that Minnesota receives about twice the rainfall of Redding. For the period July 8, 1974, through April 12, 1976, the average annual rainfall at Minnesota was 150 cm (59.2 in.) compared to 94 cm (37.4 in.) at Redding according to the data gathered by Kinkel and others (1956). The period of time during which the present study was undertaken was the driest for several years.

Sudden storm accumulation over the region, causing as high as 12.7 cm (5 in.) of rain in a day, can happen any time throughout the year. This type of heavy rainfall produces rapid increases in stream discharge because the steep slopes of largely igneous terrain with little soil development provide minimal opportunity for infiltration. The present chapter focuses on the control of solute concentrations by rainfall and discharge in mountainous streams severely affected by acid mine effluent.

Distribution of Stream Discharges, Solute Concentrations,
and Solute Loads with the Drainage Area

The Spring Creek drainage system consists primarily of Spring Creek and its two tributaries, Boulder Creek and Slickrock Creek. Boulder Creek averages 25 percent and Slickrock Creek about 5 percent of the discharge of Spring Creek below each confluence under steady-state flow conditions. These relative proportions can change dramatically during the initial rise in stream discharge when a rainstorm hits. Boulder Creek, for example, has much smaller drainage area than the upper portion of Spring Creek and consequently rises in discharge much more rapidly than Spring Creek, thereby increasing its relative discharge to 50 percent or more of the discharge of Spring Creek. Since Boulder Creek contains the major portion of the heavy metals which end up in Spring Creek, this difference in discharge during a storm event has important consequences on the downstream variations in total solute concentrations which will be discussed in the next section.

The major sources of heavy metals and acidity in Spring Creek can be identified by comparing metal loads at different parts of the stream via mass balance calculations. On April 3 and 4, 1975, a reconnaissance party sampled several sites in the drainage basin, and the analytical results from these samples identify the sources and changes in downstream transport of heavy metal solutes. The analytical concentrations were combined with the discharges to obtain total dissolved loads for iron, copper, zinc, cadmium, manganese and sulfate which are shown in table 14. The sample sites are identified by the same symbols used in figure 1. Boulder Creek (at A) is a clean mountain stream as it flows adjacent to the north side of Iron Mountain. As Boulder Creek flows downstream from A, it gradually picks up small seeps of acid mine waters leaking from the mines or entering the creek as base flow. By site C, next to the Lawson tunnel entrance of the Hornet mine, the pH drops to 3.5, and all of the solute loads increase. Between sites C and D, about 800 m, a greater increase in solutes occurs due to several small springs located along the steep west slope of the canyon. Most of the added solutes come from two springs which issue from partially buried tailings piles. During rainstorms large quantities of ground sulfide ore are washed downstream from these tailings piles, filling the creek bed with gray, floured pyrite for miles downstream. Pyrite has been found in Spring Creek reservoir muds and below the dam. The pyrite has been washing down these streams ever since they began processing sulfides at this location in 1943. The pH was 3.35 at one spring and 2.75 at the other on November 11, 1974, and Boulder Creek has a pH of 3.00 adjacent to the springs. An analysis of the spring with the highest discharge is given in table 15 and compared to an

Table 14

Comparison of Dissolved Metal and Sulfate Loads on (a) April 3 and 4, 1975, Moderate Flow Conditions and (b) June 23, 1975, Low Flow Conditions (g/min)

	<u>Site</u>	<u>Creek</u>	<u>pH</u>	<u>Fe</u>	<u>Cu</u>	<u>Zn</u>	<u>Cd</u>	<u>Mn</u>	<u>SO₄</u>
a	A	Boulder	6.6	0.8	0.4	0.4	<0.4	0.7	400
	B	Hornet mine effluent	1.0	9,300	19	1100	8.7	8.7	42,000
	C	Boulder	3.5	72	8.7	12	0.1	1.4	1,300
	D	Boulder	3.0	600	22	50	1.0	17	3,600
	F	Boulder	1.8	12,000	23	1100	9.0	26	46,000
	G	Boulder	2.4	16,000	28	1300	10	30	53,000
	I	Spring	5.9	2.1	<2.5	9.2	<2.5	<5.0	1,000
	J	Spring	2.7	14,000	40	1500	10	29	59,000
	L	Slickrock	3.4	110	15	8.7	0.07	2.2	900
	K	Spring	2.7	14,000	38	1500	11	29	66,000
	N	Spring	2.7	14,000	220	1400	10	51	63,000
b	G	Boulder	2.1	3,800	6.8	350	2.5	6.8	11,000
	J	Spring	3.0	3,800	12	410	3.5	8.7	14,000
	L	Slickrock	3.0	100	18	11	0.1	2.3	2,200
	K	Spring	2.9	3,900	59	450	3.2	14	16,000
	N	Spring	2.9	2,900	71	390	2.7	17	15,000

Table 15

Composition of Iron Mountain Tailings Spring Compared
to Boulder Creek (mg/l)

<u>Site</u>	<u>D1</u>	<u>C</u>
Name	Tailings Spring	Boulder Creek
Date	11/12/74	11/5/74
Temperature (°C)	11.0	10.0
Specific conductance (µS)	1522	478
pH	2.75	3.11
Eh (v)	0.463	0.694
Fe	140	25
Cu	3.9	2.3
Zn	45	6.5
Cd	0.24	0.056
Mn	1.25	0.69
SO ₄	819	333
Na	7.6	5.4
K	0.3	0.4
Ca	28	9.8
Mg	40	15

analysis of Boulder Creek at site C on November 5, 1974. This spring is clearly an important source of solutes entering Boulder Creek, but the occurrence of several of these springs along a steep, inaccessible slope makes any type of at-source control of water pollution impossible.

The greatest increase in the solute concentrations of Boulder Creek occurs between sites D and F. This increase is caused by the discharge of the Hornet-Richmond mine effluent into the creek after passing through a copper precipitation plant. The precipitation plant effects little change in the mine effluent other than precipitating the copper by displacement with iron from tin cans. This is indicated by comparing the sum of loads from sites B and D with the load at site F. Iron discharged into Boulder Creek from the copper plant amounts to 11,400 g/min while nearly all of the copper is removed. Of this discharge, 600 g/min comes from Boulder Creek, 9300 g/min comes from the mine effluent and 2100 g/min results from reaction within the copper plant. The efficiency of the copper plant is indicated by a decrease from 228 to 4 mg/l copper (98 percent removal) in the inflow and outflow water respectively. The iron concentration increased by about 1 g/l while zinc, cadmium, silica, sodium, potassium, calcium and magnesium showed virtually no changes. Manganese, aluminum and sulfate showed a slight increase. The differences in solute load from F to G are a result of an increase in the discharge following the beginning of precipitation at the end of the sampling day. The actual solute concentrations were all diluted nearly proportionally at site G compared to site F, confirming the onset of a storm. Allowing for error in discharge measurements, the analyses and the hydrologic imbalances of the drainage system during the beginning of a storm, the load calculations

show that most of the constituents arriving in the lower portion of Spring Creek (site N) originate from Boulder Creek. Copper and manganese show marked increases between K and N which suggest that drainage from the Benson mine (an abandoned mine near the lower portion of Spring Creek) or from South Fork Spring Creek makes some contribution to Spring Creek.

The solute load budget is reduced during low flow conditions as shown in table 14b. Changes in the distribution of solutes also show up during low flow; a major portion of the copper comes from Slickrock Creek and a larger portion of the manganese input now comes from Slickrock Creek. The copper load immediately below the confluence of Slickrock with Spring Creek still does not balance with the sum of the input loads. Twice the load of copper appears below the confluence compared to the sum of the input loads. I suggest there is a larger error associated with the copper load budgets than the other solutes, but whether this is a sampling problem, an analytical problem or a problem associated with the geochemistry of the environmental system remains to be determined. The important point is that regardless of the hydrologic conditions and the time of the year, the copper and manganese concentrations are always higher in Slickrock Creek than in Boulder or Spring Creek and that the input from Slickrock Creek has the strongest influence on the downstream concentration of these two elements. The high copper in Slickrock Creek results from mine effluent, high in copper, draining into Slickrock Creek from Iron Mountain without being precipitated in a copper plant. One water sample was collected from Slickrock Creek adjacent to the old flotation plant at the town of Iron Mountain. This analysis, given in table 16, has a copper

Table 16

Composition of Slickrock Creek at Iron Mountain,
November 14, 1974 (concentrations in mg/l)

<u>Site</u>	<u>M</u>
Temperature (°C)	11.8
Specific conductance (μS)	4520
pH	2.6
Fe	1000
Cu	115
Zn	48
Cd	0.52
Mn	9.4
SO ₄	5755
Na	7.95
K	0.65
Ca	79
Mg	265

concentration of 115 mg/l and a manganese concentration of 9.4 mg/l. The remaining solutes in table 14b, the bulk of the dissolved metals, are coming from Boulder Creek and show little variation in load during their downstream transport. For these reasons, correlation of any solutes with conductivity at site N (mouth of reservoir) is quite good except for copper and manganese.

Seasonal Variations in Rainfall, Discharge and Solute Concentrations

Water samples were collected at site N, at the point of entry of Spring Creek into Spring Creek Reservoir, every 2 to 6 wks during the study period to identify the effects of rainfall and discharge on solute concentrations. An example of the composition of Spring Creek during high, moderate and low flow is given in table 17. Spring Creek would be classified between Class I and Class II according to the categories suggested by Lundgren and other (1972) for coal mine drainage. Spring Creek, however, contains copper-zinc mine drainage with almost no neutralization from contact with carbonate-bearing rocks which are occasionally found in coal mining areas. Very little has been written about acid discharges from western United States sulfide-bearing ore bodies, and this author suggests they be classified separately from coal mine drainage and according to the type of ore deposit. These classifications hold little descriptive value except in identifying the type of mineral deposit from which the acid waters issue. In striking contrast to most natural waters, the major cations of Spring Creek are iron, aluminum, magnesium and zinc, and the only detectable anion is sulfate. The average instantaneous discharge for the period of this study was 45 cfs, although if the two highest dis-

Table 17

Composition of Spring Creek at Mouth of Reservoir Under a
Range of Flow Conditions (concentrations in mg/l)

	<u>Low flow</u>	<u>Moderate flow</u>	<u>High flow</u>
Date	Oct. 17, 1975	Apr. 3, 1975	Dec. 3, 1974
Discharge (cfs)	3.5	75.4	338
Specific conduc- tance (μ S)	3220	1385	
Temperature ($^{\circ}$ C)	13.0	8.0	9.5
pH (field)	2.55	2.72	3.09
Fe	440	110	39
Cu	7.0	1.7	2.1
Zn	50	11	4.5
Cd	0.39	0.080	0.029
Mn	2.0	0.40	0.43
Al	89	17	12
SiO ₂	42	19	12
Na	8.4	3.5	2.4
K	4.2	1.4	0.55
Ca	27	14	7.0
Mg	52	12	8.0
SO ₄	1850	495	246

charges (which lasted for only very short periods of time) are removed, the average drops to about 20 cfs.

The variations in rainfall, discharge, pH, iron concentrations and specific conductance at site N (at reservoir) are shown in figure 12 for the period November 8, 1974, to April 3, 1976. A few general trends are evident from figure 12: (1) overall there are higher total dissolved solids (as represented by specific conductance) in the summer than the winter, (2) total dissolved solids follow the normal inverse relationship with discharge because of dilution, (3) the pH also varies directly with discharge as a result of dilution but stays within the interval of 2.4 to 3.4 all year round, and (4) the iron concentration follows the same rising and falling pattern as the specific conductance. Other constituents such as aluminum, cadmium and sulfate also follow the general pattern of the specific conductance curve which can be demonstrated by the plots shown in figures 13, 14 and 15. Similar plots for copper and manganese are very poor because of the influence of Slickrock Creek as mentioned earlier. The good correlation in these plots provides a useful means of predicting heavy metal concentrations from knowledge of only the specific conductance, an easily measured water quality parameter. The excellent correlation between sulfate concentrations and specific conductance is a result of sulfate being the only major anion in these waters. Chloride, fluoride and bicarbonate, if present, would decrease the significance of the correlation, but these anions were below the limits of detection. These correlations, although very practical for the Spring Creek drainage basin, must be used with caution when applied to streams draining other massive sulfide ore bodies in Shasta County or elsewhere. If the zinc to

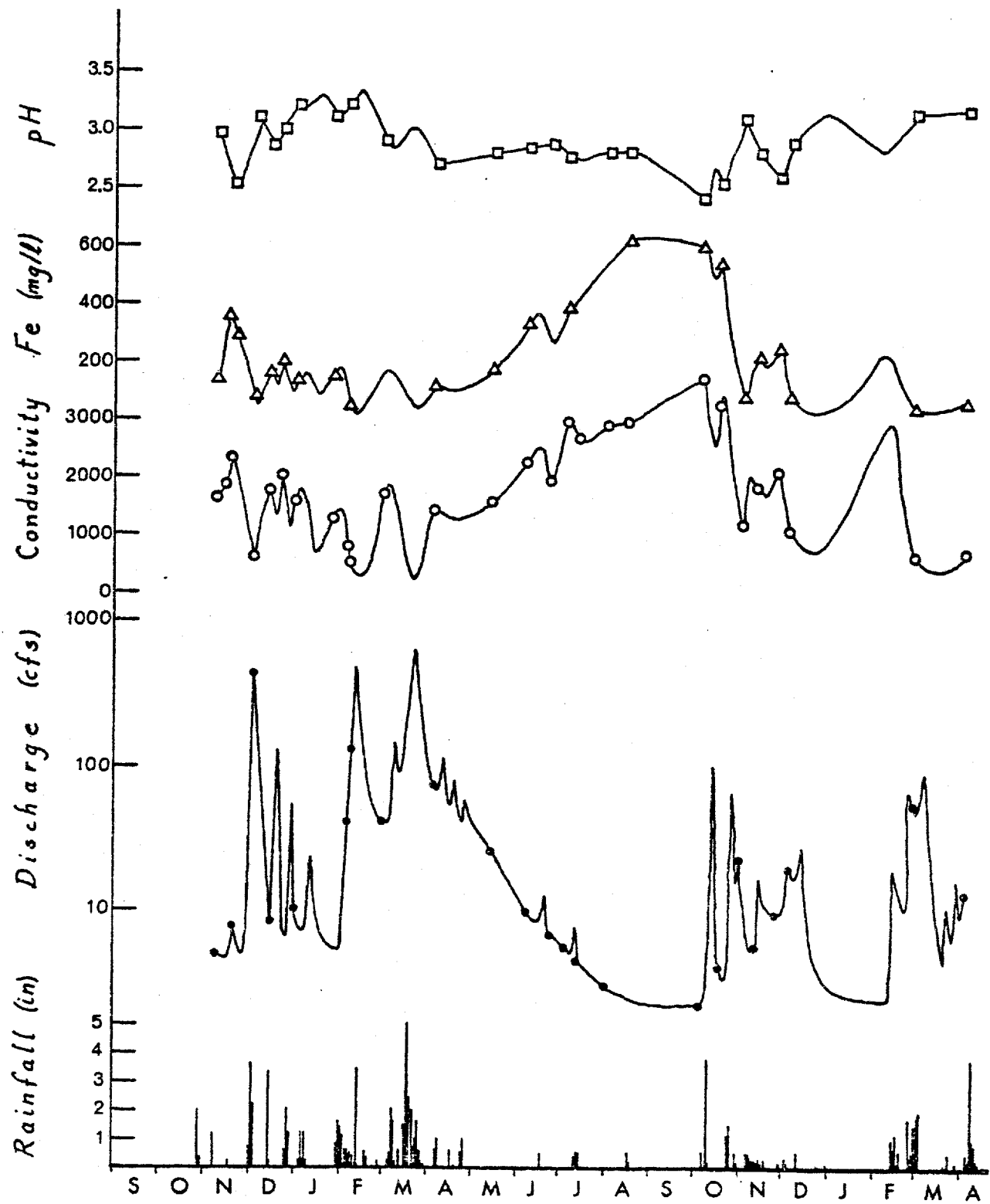


Figure 12. pH, iron and conductance variations with discharge.

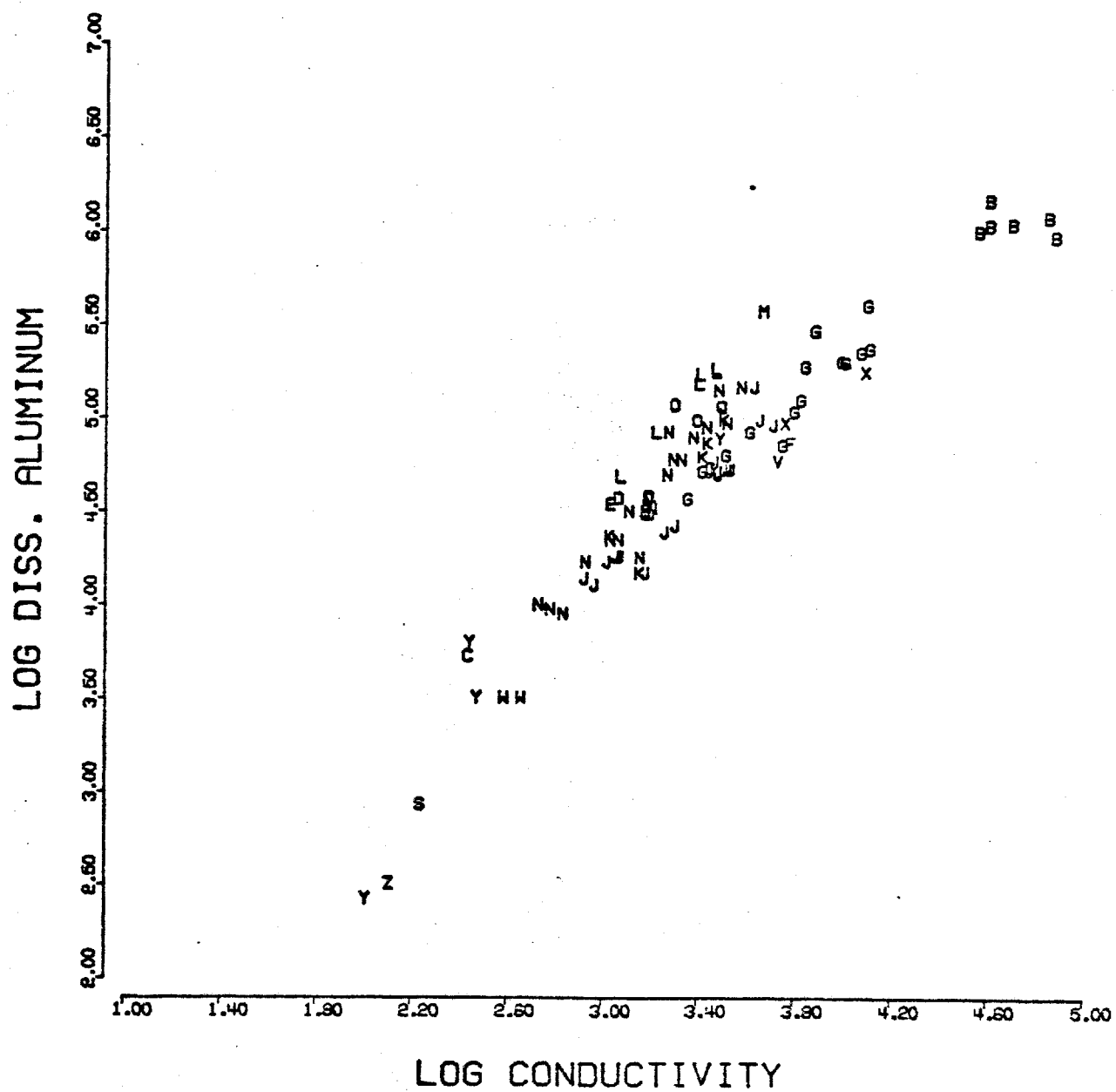


Figure 13. Correlation of the aluminum concentrations with the specific conductance. A log-log plot was used because the values covered such a large range.

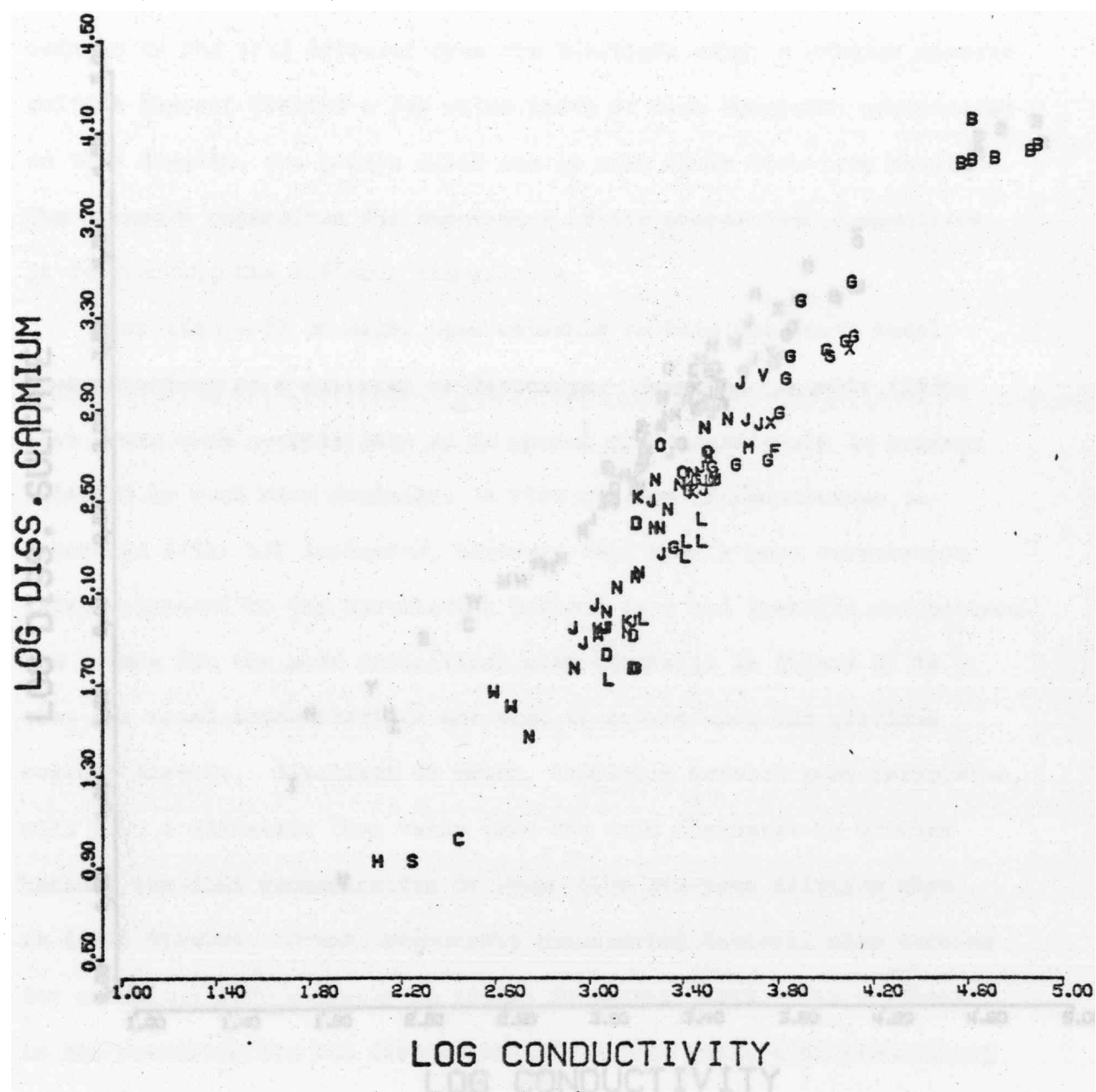


Figure 14. Correlation of the cadmium concentrations with the specific conductance.

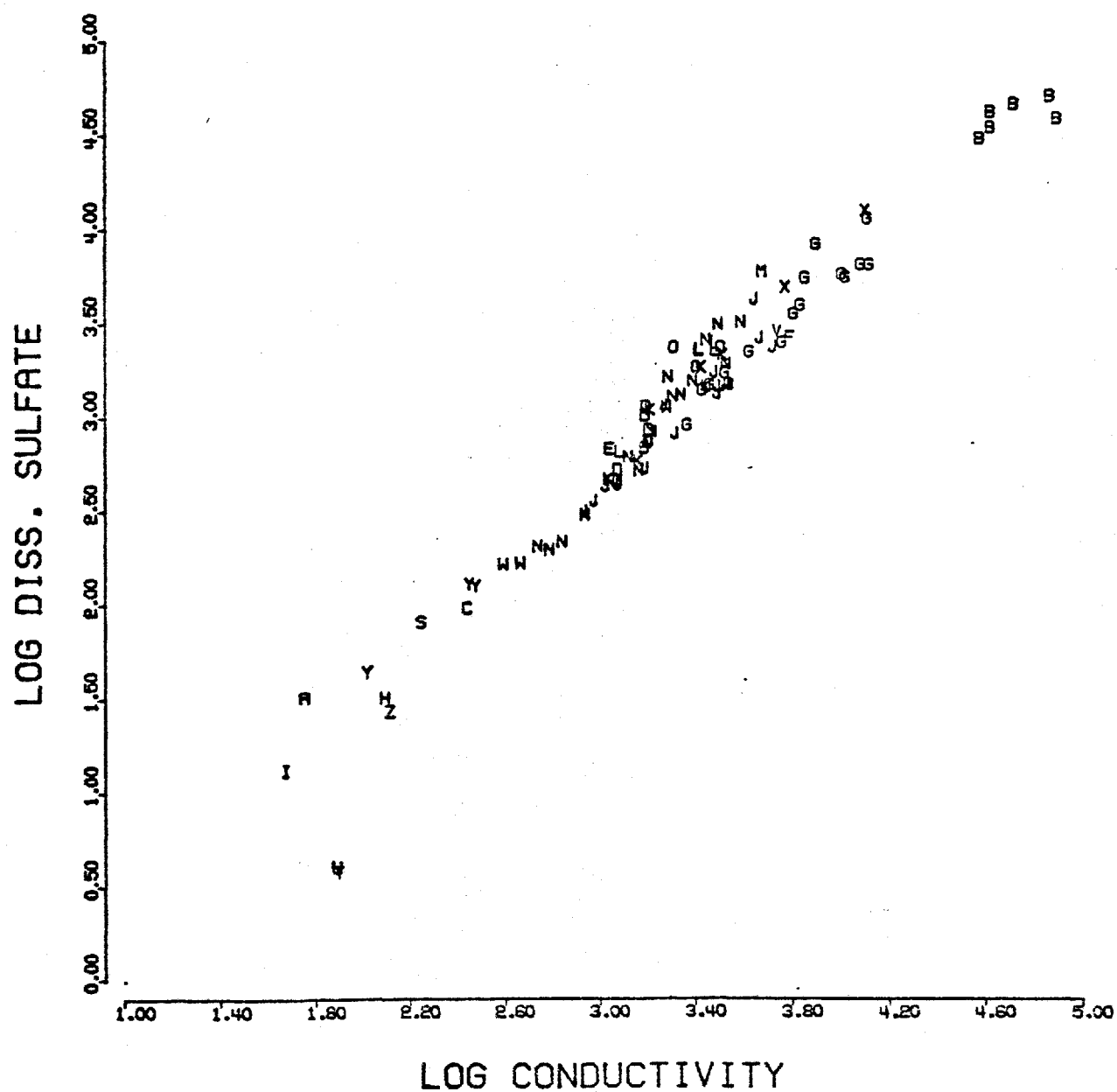


Figure 15. Correlation of the sulfate concentrations with the specific conductance.

cadmium content is relatively constant as one would expect in the Brick Flat-Richmond-Hornet ore deposit, then a good zinc-cadmium correlation in the mine effluent results (fig. 16). But when zinc and cadmium in the acid effluent from the Balaklala mine, a similar massive sulfide deposit located a few miles north of Iron Mountain, are plotted on this diagram, the points agree poorly with those from Iron Mountain. The mismatch emphasizes the importance of the source rock composition in determining the effluent composition.

From figure 12 it might seem valuable to know the heavy metal concentrations as a function of discharge. Gang and Langmuir (1974) have found such correlations to be useful predictive tools in streams affected by coal mine drainage. A plot of iron concentrations vs. discharge (fig. 17) indicates, however, that only a poor correlation exists compared to the correlation between iron and specific conductance. One reason for the poor correlation with discharge in figure 17 is that the metal concentrations are also dependent upon the previous weather history. Discharge in March, following several good rainstorms, will have a different iron value than the same discharge in October because the iron concentration is lower from previous dilution than it is in October. Other, previously unsuspected factors, also account for anomalous solute-discharge trends in Spring Creek. One of these is the precipitation and dissolution of soluble sulfate minerals along the stream banks (discussed in the last chapter) and another is the changing discharge balance between Boulder Creek and Spring Creek during a storm event. Yet another factor is whether the solute concentration corresponds to the rise or the fall of the discharge peak. This last complication is now considered in more detail.

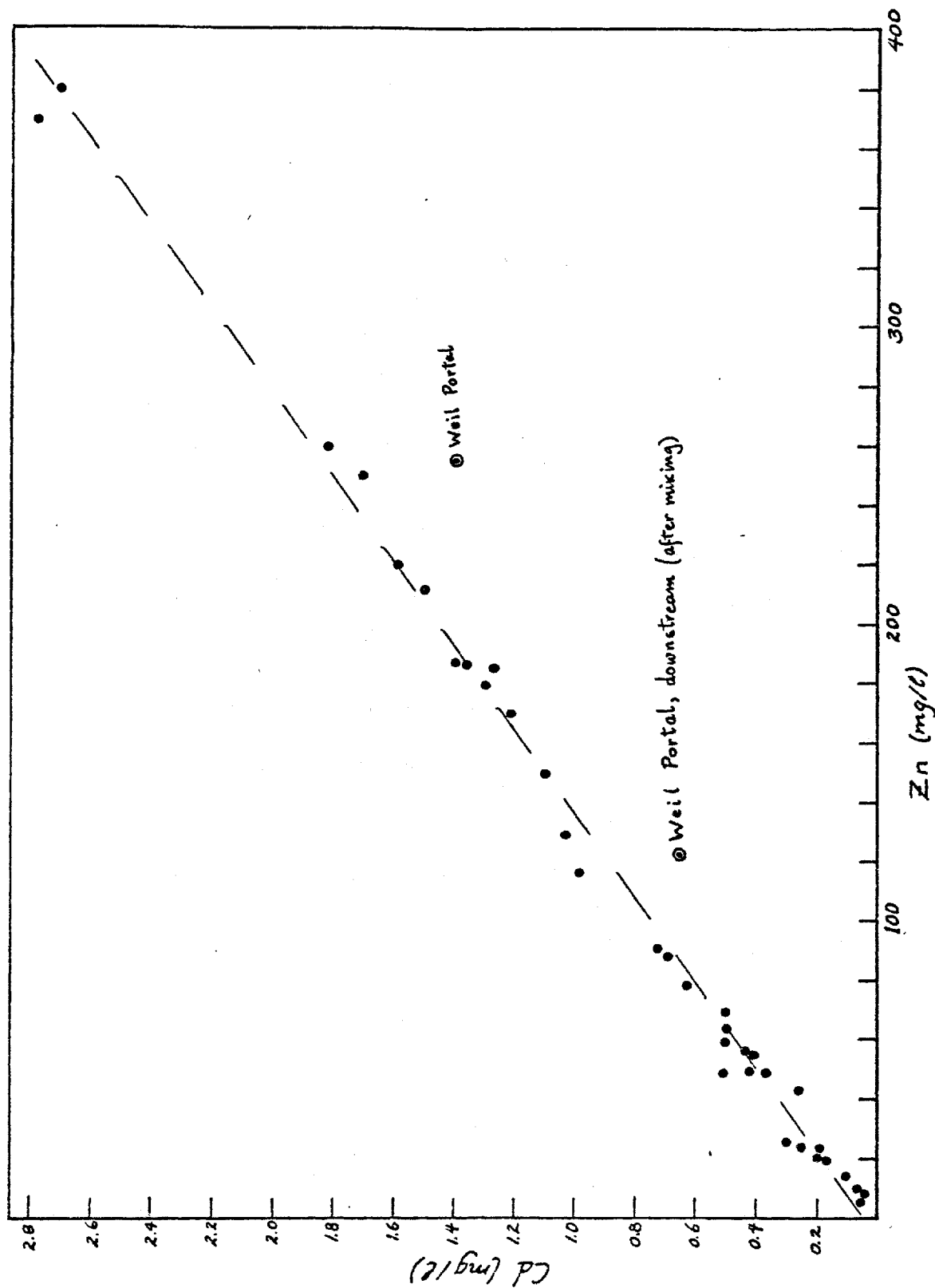


Figure 16. Correlation of the zinc and cadmium concentrations. Notice that the Weil mine drainage from the Balaklala mine, although draining a nearby and similar massive sulfide ore, does not fit the good correlation for the Iron Mountain drainage.

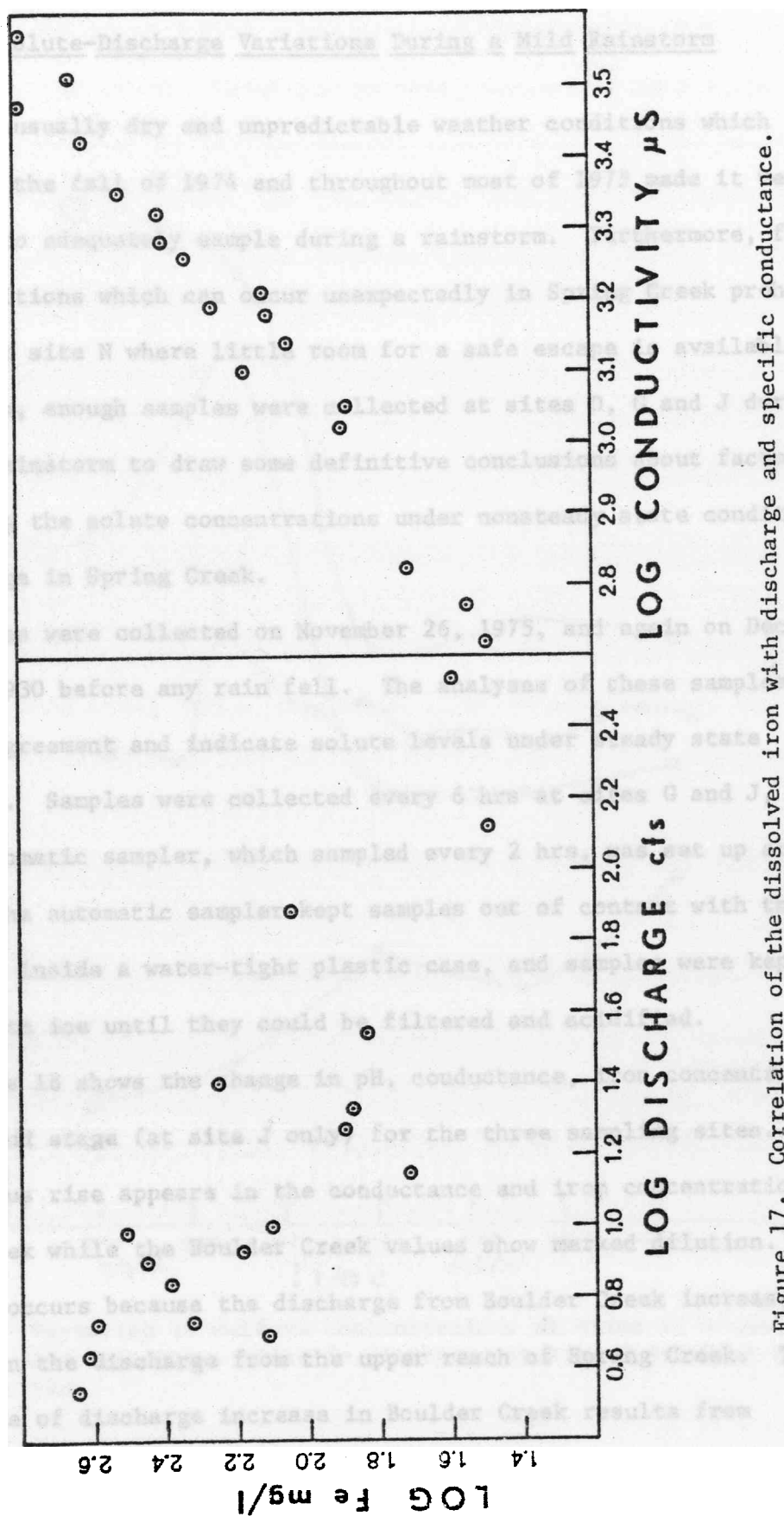


Figure 17. Correlation of the dissolved iron with discharge and specific conductance.

Solute-Discharge Variations During a Mild Rainstorm

The unusually dry and unpredictable weather conditions which existed in the fall of 1974 and throughout most of 1975 made it very difficult to adequately sample during a rainstorm. Furthermore, flash-flood conditions which can occur unexpectedly in Spring Creek prohibited sampling at site N where little room for a safe escape is available. Fortunately, enough samples were collected at sites D, G and J during one mild rainstorm to draw some definitive conclusions about factors controlling the solute concentrations under nonsteady state conditions of discharge in Spring Creek.

Samples were collected on November 26, 1975, and again on December 4, 1975, at 0930 before any rain fell. The analyses of these samples are in close agreement and indicate solute levels under steady state conditions. Samples were collected every 6 hrs at sites G and J, and an automatic sampler, which sampled every 2 hrs, was set up at site D. The automatic sampler kept samples out of contact with the atmosphere inside a water-tight plastic case, and samples were kept chilled with ice until they could be filtered and acidified.

Figure 18 shows the change in pH, conductance, iron concentration, rainfall and stage (at site J only) for the three sampling sites. An anomalous rise appears in the conductance and iron concentration of Spring Creek while the Boulder Creek values show marked dilution. This rise occurs because the discharge from Boulder Creek increases faster than the discharge from the upper reach of Spring Creek. The faster rate of discharge increase in Boulder Creek results from (1) Boulder drainage basin having a smaller area (about one-third

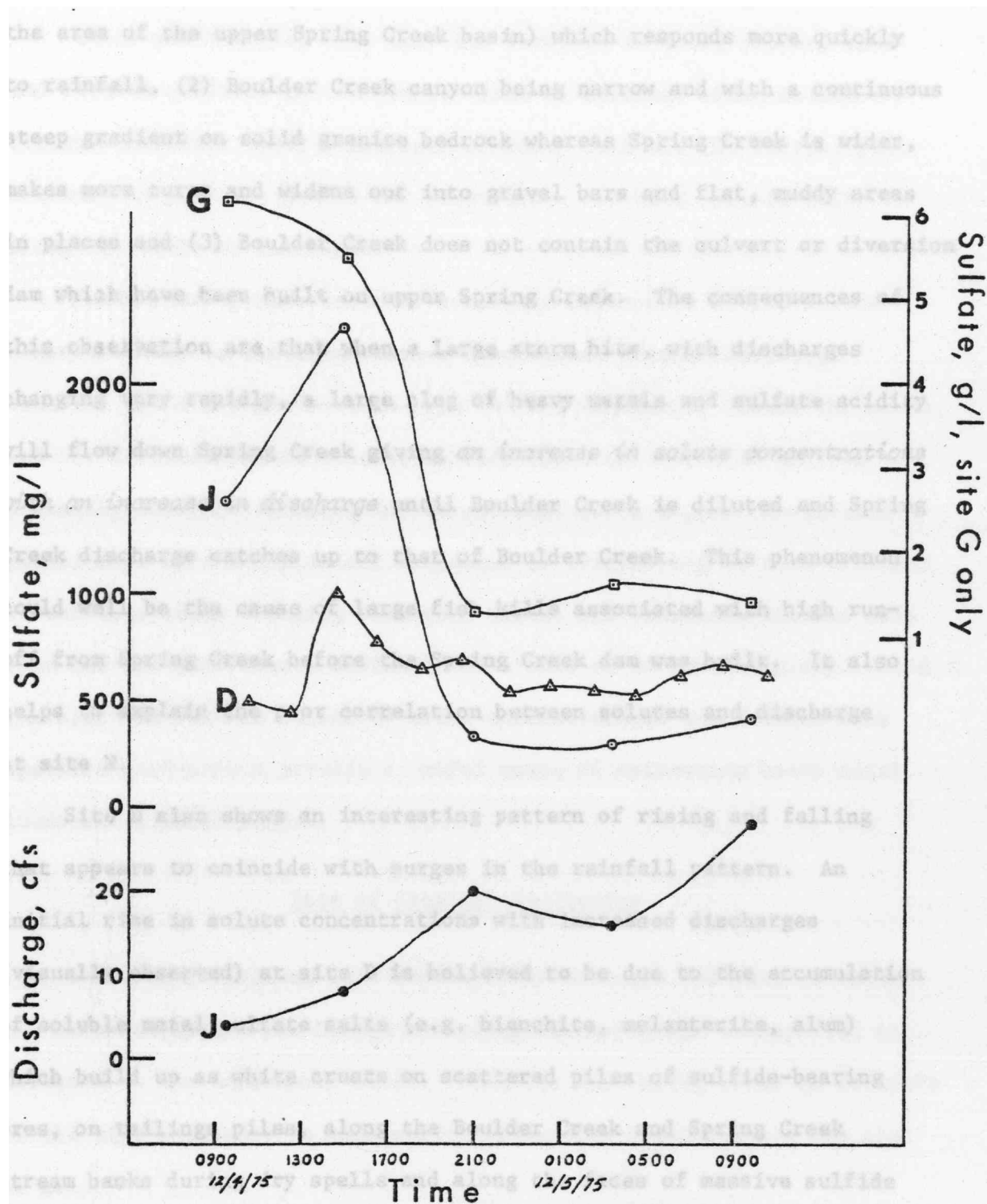


Figure 18. Variation in sulfate concentrations at sites G, J and D during a mild rainstorm. Rise in discharge at site J is shown by lowermost line.

the area of the upper Spring Creek basin) which responds more quickly to rainfall, (2) Boulder Creek canyon being narrow and with a continuous steep gradient on solid granite bedrock whereas Spring Creek is wider, makes more turns and widens out into gravel bars and flat, muddy areas in places and (3) Boulder Creek does not contain the culvert or diversion dam which have been built on upper Spring Creek. The consequences of this observation are that when a large storm hits, with discharges changing very rapidly, a large slug of heavy metals and sulfate acidity will flow down Spring Creek giving *an increase in solute concentrations with an increase in discharge* until Boulder Creek is diluted and Spring Creek discharge catches up to that of Boulder Creek. This phenomenon could well be the cause of large fish kills associated with high runoff from Spring Creek before the Spring Creek dam was built. It also helps to explain the poor correlation between solutes and discharge at site N.

Site D also shows an interesting pattern of rising and falling that appears to coincide with surges in the rainfall pattern. An initial rise in solute concentrations with increased discharges (visually observed) at site D is believed to be due to the accumulation of soluble metal sulfate salts (e.g. bianchite, melanterite, alum) which build up as white crusts on scattered piles of sulfide-bearing ores, on tailings piles, along the Boulder Creek and Spring Creek stream banks during dry spells and along the faces of massive sulfide ore exposed by mining. The dissolution of these salts along with the Boulder-Spring Creek discharge behavior makes the resultant runoff in Spring Creek a particularly hazardous pollution problem when a strong rain hits in the autumn after a long dry spell.

It is worth noting here that the increase in iron, copper, zinc and cadmium sulfates in the Hornet-Richmond effluent which occurs during the winter under conditions of heavy rainfall (L. George, pers. commun.) is probably due to the dissolution of these soluble salts along the walls of the mines.

These studies have revealed a complex dependence of the solute concentrations on previous weather conditions, present discharge behavior, relative proportions of tributary discharges within the basin, and the accumulation of soluble sulfate minerals. Iron is derived primarily from the Richmond-Hornet effluent and a copper cementation plant; most of the copper and manganese is originating in mine effluent or tailings seeps entering Slickrock Creek; all remaining solutes come from the Richmond-Hornet effluent which ends up in Boulder Creek. Good correlations between dissolved metal concentrations and sulfate with specific conductance provide a useful means of estimating heavy metal loads and sulfate loads.

Rate of Chemical Weathering

There is sufficient data available to estimate the rate at which the Richmond-Hornet ore bodies are being weathered and transported in solution to the Sacramento River. From the weathering rates an estimate of the time necessary to completely oxidize the remaining ore can also be made.

The average total dissolved iron concentration for six samples of Richmond-Hornet effluent is 10.45 g/l. By making a conservative estimate of 100 gal/min for the average annual flow rate (L. George, pers. commun.), the total discharge of iron is about 4000 g/min or 21,000 metric tons/yr.

Since the remaining ore is dominantly pyrite and therefore 50 percent iron, the ore bodies are being weathered at the rate of approximately 42,000 tons/yr. Some of the weathering products are seeping into Boulder Creek and Slickrock Creek without reaching the Hornet or Richmond effluent pipes. The volume of water in these seeps is quite small compared to the Richmond-Hornet discharge, and it should not make a significant change to the total weathering rate.

Ten million tons of ore remain in the Richmond-Hornet ore bodies, and at the estimated rate of weathering it would take 238 yrs to completely oxidize all of this ore. This weathering rate is based on a conservative average for the Richmond-Hornet discharge. If a maximum average annual discharge of 250 gal/min is used, then it would take 100 yrs to oxidize the remaining ore. It is clear from these calculations that these acid mine waters, if allowed to continue discharging under present conditions, will persist for a considerable length of time. Furthermore, over 3000 tons of zinc, 23 tons of cadmium, 21,000 tons of iron and 82,000 tons of sulfate will be irreversibly transported into Spring Creek and the Sacramento River each year for the next 100 to 250 yrs.

MINERAL EQUILIBRIA CONTROLS ON THE COMPOSITION OF ACID MINE WATERS

The chemical composition of any natural water is partly determined by the dissolution and precipitation of minerals in contact with that water. Interactions between minerals and natural waters include both kinetic and equilibrium processes, but an equilibrium model provides the limiting situation. The application of equilibrium thermodynamics can define the extent to which a natural water has reached chemical equilibrium even though it may be undergoing dynamic changes in fluid flow, heat flow or mass transfer. The assumption of local equilibrium is a fundamental principle of irreversible thermodynamics which permits the calculation of equilibrium properties in a system which is irreversible overall (Onsager, 1931; Thompson, 1959; Helgeson, 1968).

Chemical equilibrium models have been successfully used to calculate the chemical potentials of dissolved solutes under a range of conditions both in the laboratory and in aquatic environments. There are two basic types of models: (1) the ion association model which utilizes some form of Debye-Hückel theory along with the MacInnes convention for individual ion activities and (2) the Bronsted-Guggenheim specific ionic interaction theory which considers neutral salt components (mean activity coefficients) rather than individual ions and complexes. The ion association model is advantageous for natural water systems because of the relative abundance of thermodynamic data on mineral solubility product constants and complex stability constants, but the

model suffers from its inability to calculate accurate activities above about 0.1 molal ionic strength. The specific ionic interaction (SII) theory is considered more fundamental in principle and yields reliable activities up to several molal (Pitzer, 1973) but lacks sufficient thermodynamic data for applications to a wide range of natural waters. Useful data for the SII theory are accumulating, however, and some applications should be forthcoming in the next few years. For example, Lafon (1975) has used one form of SII theory to examine the solubility of barite and gypsum in sodium chloride solutions. Wood (1975) has successfully modeled quaternary and ternary salt brines ($I > 10$ molal) by using Harned's rule along with Scatchard's modified form of the Debye-Hückel equation. Activity coefficients for several trace components calculated from SII theory have been published by Watson and others (1975) and Whitfield (1975) for the ionic strength of sea water and up to 3 molal.

Following the introduction of an iterative calculation procedure to determine the equilibrium distribution of solutes among free ions and complexes in sea water (Garrels and Thompson, 1962), several equilibrium models, based on ion association, have been developed and applied to solution geochemistry. Paces (1972) described water-rock equilibration in the Bohemian massif; Jones and others (1974) found that dissolved aluminum and iron concentrations in stream samples agreed with solubility data on kaolinite and amorphous iron hydroxide; Helz and Sinex (1974) determined equilibrium saturation with respect to calcite and dolomite in some Virginia thermal springs; Gang and Langmuir (1974) tested several acid mine waters for solubility control by ferric oxyhydroxide, siderite, kaolinite, amorphous aluminum hydroxide, gypsum,

cobalt hydroxide, cobaltocalcite, silver and chromium hydroxide; Bricker and Troup (1975) have shown the control of iron concentrations by siderite and vivianite in Chesapeake Bay sediment waters; and Nordstrom and Jenne (1977) have shown fluorite to be an important solubility control in hot springs of the western United States.

Computer programs based on ion association theory which can compute ion activities from the temperature, pH, Eh and water analysis have been developed by Kharaka and Barnes (1973) and Truesdell and Jones (1974). These programs take into account the temperature dependence of equilibrium constants and the effects of complexing, and they output the activity products for many minerals. The PL/1 program WATEQ (Truesdell and Jones, 1974) was used to test mineral solubility equilibria in this investigation after several modifications of the original program. The experiences of Nordstrom and Jenne (1977) have shown that careful evaluation of the thermodynamic properties for the minerals and complexes which are going to be considered as solubility controls is required for a reliable testing of equilibria. For the acid mine waters studied in this investigation it was necessary to compile and evaluate the sulfate complexes for all the major cations, the hydroxide complexes of iron and aluminum, and the minerals jarosite, gypsum, and various forms of iron hydroxides. In addition, thermodynamic data on copper, zinc and cadmium complexes and minerals were added to the program. The final modified form of WATEQ used in this study has been renamed WATEQ2.

Thermodynamic Data for Metal Sulfate and Hydroxide Complexes

Published values of the association constant and association enthalpy of metal sulfate ion pairs and triplets have been compiled and evaluated numbers are listed in table 18. Stability constants of the same complex determined by different investigators show good agreement (± 10 percent) with the exception of $\text{NaSO}_4^-(\text{aq})$. The log K values for the association of $\text{NaSO}_4^-(\text{aq})$ range from 0.226 (Lafon and Truesdell, 1971) to 1.17 (Pytkowicz and Kester, 1969, as cited by Fisher, 1975, with correction to zero ionic strength). If the one low value of Lafon and Truesdell (1971) and the high values offered by Fisher and Fox (1975) and Fisher (1975) are dropped, the remaining four values average 0.70 ± 0.05 which is quite acceptable. The final value chosen was 0.72 based on an evaluation of Jenkins and Monk's (1950) data using the Fuoss equation (Siebert and Christ, pers. commun.).

After compilation of the association constants for metal sulfate complexes, the enthalpy values had to be compiled and evaluated. The discrepancies between investigators for enthalpy data were worse than for association constants. Fortunately, the temperature dependence of most of the sulfate complexes had been evaluated with the Fuoss equation (see Bockris and Reddy, 1970, p. 261) by Siebert and Christ (pers. commun.).¹ For several association constants the enthalpy derived from the Fuoss method was in good agreement with those obtained from some of the more reliable measurements. Not all stability constants

¹Enthalpies were calculated from 0° to 40°C data assuming linearity in the log K over this temperature interval.

Table 18

Log K and Enthalpies of Association for Sulfate Complexes Used
to Calculate Mineral Equilibria in Acid Mine Waters

Complex	log K	$\frac{H^\circ}{-R}$ (kcal mole ⁻¹)
NaSO_4^-	0.72	1.12
KSO_4^-	0.85	2.25
CaSO_4^0	2.31	1.47
MgSO_4^0	2.25	4.60
MnSO_4^0	2.25	3.23
FeSO_4^0	2.25	3.23
ZnSO_4^0	2.37	3.33
$\text{Zn}(\text{SO}_4)_2^{2-}$	3.28	2.64
CdSO_4^0	2.04	1.08
AlSO_4^+	3.02	2.15
$\text{Al}(\text{SO}_4)_2^-$	4.92	2.84
FeSO_4^+	3.92	3.91
$\text{Fe}(\text{SO}_4)_2^-$	5.4	4.60

can be evaluated by the Fuoss method, but the procedures are beyond the scope of this thesis.

To maintain consistency and reliability, the association constants and enthalpies for the metal sulfate complexes given in table 18 have been adopted from Siebert and Christ (pers. commun.) with one exception. The exception is the ferric double sulfate complex which was not given by Siebert and Christ. The log K for this reaction is the average of those given by Izatt and others (1972) and Mattoo (1959) which differ by less than 1 percent. The enthalpy of association has only been measured by D. J. Eatough (unpub. data) using calorimetric titration. Unfortunately, this method gives enthalpy values which are consistently lower than those derived from other types of measurements and are therefore of questionable reliability. The enthalpy value of the ferric double sulfate association was obtained by assuming that the difference between it and the single sulfate value was the same as the difference between the aluminum double sulfate and its single sulfate complex.

Association constants and enthalpies of association for ferrous, ferric, manganous and aluminum hydroxides have been evaluated by Baes and Mesmer (1974) and Mesmer and Baes (1975) as well as by Siebert and Christ (pers. commun.). There are negligible differences between the two compilations, and all the values used in this study were taken from the former authors because data covering more complexes pertinent to acid mine waters were available from them.

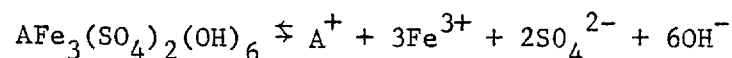
Thermodynamic Data on Jarosites, Gypsum and Other Sulfate Minerals

Limited thermodynamic data on jarosites are available and are compiled in table 19 for the three major jarosite minerals found in

Table 19
Thermodynamic Data for Three Major Jarosites

$\Delta G_{f,298}$ (kcal mole ⁻¹)	pKsp, 298	Reference
Jarosite, $\text{KFe}_3(\text{SO}_4)_2(\text{OH})_6$		
-788.64		Kashkai and others (1975)
-791.2	98.56	Vlek and others (1974)
-794		Brown (1971)
	96.5	Brown (1970) as cited by Vlek and others (1974)
-790	97.8	Zotov and others (1973)
Natrojarosite, $\text{NaFe}_3(\text{SO}_4)_2(\text{OH})_6$		
-778.37		Kashkai and others (1975)
-781.50	95.2	G. Clifton (pers. commun.)
Hydronium jarosite, $(\text{H}_3\text{O})\text{Fe}_3(\text{SO}_4)_2(\text{OH})_6$		
-772.54	82.1	Kashkai and others (1975)

nature: jarosite, natrojarosite and hydronium jarosite. The equilibrium constants are given for the reaction:



where A is Na, K or H₃O. The values reported for jarosite are in fairly good agreement and the pK of 97.8 (Zotov and others, 1973) was chosen as a reasonable average value. G. Clifton's (pers. commun.) pK of 95.2 was chosen for natrojarosite because his experiments were reversed showing approach to equilibrium, and they were run at higher temperatures to speed up reaction rates. The pK for hydronium jarosite was calculated from the free energy data of Kashkai and others (1975) using the free energies of ions from Wagman and others (1968).

No significant differences in the free energy of formation or the solubility product constant of gypsum were found among major compilations of thermodynamic data, and the original value in WATEQ of pK = 4.85 was left unchanged.

Several other sulfate minerals were added to WATEQ2 program, but further evaluation was beyond the time limitations of the thesis. Further evaluation and refinement by simultaneous multiple regression analysis such as that provided by the computer program PHAS20 (Haas and Fisher, 1976) is needed. Unfortunately, temperature dependent data which are essential for such an evaluation have not been measured for most of the minerals added to WATEQ2.

Modifications of a Water-Mineral Equilibria Computing Program for Acid Mine Water

The original computer program, WATEQ, could use a water analysis containing all of the common major constituents normally found in

natural waters. Most trace elements such as copper, zinc and cadmium which are major solutes in acid mine waters draining copper-zinc mines could not be considered in the computations. To accomodate the necessary heavy metals, WATEQ was considerably modified to yield WATEQ2.

Activity coefficients were originally calculated using the extended Debye-Hückel equation and whenever a new complex was added to the program it was necessary to estimate the α parameter. This problem was overcome by substituting the more general Davies equation which is just as reliable at low ionic strengths and usually more accurate at high ionic strengths (Butler, 1964). Since acid mine waters can have ionic strengths approaching that of sea water, it is desirable to use a theory for activity coefficients that can reach somewhat above 0.1 molal, the usual upper limit for extended Debye-Hückel calculations. The Davies equation is considered satisfactory to 0.5 molal.

The computation of ferrous and ferric iron solutes was changed, so that any one of the following situations can be considered by WATEQ2: (1) both field Eh and ferrous-ferric concentrations are input, and a calculated Eh based on ferrous and ferric ion activities can be compared to the measured field Eh; (2) field Eh and total iron are input, and the ferrous and ferric ion concentrations as well as activities are calculated from these values; and (3) only ferrous and ferric ion concentrations are input, and the Eh is calculated from the ferrous-ferric activity ratio. In the third situation the redox state of all other redox species is determined by the calculated Eh unless they are analyzed.

Chloride, fluoride, hydroxide and sulfate complexes of zinc, cadmium, copper and manganese were added to the program as well as

several oxide, carbonate and sulfate minerals of the same metals. WATEQ2 now considers a total of 186 minerals and 181 solutes with 340 equilibrium constants for activity and activity product calculations.

Activity Product Trends and Mineral Equilibria in the
Richmond-Hornet, Boulder Creek and
Spring Creek Drainages

The modifications of WATEQ which produced WATEQ2 permit the testing of acid mine waters for mineral saturation. In addition, comparison of mineral equilibria calculations with field observations of minerals that have been found to precipitate from acid mine waters can be made for the Spring Creek drainage system. By continual checking of mineral equilibria calculations with actual geologic circumstances, inaccuracies in chemical models such as WATEQ2 can be discovered, evaluated, and corrected. Much more of this type of cross-checking of equilibrium calculations must be made before definitive statements can be made as to whether certain waters show a tendency to be at equilibrium or out of equilibrium.

The saturation state of a natural water with respect to any mineral is defined by the actual chemical potential relative to the chemical potential at an equilibrium reference state. More specifically, the saturation state is measured by the saturation index or disequilibrium index (e.g. Paces, 1972): $\log AP/K$, where AP is the activity product for a mineral and K is the temperature dependent solubility product constant. Positive values for the saturation index indicate supersaturation, negative values indicate undersaturation, and zero indicates equilibrium. Since errors from analytical techniques and equilibrium thermodynamic properties are inescapable, an "equilibrium zone" of

±5 percent around the log K shall be used to bracket the region of saturation. Saturation indices must be greater than 5 percent above the log K to demonstrate supersaturation and less than 5 percent below the log K to demonstrate undersaturation.

The occurrence of mineral precipitates within the watershed partially dictates which minerals should be tested for saturation. The dominant minerals which have been found in contact with acid mine waters are described here along with any important characteristics of their X-ray diffractogram patterns.

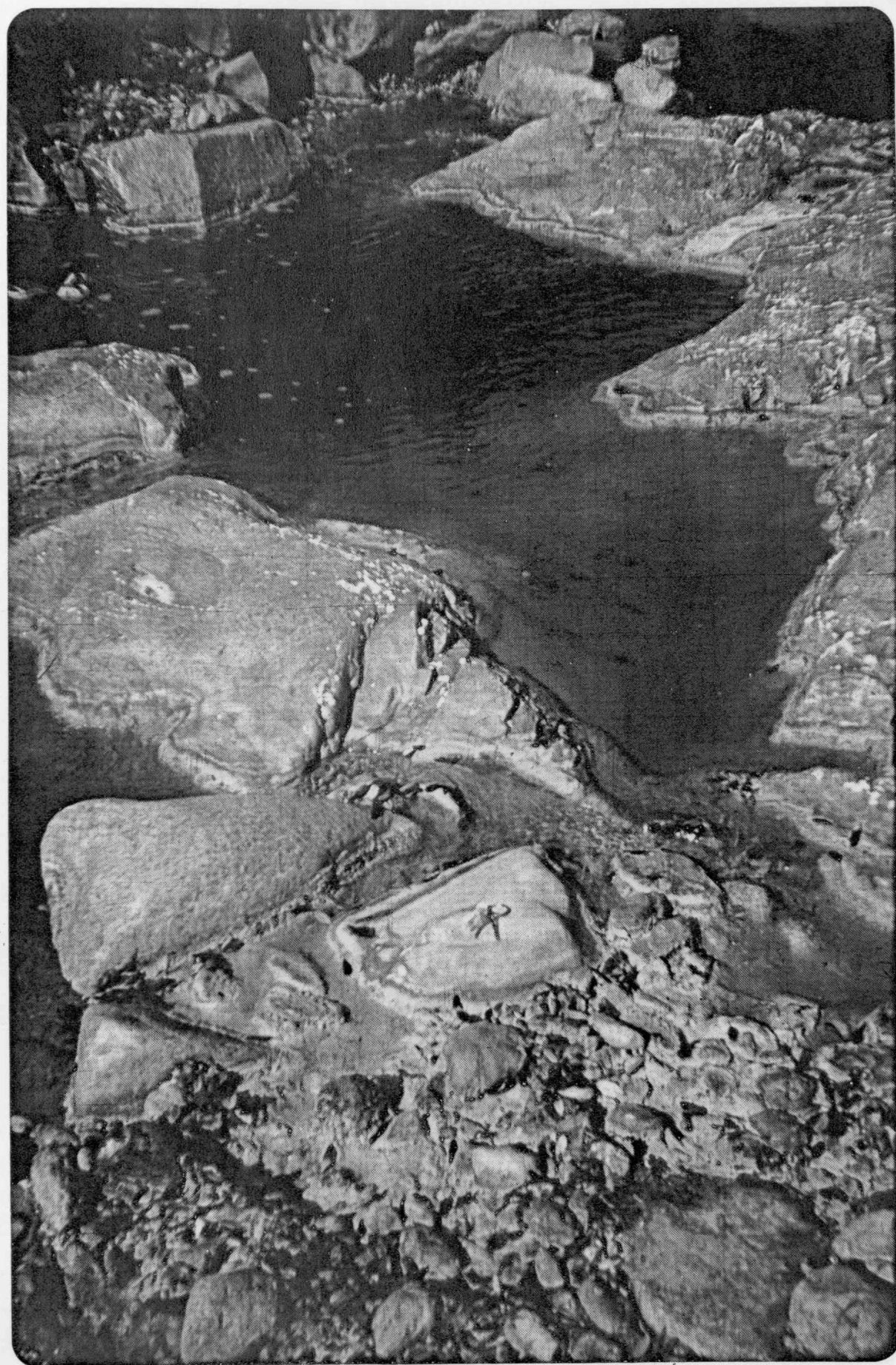
Melanterite ($\text{FeSO}_4 \cdot 7\text{H}_2\text{O}$)

Pale-blue-green clusters of crystals are often found on the surface of massive sulfide ore and may contain variable amounts of copper, zinc, and magnesium either as separate phases (i.e. chalcantinite, goslarite and epsomite) or as solid substitution. The exposed surface of the Brick Flat ore body often shows well-developed crusts of melanterite. Crystals are also found lining the flume which collects the Richmond-Hornet effluent. Since several hydrated sulfate minerals (such as melanterite and chalcantinite) have very similar structure, their X-ray patterns tend to be very similar.

Jarosite ($\text{KFe}_3(\text{SO}_4)_2(\text{OH})_6$)

A fine-grained yellow precipitate forms in Boulder Creek every summer and fall (pl. 6) which when washed and filtered gives a good X-ray pattern for potassium jarosite. A wet sample (containing acid mine water and bacterial slime) gives a poor diffractogram pattern. The ratio of the peak intensities indicates that the material is

Plate 6. Precipitation of jarosite minerals (yellow) and efflorescent sulfate minerals (white crusts) in Boulder Creek at site G. Keys on rock in foreground provide scale.



dominantly potassium jarosite and that natrojarosite or hydronium jarosite is either absent or present in small amounts.

Goethite (FeOOH)

Fine-grained, orange-brown precipitates in Spring Creek show the main peak for goethite on an X-ray pattern, but the material is very poorly crystalline. Darker layers of iron oxyhydroxide (goethite) have been found on the surface of stable cobbles and boulders in the creek, and they give the appearance of having been aged and polished by the stream water. These dark layers show greater crystallinity as evidenced by their X-ray patterns.

Soda alum (NaAl(SO₄)₂·12H₂O)

Near the outlet from Spring Creek Dam, an abundance of white and yellow efflorescent crusts, which form by reaction of the albite granite (scattered rockfill for dam) with the acid waters of Spring Creek, occur at the water's edge. Pools on either side of the discharge buttresses are not flowing or circulating significantly, and there tends to be a build-up of mineral crusts along the pool's edges. The white crusts are dominantly composed of soda alum which is preferentially produced over potash alum because of the abundance of sodium in the albite granite.

The high calcium, magnesium and sulfate content of these acid mine waters suggests that gypsum and epsomite should be considered for mineral saturation, although they have not been found as naturally occurring.

The results of the mineral equilibria calculations compare favorably with field observations. In figure 19 the saturation indices for

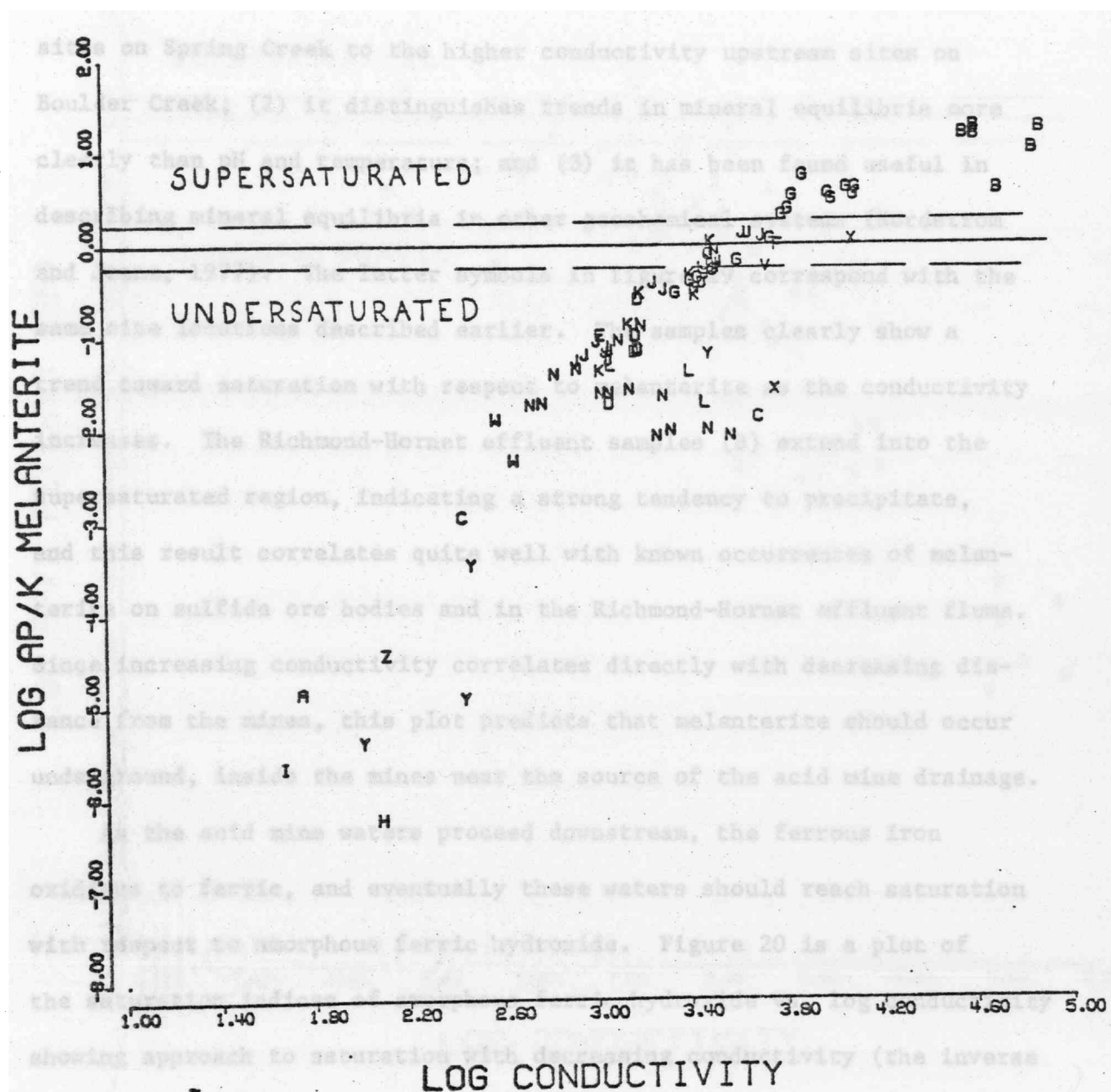


Figure 19. Saturation indices for melanterite as a function of the log conductivity showing that supersaturation is reached in the Hornet-Richmond effluent.

melanterite are plotted against the log conductivities. Log conductivity has been chosen as the independent variable because (1) it corresponds to a spatial change from the lower conductivity downstream sites on Spring Creek to the higher conductivity upstream sites on Boulder Creek; (2) it distinguishes trends in mineral equilibria more clearly than pH and temperature; and (3) it has been found useful in describing mineral equilibria in other geochemical systems (Nordstrom and Jenne, 1977). The letter symbols in figure 19 correspond with the same site locations described earlier. The samples clearly show a trend toward saturation with respect to melanterite as the conductivity increases. The Richmond-Hornet effluent samples (B) extend into the supersaturated region, indicating a strong tendency to precipitate, and this result correlates quite well with known occurrences of melanterite on sulfide ore bodies and in the Richmond-Hornet effluent flume. Since increasing conductivity correlates directly with decreasing distance from the mines, this plot predicts that melanterite should occur underground, inside the mines near the source of the acid mine drainage.

As the acid mine waters proceed downstream, the ferrous iron oxidizes to ferric, and eventually these waters should reach saturation with respect to amorphous ferric hydroxide. Figure 20 is a plot of the saturation indices of amorphous ferric hydroxide vs. log conductivity showing approach to saturation with decreasing conductivity (the inverse of fig. 19). Most of the samples for the lower sites on Spring Creek (J, L, N) fall within the equilibrium zone for amorphous iron hydroxide which correlates well with the known oxidation kinetics of dissolved iron in Spring Creek and the fine-grained nature of the iron hydroxides found there. Figure 21 plots the saturation index for goethite and

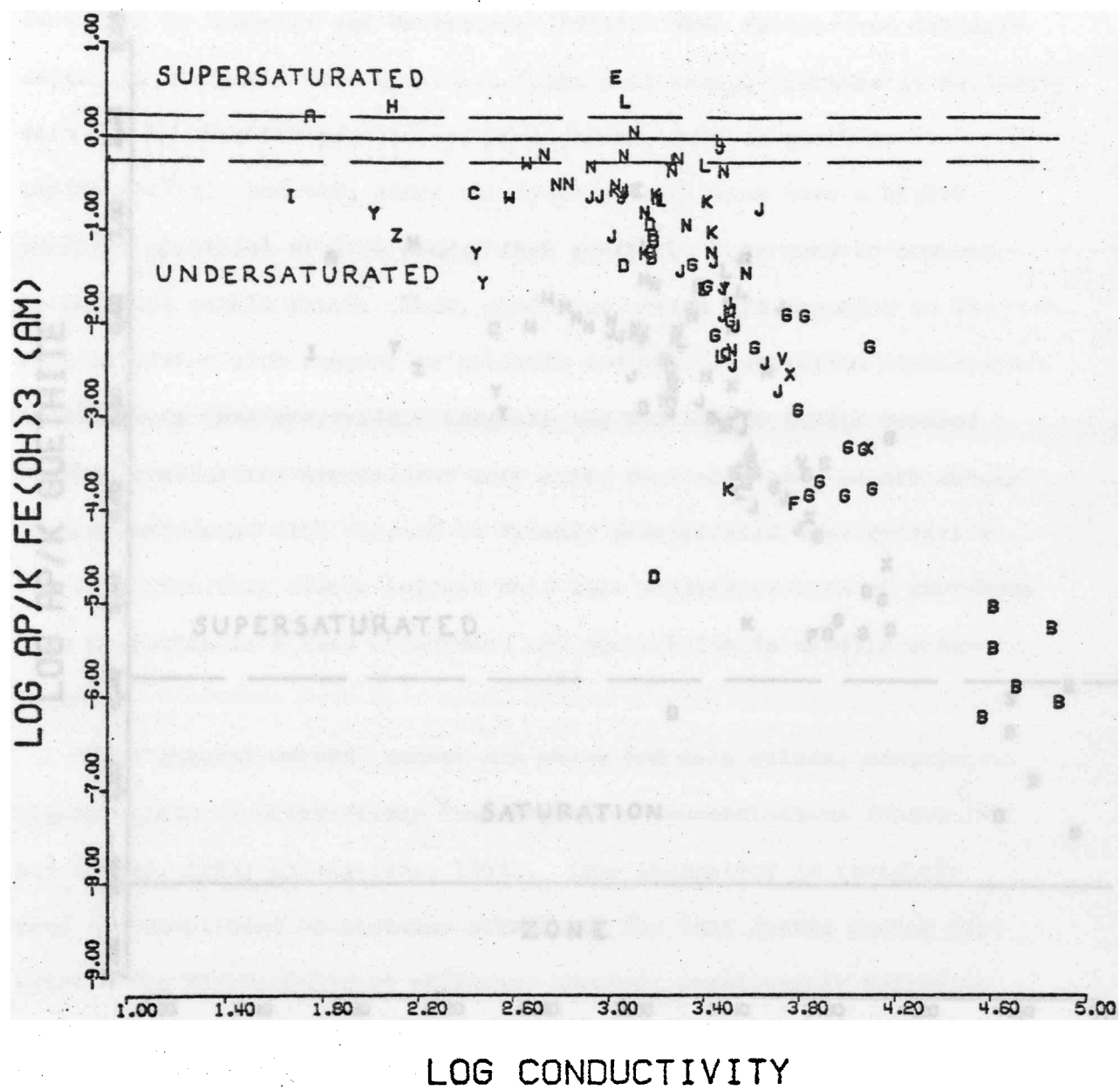


Figure 20. Saturation indices for amorphous iron hydroxide showing that saturation is reached by the diluted downstream waters.

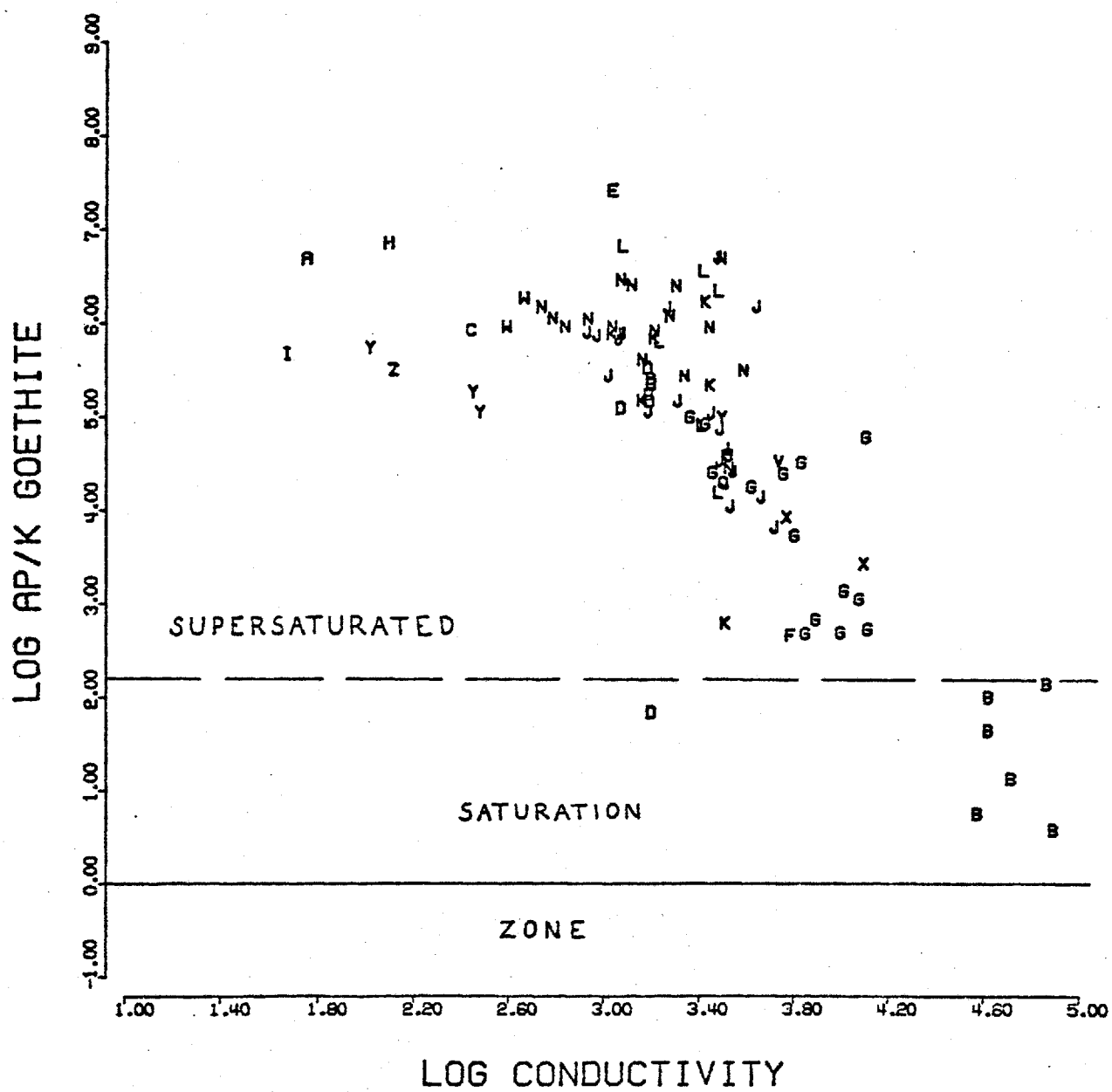


Figure 21. Saturation indices for goethite demonstrating supersaturation for nearly all of the samples.

shows nearly all of the samples are supersaturated. The relationship between freshly precipitated iron hydroxide and goethite has been described by Langmuir and Whittemore (1971). When ferric iron precipitates, an amorphous iron hydroxide forms most readily because it nucleates more easily than the more crystalline phases, such as goethite or lepidocrocite. However, since the fresh precipitates have a higher chemical potential or free energy than goethite, they tend to convert to the more stable phase. Thus, acid mine waters are expected to be supersaturated with respect to goethite and near equilibrium with respect to amorphous iron hydroxide. Langmuir and Whittemore (1971) reached similar conclusions except that they state that acid mine waters should be supersaturated with respect to freshly precipitated iron hydroxide. The data from this thesis suggest that this supersaturation of amorphous iron hydroxide is a rare occurrence and equilibrium is usually maintained.

Most natural waters, except sea water and salt brines, contain higher calcium concentrations than magnesium concentrations (White and others, 1963; Livingstone, 1963). This inequality is certainly true for unpolluted mountainous streams in the West Shasta mining district. The Richmond-Hornet effluent, however, consistently maintains higher magnesium values than calcium. The abrupt change in the calcium to magnesium ratio can be explained by the limiting solubility of gypsum during the decomposition of Balaklala Rhyolite by acid mine waters. Increasing amounts of calcium and magnesium are leached from the rhyolite until saturation is reached with respect to gypsum, and then calcium concentrations are prevented from increasing further because of the precipitation of gypsum. The first magnesium sulfate mineral likely

to precipitate is epsomite, but its solubility is much greater than gypsum, and it is more commonly found with oxidizing ore bodies which have a high magnesium content in the country rock (such as at Almaden, California, or the Gilman district, Colorado). In figures 22 and 23, the saturation indices for gypsum and epsomite are plotted. These plots indicate that, as one approaches the higher conductivity waters and the source of the acid mine water production, gypsum saturation is reached whereas the waters remain undersaturated with respect to epsomite.

In summary, activity product calculations on several minerals expected or observed to occur in acid mine waters demonstrate the tendency for soluble sulfate minerals to precipitate at or close to the source of the oxidizing ore bodies. As acid mine waters are transported and diluted downstream a greater tendency for ferric iron minerals to precipitate is observed, in keeping with field observations. These calculations provide a means of determining water-rock reactions in subsurface environments that are inaccessible to direct observation and they assist predictions of solute-discharge patterns with changing weather conditions.

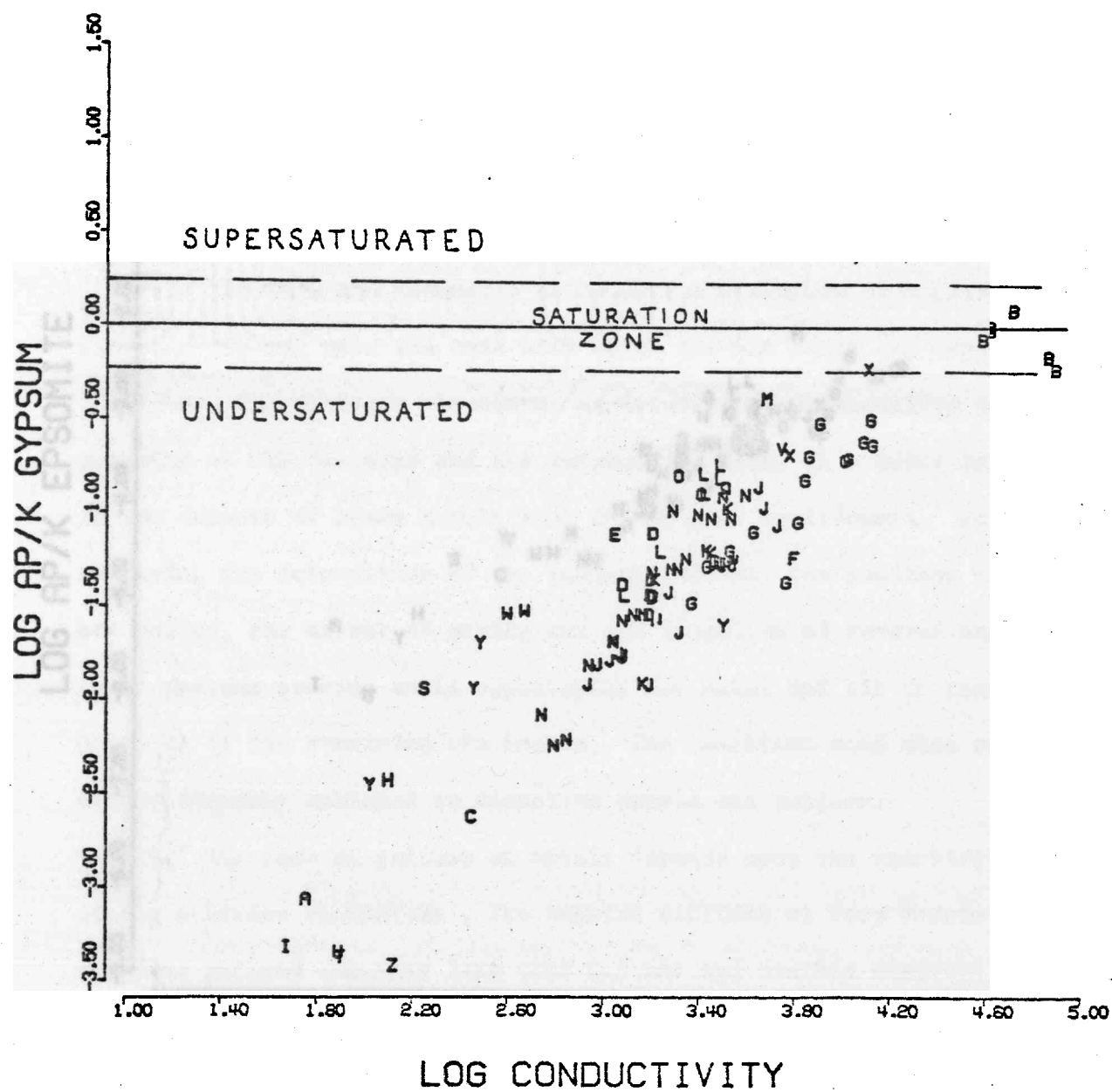


Figure 22. Saturation indices for gypsum indicating saturation is reached in the undiluted mine waters issuing directly from the mines.

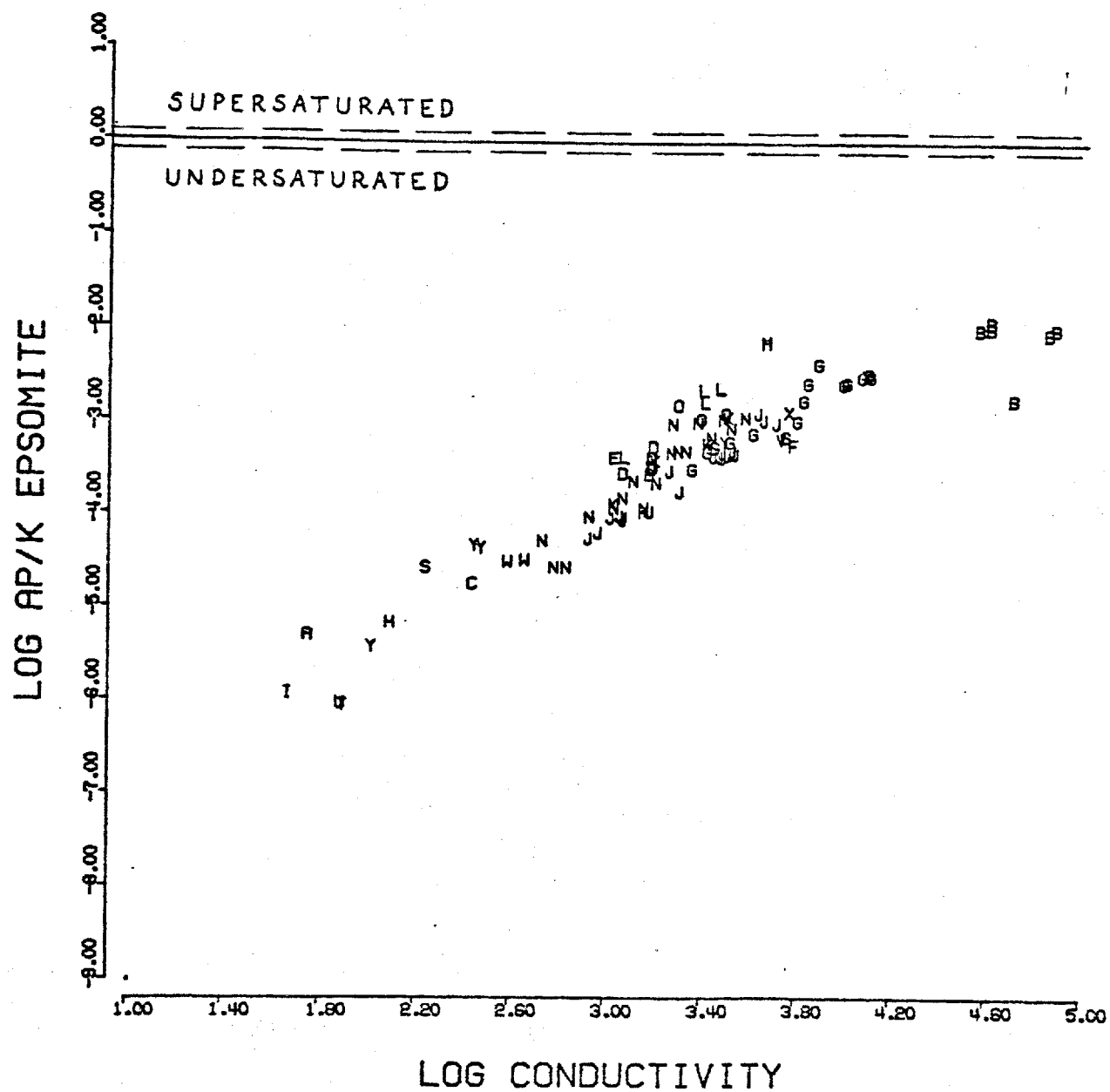


Figure 23. Saturation indices for epsomite showing that saturation is never reached by these waters.

CONCLUSIONS

A detailed investigation of acid mine drainage in the Spring Creek watershed has shown that several important factors affect the release, transport and destination of heavy metals mobilized during the oxidation of massive sulfide deposits.

1. The rate and intensity of oxidative breakdown of sulfide deposits depends upon the ease with which air and water can reach the sulfides. The geologic structure, especially the permeability and porosity of the deposits and the surrounding rocks is a major factor in the release of heavy metals into the aquatic environment. At Iron Mountain, the deformation of the volcanic strata, the position of the ore bodies, the extent of mining and the locations of several major fault systems provide ample opportunity for water and air to reach large portions of the remaining ore bodies. The resultant acid mine effluent is considerably enriched in dissolved metals and sulfate.

2. The rate of release of metals depends upon the reactivity of the sulfides themselves. The massive sulfides at Iron Mountain are fine grained (usually less than 0.5 mm) and contain numerous fractures which help to make the sulfides react quite readily. The composition and mineralogy of the sulfides (mainly pyrite, sphalerite and chalcopyrite) determine the major metal concentrations in the acid mine effluent (iron, zinc and copper).

3. The composition and mineralogy of the major rock types in the watershed determine the concentrations of common metal cations in the

drainage and affect the degree of acid development and total dissolved solid concentrations. No neutralizing rock types such as limestone or dolomite strata occur in the Spring Creek region and since the common rock-forming silicates are poor neutralizers of acid waters, pH values as low as 0.8 and sulfate concentrations (roughly half of the total dissolved solids) of 50,000 mg/l are produced.

4. The presence of *Thiobacillus ferrooxidans* appreciably increases the oxidation rate of iron sulfide and of dissolved ferrous iron in the effluent water. Downstream rates of ferrous iron oxidation can be as high as 3.0 mM/hr when sufficient bacteria are present. The bacterial catalysis of ferrous iron oxidation leads to high concentrations of ferric iron and forces the precipitation of jarosite in low pH (<2.0) waters and ferric hydroxide in slightly higher pH (2.0 to 4.0) waters. Without bacterial oxidation all of the iron would remain dissolved in the drainage system.

5. Large variations in solute concentrations of stream waters containing acid mine drainage can be observed over long term (1 year or more) and short term (3 days) intervals. Rainfall history, relative drainage areas and resultant discharge patterns all have an important role in determining solute concentrations in different parts of the Spring Creek watershed at different times. For Spring Creek itself the largest load of metals occurs within a few hours of the initial onset of a rainstorm.

6. Solute concentrations, especially heavy metals, can be decreased and increased by precipitation and dissolution of soluble sulfate minerals such as melanterite. In Boulder Creek the solute concentrations

rose during the first few hours of a rainstorm due to dissolution of soluble sulfates occurring along the edge of the stream.

7. Mineral solubilities play an important role in providing an upper limit to observed solute concentrations. WATEQ2, a mineral equilibria computer model developed for acid mine waters, has proven successful in demonstrating that waters in the Spring Creek region reach saturation with respect to melanterite, amorphous iron hydroxide and gypsum. Further results from this investigation have demonstrated that field Eh measurements in acid mine waters can be thermodynamically related to the ferrous-ferric redox couple.

REFERENCES

- Ahluwalia, J. C., and Cobble, J. W., 1964, The thermodynamic properties of high temperature aqueous solutions. III. The partial molal heat capacities of hydrochloric acid from 0 to 100° and the third-law potentials of the silver-silver chloride and calomel electrodes from 0 to 100°: Jour. Phys. Chem., v. 86, p. 5381-5384.
- Albers, J. P., 1961, Gold deposits in the French Gulch-Deadwood district, Shasta and Trinity Counties, California: U. S. Geol. Survey Prof. Paper 424-C, p. 1-4.
- 1964, Geology of the French Gulch quadrangle, Shasta and Trinity Counties, California: U. S. Geol. Survey Bull. 1141-J, p. 1-70.
- 1966, Economic deposits of the Klamath Mountains: Calif. Div. Mines and Geology Bull. 190, p. 51-60.
- Alexander, M., 1961, Introduction to Soil Microbiology: New York, Wiley and Sons, 472 p.
- Aubury, L. E., 1905, The copper resources of California: Calif. Min. Bur. Bull. 23, 282 p.
- 1908, The copper resources of California: Calif. Min. Bur. Bull. 50, p. 38-114.
- Bass-Becking, L. G. M., Kaplan, I. R., and Moore, D., 1960, Limits of the natural environment in terms of pH and oxidation-reduction potentials: Jour. Geology, v. 68, p. 243-284.
- Baes, C. F., Jr., and Mesmer, R. E., 1974, The hydrolysis of cations, a critical review of hydrolytic species and their stability constants in aqueous solutions, pt. I: ORNL-NSF-EATC-3.
- Baker, R. A., 1972, Evaluation of pyritic oxidation by Mossbauer spectrometry: Water Res., v. 6, p. 9-17.
- Bates, R. G., 1973, Determination of pH: New York, Wiley and Sons, 479 p.
- Beck, J. V., and Brown, G. D., 1968, Direct sulfide oxidation in the solubilization of sulfide ores by *Thiobacillus ferrooxidans*, Jour. Bacteriol., v. 96, p. 1433-1434.
- Beck, J. V., and Hatch, A. L., 1969, Effect of ferric iron and the oxidation of iron and copper sulfide ores by *Thiobacillus ferrooxidans*: Bacteriol. Proc., v. 64.

- Belly, R. T., Bohlool, B. B., and Brock, T. D., 1973, The genus *Thermoplasma*, in Mycoplasma and mycoplasma-like agents of human, animal and plant diseases: Ann. New York Acad. Sci., v. 225, p. 94-107.
- Belly, R. T., and Brock, T. D., 1974, Widespread occurrence of acidophilic strains of *Bacillus coagulans* in hot springs: Jour. Appl. Bact., v. 37, p. 175-177.
- Bennett, H. D., 1969, Algae in relation to mine water: Castanea, v. 34, p. 306-331.
- Berner, R. A., 1963, Electrode studies of hydrogen sulfide in marine sediments: Geochim. et Cosmochim. Acta, v. 27, p. 563-575.
- de Bethune, A. J., and Loud, N. A. S., 1964, Standard aqueous electrode potentials and temperature coefficients at 25°C: Skokie, Ill., C. A. Hampel, 19 p.
- Bloomfield, C., 1972, The oxidation of iron sulfides in soils in relation to the formation of acid sulfate soils, and of ochre deposits in field drains: Jour. Soil Sci., v. 23, p. 1-16.
- Bockris, J. O'M., and Reddy, A. K. N., 1970, Modern Electrochemistry, an introduction to an interdisciplinary area, v. 1: New York, Plenum Press, 622 p.
- Bohlool, B. B., and Brock, T. D., 1974, Immunofluorescence approach to the study of the ecology of *Thermoplasma acidophilum* in coal refuse material: Appl. Microbiol., v. 28, p. 11-16.
- Bricker, O. P., III, and Troup, B. N., 1975, Sediment-water exchange in Chesapeake Bay, in Chemistry, biology and the estuarine system, v. 1 of Estuarine Research: New York, Academic Press, Inc., p. 3-27.
- Brock, T. D., 1973, Lower pH limit for the existence of blue-green algae: evolutionary and ecological implications: Science, v. 179, p. 480-483.
- 1974, Biology of Microorganisms, 2d ed.: New York, Prentice-Hall, 852 p.
- Brock, T. D., Brock, K. M., Belly, R. T., and Weiss, R. L., 1972, *Sulfolobus*: a new genus of sulfur-oxidizing bacteria living at low pH and high temperature: Arch. Mikrobiol., v. 84, p. 54-68.
- Brown, J. B., 1970, A chemical study of some synthetic potassium-hydroxide jarosites: Am. Mineralogist, v. 10, p. 696-703.
- 1971, Jarosite-goethite stabilities at 25°C, 1 atm: Mineral. Deposita, v. 6, p. 245-252.
- Bryner, L. C., and Anderson, R., 1957, Microorganisms in leaching sulfide minerals: Ind. Eng. Chem., v. 49, p. 1721-1724.

- Bryner, L. C., Beck, J. V., Davis, D. B., and Wilson, D. G., 1954, Microorganisms in leaching sulfide minerals: *Ind. Eng. Chem.*, v. 46, p. 2587-2592.
- Bryner, L. C., and Jameson, A. K., 1958, Microorganisms in leaching sulfide minerals: *Appl. Microbiol.*, v. 6, p. 281-287.
- Bryner, L. C., and Jones, S. W., 1965, Studies on microbial leaching of sulfide minerals: *Dev. Ind. Microbiol.*, v. 7, p. 287-297.
- Buchanan, R. E., and Gibbon, N. E., eds., 1974, *Bergey's manual of determinative bacteriology*, 8th ed.: Baltimore, William and Wilkins Co., 1246 p.
- Burchfiel, B. C., and Davis, G. A., 1972, Structural framework and evolution of the southern part of the Cordilleran orogen, western United States: *Am. Jour. Sci.*, v. 272, p. 97-118.
- 1975, Nature and controls of Cordilleran orogenesis, western United States: extensions of an earlier synthesis: *Am. Jour. Sci.*, v. 275-A, p. 363-396.
- Burkin, A. R., 1966, *The chemistry of hydrometallurgical processes*: Princeton, New Jersey, Van Nostrand Inc., 157 p.
- Butler, J. N., 1964, *Ionic equilibrium, a mathematical approach*: New York, Addison-Wesley, 547 p.
- Charlot, G., 1971, *Selected constants, oxidation-reduction potentials of inorganic substances in aqueous solutions*: London, Butterworths, IUPAC, Anal. Chem. Div.
- Chateau, H., 1954, Determinations precises des potentiels de reference donnees par les electrodes au calomel entre 5 et 70°C: *J. de Chimie Physique*, v. 51, p. 590-593.
- Christensen, J. J., Eatough, D. J., and Izatt, R. M., 1975, *Handbook of metal ligand heats and related thermodynamic quantities*, 2d ed.: New York, Marcel Dekker, 495 p.
- Colmer, A. R., and Hinkle, M. E., 1947, The role of microorganisms in acid mine drainage: a preliminary report: *Science*, v. 106, p. 253-256.
- Colmer, A. R., Temple, K. L., and Hinkle, M. E., 1950, An iron-oxidizing bacterium from the acid drainage of some bituminous coal mines: *Jour. Bacteriol.*, v. 59, p. 317-328.
- Corrick, J. D., and Sutton, J. A., 1961, Three chemosynthetic autotrophic bacteria important to leaching operations at Arizona copper mines: *U. S. Bur. Mines Rep. Inv.* 5718, 8 p.

- Corrick, J. D., and Sutton, J. A., 1965, Copper extraction from a low-grade ore by *Ferrobacillus ferrooxidans*: effect of environmental and nutritional factors: U. S. Bur. Mines Rep. Inv. 6714, 21 p.
- Covington, A. K., 1969, Reference electrodes, ch. 4 of *Ion-Selective Electrodes*: N.B.S. Spec. Pub. 314, p. 107-141.
- Curtis, G. H., Evernden, J. F., and Lipson, J. I., 1958, Age determination of some granitic rocks in California by the K-Ar method: Calif. Div. Mines Spec. Rept. 54, 16 p.
- Daniels, S. L., 1972, The adsorption of microorganisms onto solid surfaces: a review: *Dev. Ind. Microbiol.*, v. 13, p. 211-253.
- Darland, G., Brock, T. D., Samsonoff, W., and Conti, S. F., 1970, A thermophilic, acidophilic mycoplasma isolated from a coal refuse pile: *Science*, v. 170, p. 1416-1418.
- Davis, G. A., 1966, Metamorphic and granitic history of the Klamath Mountains: *Calif. Div. Mines and Geology Bull.* 190, p. 39-50.
- 1969, Tectonic correlations, Klamath Mountains and western Sierra Nevada, California: *Geol. Soc. America Bull.* 80, p. 1095-1108.
- Davis, S. N., and DeWiest, R. J. M., 1966, *Hydrogeology*: New York, John Wiley and Sons, 463 p.
- DeCuyper, J. A., 1964, Bacterial leaching of low grade copper and cobalt ores: *Metall. Soc. Conf., Can. Met. Quart.*, v. 3, p. 43-45.
- Dickinson, W. R., 1970, Relations of andesites, granites, and derivative sandstones to arc-trench tectonics: *Geophys. Space Phys. Rev.*, v. 8, p. 812-860.
- Doemel, W. N., and Brock, T. D., 1971, The physiological ecology of *Cyanidium caldarium*: *Jour. Gen. Micro.*, v. 67, p. 17-32.
- Doyle, R. W., 1968, The origin of the ferrous ion-ferric oxide Nernst potential in environments containing dissolved ferrous iron: *Am. Jour. Sci.*, v. 266, p. 840-859.
- Dugan, P. R., MacMillan, C. B., and Pfister, R. M., 1970a, Aerobic heterotrophic bacteria indigenous to pH 2.8 acid mine water: microscopic examination of acid streamers: *Jour. Bacteriol.*, v. 101, p. 973-981.
- 1970b, Aerobic heterotrophic bacteria indigenous to pH 2.8 acid mine water: predominant slime-producing bacteria in acid streamers: *Jour. Bacteriol.*, v. 101, p. 982-988.

- Duncan, D. W., and Trussell, P. C., 1964, Advances in the microbiological leaching of sulfide ores: *Can. Met. Quart.*, v. 3, p. 43-55.
- Duncan, D. W., Trussell, P. C., and Walden, C. C., 1964, Leaching of chalcopyrite with *Thiobacillus ferrooxidans*: effect of surfactants and shaking: *Appl. Microbiol.*, v. 12, p. 122-126.
- Duncan, D. W., and Walden, C. C., 1972, Microbiological leaching in the presence of ferric iron: *Dev. Ind. Microbiol.*, v. 13, p. 66-75.
- Eaton, W. A., George, O., and Hanania, G. I. H., 1967, Thermodynamic aspects of the potassium hexacyanoferrate (III)-(II) system. I. Ion association: *Jour. Phys. Chem.*, v. 71, p. 2016-2021.
- Ehrlich, H. L., 1963a, Bacterial action on orpiment: *Econ. Geology*, v. 58, p. 991-994.
- 1963b, Microorganisms in acid drainage from a copper mine: *Jour. Bacteriol.*, v. 86, p. 350-352.
- 1964, Bacterial oxidation of arsenopyrite and enargite, *Econ. Geology*, v. 59, p. 1306-1312.
- Ferguson, J., and Bubella, B., 1974, The concentration of Cu (II), Pb (II) and Zn (II) from aqueous solutions by particulate algal matter: *Chem. Geology*, v. 13, p. 163-186.
- Fisher, F. H., 1975, Dissociation of Na_2SO_4 from ultrasonic-absorption reduction in MgSO_4 - NaCl solutions: *Jour. Sol. Chem.*, v. 4, p. 237-240.
- Fisher, F. H., and Fox, A. P., 1975, NaSO_4^- ion pairs in aqueous solutions at pressures up to 2000 atm: *Jour. Sol. Chem.*, v. 4, p. 225-236.
- Fleischer, M., 1955, Minor elements in some sulfide minerals: *Econ. Geology*, 50th Anniv. Vol., p. 970-1024.
- Fott, B., McCarthy, A. J., and McCarthy, S. J., 1964, Three acidophilic volvocine flagellates in pure cultures: *Jour. Protozool.*, v. 11, p. 116-120.
- Gang, M. W., and Langmuir, D., 1974, Controls on heavy metals in surface and ground waters affected by coal mine drainage; Clarion River-Redbank Creek watershed, Pennsylvania: *Natl. Coal Assoc.*, 5th Symp. on Coal Mine Drainage Res., p. 39-69.
- Garrels, R. M., 1960, *Mineral Equilibria*: New York, Harper and Brothers, 254 p.

- Garrels, R. M., and Christ, C. L., 1965, *Solutions, Minerals and Equilibria*: New York, Harper and Row, 450 p.
- Garrels, R. M., and Thompson, M. E., 1960, Oxidation of pyrite in ferric sulfate solution: *Am. Jour. Sci.*, v. 258, p. 57-67.
- 1962, A chemical model for sea water at 25°C and one atmosphere total pressure: *Am. Jour. Sci.*, v. 260, p. 57-66.
- Haas, J. L., Jr., and Fisher, J., 1976, Simultaneous evaluation and correlation of thermodynamic data: *Am. Jour. Sci.*, v. 276, p. 525-545.
- Hanania, G. I. H., Irvine, D. H., Eaton, W. A., and George, P., 1967, Thermodynamic aspects of the potassium hexacyanoferrate (III)-(II) system. II. Reduction potential: *Jour. Phys. Chem.*, v. 71, p. 2022-2030.
- Harned, H. S., and Owen, B. B., 1958, *The Physical Chemistry of Electrolytic Solutions*, 3d ed.: New York, Reinhold Pub. Corp., 354 p.
- Helgeson, H. C., 1968, Evaluation of irreversible reactions in geochemical processes involving minerals and aqueous solutions, I. Thermodynamic relations: *Geochim. et Cosmochim. Acta*, v. 32, p. 853-877.
- Helz, G. G., and Sinex, S. A., 1974, Chemical equilibria in the thermal spring waters of Virginia: *Geochim. et Cosmochim. Acta*, v. 38, p. 1807-1820.
- Hem, J. D., 1960, Complexes of ferrous iron with tannic acid: U. S. Geol. Survey Water-Supply Paper 1459-D, 94 p.
- Hemley, J. J., and Jones, W. R., 1964, Chemical aspects of hydrothermal alteration with emphasis on hydrogen metasomatism: *Econ. Geology*, v. 59, p. 538-569.
- Hepler, J. R., Sweet, J. R., and Jesser, R. A., 1960, Thermodynamics of aqueous ferricyanide, ferrocyanide, and cobalticyanide ions: *Jour. Am. Chem. Soc.*, v. 82, p. 304-306.
- Hinds, N. E. A., 1933, Geologic formations of the Redding-Weaverville districts, northern California: *Calif. Jour. Mines Geology*, v. 29, p. 76-122.
- Hollister, V. F., and Evans, J. R., 1965, *Geology of the Redding quadrangle, Shasta County, California*: Calif. Div. Mines Geology Map Sheet 4.
- Hutchinson, M., Johnstone, K. I., and White, D., 1966, Taxonomy of the acidophilic *Thiobacilli*: *Jour. Gen. Microbiol.*, v. 44, p. 373-381.

- Hutchinson, M., Johnstone, K. I., and White, D., 1969, Taxonomy of the genus *Thiobacillus*: the outcome of numerical taxonomy applied to the group as a whole: Jour. Gen. Microbiol., v. 57, p. 397-410.
- Irwin, W. P., 1966, Geology of the Klamath Mountains province: Calif. Div. Mines Geology Bull. 190, p. 17-37.
- Ivanon, V. I., Nagirnyak, F. F., and Stepanov, B. A., 1962, Bacterial oxidation of sulfide ores: Microbiology [U.S.S.R., English trans.], v. 30, p. 575-578.
- Ivarson, K. C., 1973, Microbiological formation of basic ferric sulfates: Can. Jour. Soil Sci., v. 53, p. 315-323.
- Izatt, R. M., Eatough, D. J., and Christensen, J. J., 1972, unpub. data.
- Jackson, J. T., Moriarty, D. J. H., and Nicholas, D. J. D., 1968, Deoxyribonucleic acid base composition of the *Thiobacilli* and some nitrifying bacteria: Jour. Gen. Microbiol., v. 53, p. 53-60.
- Jayson, G. G., Parsons, B. J., and Swallow, A. J., 1972, Oxidation of ferrous ions by hydroxyl radicals: Jour. Chem. Soc., Far. Trans., v. 11, p. 2053-2058.
- Jenkins, I. L., and Monk, C. B., 1950, The conductances of sodium, potassium and lanthanum sulfates at 25°C: Jour. Am. Chem. Soc., v. 72, p. 2695-2698.
- Jenne, E. A., 1968, Controls on Mn, Fe, Co, Ni, Cu, and Zn concentrations in soils and waters: the significant role of hydrous Mn and Fe oxides, in Trace Inorganics in Water: Am. Chem. Soc. Series no. 73, p. 337-387.
- Jones, B. R., Kennedy, V. C., and Zellweger, G. W., 1974, Comparison of observed and calculated concentrations of dissolved Al and Fe in stream water: Water Resources Res., v. 10, p. 791-793.
- Joseph, J. M., 1953, Microbiological study of acid mine waters: preliminary report: Ohio Jour. Sci., v. 53, p. 123-127.
- Kashkai, C., Borovskaya, Y. B., and Babozade, M. A., 1975, $\Delta G_{f,298}^{\circ}$ determination of synthetic jarosite and its sulfate analogues: Geokhimiya, v. 5, p. 778-784.
- Kessler, E., 1967, Physiologische and biochemische Beiträge zur Taxonomie der Gattung *Chlorella*. III. Merkmale von 8 autotrophen: Arten. Archiv. für Mikrobiologie, v. 55, p. 356-357.
- Kett, W. F., 1947, Fifty years of operation by the Mountain Copper Company, Ltd., in Shasta County, California: Calif. Jour. Mines Geology, v. 43, p. 105-162.

- Kharaka, Y. K., and Barnes, I., 1973, SOLMNEQ: Solution-mineral equilibrium computations: U. S. Geol. Survey Computer Contr., U. S. Dept. Commerce, Natl. Tech. Inf. Service, Springfield, Va. 22151, Rept. PB-215 899, 82 p.
- Kinkel, A. R., Jr., Hall, W. E., and Albers, J. P., 1956, Geology and base-metal deposits of the West Shasta copper-zinc district, Shasta County, California: U. S. Geol. Survey Prof. Paper 285, 156 p.
- Kolthoff, I. M., and Tomsicek, W. J., 1935, The oxidation potential of the system potassium ferrocyanide-potassium ferricyanide at various ionic strengths: Jour. Phys. Chem., v. 39, p. 945-954.
- Kuznetsov, S. I., Ivanov, M. V., and Lyalikova, N. N., 1963, Introduction to Geological Microbiology: New York, McGraw-Hill Book Co., 252 p.
- Lacey, D. T., and Lawson, F., 1970, Kinetics of the liquid-phase oxidation of acid ferrous sulfate by the bacterium *Thiobacillus ferrooxidans*: Biotech. Bioeng., v. 12, p. 29-50.
- Lackey, J. B., 1938, The flora and fauna of surface waters polluted by acid mine drainage: Public Health Rep., v. 53, p. 1499-1507.
- Lafon, G. M., 1975, The calculation of chemical potentials in natural waters. Application to mixed chloride-sulfate solutions, in Marine Chemistry in the Coastal Environment, T. M. Church, ed.: Am. Chem. Soc. Symposium Ser. 18, Am. Chem. Soc., p. 97-111.
- Lafon, G. M., and Truesdell, A. H., 1971, Temperature dependence of sodium sulfate complexing in aqueous solutions [abs.]: Am. Geophys. Union Trans., v. 52, p. 362.
- Langmuir, D., 1971, Eh-pH determinations, in Carver, R. E., ed., Proceedings in Sedimentary Geology: New York, Wiley-Interscience, p. 598-635.
- Langmuir, D., and Whittemore, D. O., 1971, Variations in the stability of precipitated ferric oxyhydroxides, in Nonequilibrium systems in natural water chemistry: Am. Chem. Soc., Ser. no. 106, p. 209-234.
- Laskin, A. I., and Lechevalier, H. A., eds., 1973, Handbook of Microbiology: CRC Press.
- Lazaroff, N., 1963, Sulfate requirement for iron oxidation by *Thiobacillus ferrooxidans*: Jour. Bacteriol., v. 85, p. 78-83.
- Leathen, W. W., Kinsel, N., and Braley, S. A., 1956, *Ferrobacillus ferrooxidans*, a chemosynthetic autotrophic bacterium: Jour. Bacteriol., v. 72, p. 700-704.

- Lewis, G. N., and Randall, M., 1961, Thermodynamics: New York, McGraw-Hill Book Co., 723 p.
- Lewis, R. H., 1963, Recommended flow releases from Spring Creek debris dam for the protection of salmonid fishes in the Sacramento River: Calif. Dept. Fish and Game Rept., unpub., 8 p.
- Lin, J., and Breck, W. G., 1965, Entropy differences for some related pairs of complex ions: Can. Jour. Chem., v. 43, p. 766-771.
- Livingstone, D. E., 1963, Chemical composition of rivers and lakes: U. S. Geol. Survey Prof. Paper 440-G, 64 p.
- Lloyd, R., 1965, Factors which affect the tolerance of fish to heavy metal poisoning, *in* Biological Problems in Water Pollution: U. S. Dept. Health, Educ., Welfare, 3d seminar, Aug. 13-17, 1962, Public Health Service 999-WP-25, p. 181-186.
- Lundgren, D. G., Anderson, K. J., Remson, C. C., and Mahoney, R. P., 1964, Culture, structure and physiology of the chemoautotroph *Ferrobacillus ferrooxidans*: Dev. Ind. Microbiol., v. 6, p. 250-259.
- Lundgren, D. G., Vestal, J. R., and Tabita, F. R., 1974, The iron-oxidizing bacteria, *in* Neillands, J. B., ed., Microbial Iron Metabolism: a comprehensive treatise: New York, Academic Press, p. 457-473.
- Lydon, P. A., and O'Brien, J. C., 1974, Mines and mineral resources of Shasta County: Calif. Div. Mines Geology County Rept. 6, 154 p.
- Lynn, R., and Brock, T. D., 1969, Notes on the ecology of a species of *Zygogonium* (Kütz) in Yellowstone National Park: Jour. Phycology, v. 5, p. 181-185.
- Majima, H., 1971, Electrochemistry of pyrite and its significance in sulphide flotation: AIME preprint 71-B-85, 27 p.
- Mattoo, B. N., 1959, Stability of metal complexes in solution. III. Ion association in ferric sulfate and nitrate solutions at low Fe III concentration: Z. Phys. Chem. [Frankfurt], v. 19, p. 156-167.
- Mesmer, R. E., and Baes, C. F., Jr., 1975, The hydrolysis of cations, a critical review of hydrolytic species and their stability constants in aqueous solutions, pt. II: ORNL-NSF-EATC-3, 153 p.
- Morisawa, M., 1968, Streams, their Dynamics and Morphology: New York, McGraw-Hill Book Co., 175 p.
- Morgan, J. J., and Stumm, W., 1965, The role of multivalent metal oxides in limnological transformations, as exemplified by iron and manganese, *in* Jaag, O., ed., Advances in Water Pollution Research: New York, Pergamon Press; v. 1, p. 103-131.

- Morris, J. C., and Stumm, W., 1967, Redox equilibria and measurements of potentials in the aquatic environment, *in* Equilibrium Concepts in Natural Water Systems: Am. Chem. Soc. Adv. in Chemistry Ser., v. 67, p. 270-285.
- Murray, R. C., Jr., and Rock, P. A., 1968, The determination of the ferrocyanide-ferricyanide standard electrode potential at 25°C in cells without liquid junction using cation-sensitive glass electrodes: *Electrochim. Acta*, v. 13, p. 969-975.
- Natarajan, K. A., and Iwasaki, I., 1974, Eh measurements in hydro-metallurgical systems: *Min. Sci. Eng.*, v. 6, p. 35-44.
- Nelson, M., Nordstrom, D. K., and Leckie, J. O., 1976, Ferrous iron analysis in the presence of ferric by the modified Ferrozine method with application to acid mine waters: in prep.
- Nielson, A. M., and Beck, J. V., 1972, Chalcocite oxidation and coupled carbon dioxide fixation by *Thiobacillus ferrooxidans*: *Science*, v. 175, p. 1124-1126.
- Nordstrom, D. K., and Averett, R. C., 1977, Heavy metal discharges into Shasta Lake and Keswick Reservoirs on the Upper Sacramento River, California: a reconnaissance during low flow: U. S. Geol. Survey Open-File Rept. 76-49.
- Nordstrom, D. K., and Jenne, E. A., 1977, Fluorite solubility equilibria in selected geothermal waters: *Geochim. et Cosmochim. Acta*, v. 41, p. 175-188.
- O'Brien, J. C., 1957, Copper, *in* Mineral commodities of California: Calif. Div. Mines Bull. 176, p. 169-182.
- Onsager, L., 1931, Reciprocal relations in irreversible processes: *Phys. Rev.*, v. 37, p. 405-426.
- O'Shaughnessy, M. M., 1899, The copper resources of California: Calif. Miners' Assoc., Calif. Mines and Minerals, p. 206-211.
- Paces, T., 1972, Chemical characteristics and equilibration in natural water-felsic rock-CO₂ system: *Geochim. et Cosmochim. Acta*, v. 36, p. 217-240.
- Pauling, L., 1964, College chemistry, 3d ed.: San Francisco, W. H. Freeman and Co., 832 p.
- Peters, E., and Majima, H., 1968, The physical chemistry of leaching of sulphide minerals: TMS Trans. Paper A68-32, 34 p.
- Pitzer, K. S., 1973, Thermodynamics of electrolytes. I. Theoretical basis and general equations: *Jour. Phys. Chem.*, v. 77, p. 268-277.
- Potter, R. W., II, 1976, The weathering of sulfide ores in Shasta County, California and its relationship to pollution associated with acid mine drainage: U. S. Geol. Survey Open-File Rept. 76-395, 17 p.

- Pouradier, J., and Chateau, H., 1953, Influence de la temperature sur le potentiel normal de l'electrode au calomel: Compt. Rend., v. 237, p. 711-713.
- Razzell, W. E., and Trussell, P. C., 1963, Microbiological leaching of metallic sulfides: Appl. Microbiol., v. 11, p. 105-110.
- Rock, P. A., 1966, The standard oxidation potential of the ferrocyanide-ferricyanide electrode at 25°C and the entropy of ferrocyanide ion: Jour. Phys. Chem., v. 70, p. 576-580.
- Roy, A. B., and Trudinger, P. A., 1970, The Biochemistry of Inorganic Compounds of Sulphur: Cambridge Univ. Press.
- Sato, M., 1960a, Oxidation of sulfide ore bodies. I. Oxidation mechanisms of sulfide minerals at 25°C: Econ. Geology, v. 55, p. 1202-1231.
- 1960b, Oxidation of sulfide ore bodies. II. Oxidation mechanisms of sulfide minerals at 25°C: Econ. Geology, v. 55, p. 1202-1231.
- Schnaitman, C. A., Korczynski, M. S., and Lundgren, D. G., 1969, Kinetic studies of iron oxidation by whole cells of *Ferrobacillus ferrooxidans*: Jour. Bacteriol., v. 99, p. 552-557.
- Silver, M., 1970, Oxidation of elemental sulfur and sulfur compounds and CO₂ fixation by *Ferrobacillus ferrooxidans* (*Thiobacillus ferrooxidans*): Can. Jour. Microbiol., v. 16, p. 845-849.
- Silver, M., and Torma, A. E., 1974, Oxidation of metal sulfides by *Thiobacillus ferrooxidans* grown on different substrates: Can. Jour. Microbiol., v. 20, p. 141-147.
- Silverman, M. P., 1967, Mechanism of bacterial pyrite oxidation: Jour. Bacteriol., v. 94, p. 1046-1051.
- Silverman, M. P., and Ehrlich, H. L., 1964, Microbiol formation and degradation of minerals: Adv. Appl. Microbiol., v. 6, p. 153-206.
- Silverman, M. P., and Lundgren, D. G., 1959, Studies on the chemoautotrophic iron bacterium *Ferrobacillus ferrooxidans*. I. An improved medium and a harvesting procedure for securing high cell yields: Jour. Bacteriol., v. 77, p. 642-647.
- Silverman, M. P., Rogoff, M. H., and Wender, I., 1961, Bacterial oxidation of pyrite materials in coal: Appl. Microbiol., v. 9, p. 491-496.
- Singer, P. C., and Stumm, W., 1970a, Acid mine drainage: the rate-determining step: Science, v. 167, p. 1121-1123.
- 1970b, Oxygenation of ferrous iron: FWQA Rept. 14010-06/69, 197 p.

- Skopintsev, B. A., Romenskaya, N. N., and Smirnov, E. V., 1966, New determinations of the oxidation-reduction potential in Black Sea water: *Oceanology*, v. 6, p. 653-659.
- Smith, E. E., and Shumate, K. S., 1970, Sulfide to sulfate reaction mechanism: FWQA Rept. 14010 FPS 02/70.
- Smith, E. E., Shumate, K. S., and Svanks, K., 1968, Sulfide to sulfate reaction studies: Second Symp. Coal Mine Drainage Res., Pittsburgh, Pa., p. 1-11.
- Sokolova, G. A., and Karavaiko, G. I., 1968, Physiology and geochemical activity of *Thiobacilli* [Russian trans.]: Israel Prog. for Scientific Transl., 283 p.
- Standard Methods for the Examination of Water and Waste Water, 1971, 13th ed.: Washington, D. C., APHA, 874 p.
- Stokes, H. N., 1901, On pyrite and marcasite: U. S. Geol. Survey Bull. 186.
- Stumm, W., 1966, Redox potential as an environmental parameter; conceptual significance and operational limitation: Third Internat. Conf. on Water Pollution Res., Munich, Proc., p. 1-16.
- Stumm, W., and Morgan, J. J., 1970, Aquatic Chemistry: an introduction emphasizing chemical equilibria in natural waters: New York, Wiley-Interscience, 583 p.
- Sutton, J. A., and Corrick, J. D., 1961, Bacteria in mining and metallurgy. Leaching selected ores and minerals. Experiments with *Thiobacillus ferrooxidans*: U. S. Bur. Mines Rep. Inv. 5829, 16 p.
- 1963, Leaching copper minerals by means of bacteria: *Mining Eng.*, v. 15, p. 37-40.
- "Tannin", 1911, in *The Encyclopaedia Britannica*, 11th ed.: New York, The Encyclopaedia Britannica Co., v. 26, p. 397-398.
- "Tannin", 1958, in *Van Nostrand's Scientific Encyclopedia*, 3d ed.: New Jersey, D. Van Nostrand Co., Inc., p. 1646-1647.
- Temple, K. L., and Colmer, A. R., 1951, The autotrophic oxidation of iron by a new bacterium: *Thiobacillus ferrooxidans*: *Jour. Bacteriol.*, v. 62, p. 605-611.
- Thompson, J. B., Jr., 1959, Local equilibrium in metasomatic processes, in Abelson, P. H., ed., *Researches in Geochemistry*: New York, John Wiley, p. 427-457.
- Thorstenson, D. C., 1970, Equilibrium distribution of small organic molecules in natural waters: *Geochim. et Cosmochim. Acta*, v. 34, p. 745-770.

- Torma, A. E., 1971, Microbiological oxidation of synthetic cobalt, nickel and zinc sulfides by *Thiobacillus ferrooxidans*: Rev. Can. Biol., v. 30, p. 209-216.
- Truesdell, A. H., and Jones, B. F., 1974, WATEQ, a computer program for calculating chemical equilibria of natural waters: U. S. Geol. Survey Jour. Res., v. 2, p. 233-248.
- Tuovinen, O. H., and Kelly, D. P., 1972, Biology of *Thiobacillus ferrooxidans* in relation to the microbiological leaching of sulphide ores: Z. Allg. Mikrobiol., v. 12, p. 311-346.
- Tuttle, J. H., 1969, Aspects of iron and sulfur oxidations by the chemoautotroph *Thiobacillus ferrooxidans* with emphasis on inhibition by organic compounds: Ohio State Univ. Ph.D. thesis, 299 p.
- Unz, R. F., and Lundgren, D. G., 1961, A comparative nutritional study of three chemoautotrophic bacteria: *F. ferrooxidans*, *T. ferrooxidans*, and *T. thiooxidans*: Soil Sci., v. 93, p. 302-313.
- Vlek, P. L. G., Blom, T. J. M., Beek, J., and Lindsay, W. L., 1974, Determination of the solubility product of various iron hydroxides and jarosite by the chelation method: Soil Sci. Soc. Am. Proc., v. 38, p. 429-432.
- Wadsworth, M. E., 1973, Kinetics of heterogeneous systems: Ann. Rev. Phys. Chem., v. 23, p. 355-384.
- Wagman, D. D., Evans, W. H., Parker, V. B., Halow, I., Bailey, S. M., and Schumann, R. B., 1968, Selected values of thermodynamic properties: Natl. Bur. Standards Tech. Note 270-3.
- 1969, Selected values of thermodynamic properties: Natl. Bur. Standards Tech. Note 270-4.
- Wakita, H., 1970, Abundance of cadmium in rock-forming minerals, in Handbook of geochemistry, K. H. Wedepohl, ed., v. II/3: Berlin, Springer-Verlag.
- Watson, M. W., Wood, R. H., and Millero, F. J., 1975, The activity of trace metals in artificial seawater at 25°C, in Church, T. M., ed., Marine chemistry in the Coastal Environment: Am. Chem. Soc. Ser. 18, p. 112-118.
- The Weekly Shasta Courier, 1897, Shasta, Calif.: Jan. 2 and 9 eds.
- White, D. E., Hem, J. D., and Waring, G. A., 1963, Chemical composition of subsurface waters: U. S. Geol. Survey Prof. Paper 440-F, 67 p.
- Whitfield, M., 1969, Eh as an operational parameter in estuarine studies: Limnol. Oceanogr., v. 14, p. 547-558.

- Whitfield, M., 1974, Thermodynamic limitations on the use of the platinum electrode in Eh measurements: *Limnol. Oceanogr.*, v. 19, p. 857-865.
- 1975, The extension of chemical models for sea water to include trace components at 25°C and 1 atm pressure: *Geochim. et Cosmochim. Acta*, v. 39, p. 1545-1557.
- Wood, J. R., 1975, Thermodynamics of brine-salt equilibria. I. The systems $\text{NaCl-KCl-MgCl}_2\text{-CaCl}_2\text{-H}_2\text{O}$ and $\text{NaCl-MgSO}_4\text{-H}_2\text{O}$ at 25°C: *Geochim. et Cosmochim. Acta*, v. 39, p. 1147-1163.
- Zajic, J. A., 1969, *Microbial Biogeochemistry*: New York, Academic Press, 345 p.
- ZoBell, C. E., 1946, Studies on redox potential of marine sediments: *Am. Petrol. Geol. Bull.*, v. 30, p. 477-509.

APPENDIX I

Tables of Water Analyses (all concentrations in mg/l)

Appendix I. Set 1

<u>I.D.</u>	<u>Log no.</u>	<u>Dataset</u>	<u>Date</u>	<u>Discharge (cfs)</u>	<u>Temp (°C)</u>	<u>pH</u>	<u>Eh (mv)</u>	<u>Conductivity (μS)</u>
Q	SPC8301	1470	300874	-	23.5	2.60	-	3030
P	SPC8302	1471	300874	-	27.0	7.60	-	882
R	CUC8303	1472	300874	-	27.0	6.75	-	518
N	SPC8311	1473	310874	-	24.5	3.40	-	2800
H	74WA156	1474	051174	1.5	10.5	6.40	385	119
C	74WA157	1475	051174	0.5	10.0	3.02	694	4780†
B	74WA158	1476	051174	0.1	23.0	0.92	-	45000
G	74WA165	1477	061174	-	10.5	1.85	625	7500
J	74WA166	1478	061174	3.24	11.5	2.32	640	4450
G	74WA171	1479	071174	5.26	10.5	1.9	617	6800
G	74WA172	1480	071174	5.25	10.5	1.9	-	5600
N	74WA179	1481	081174	4.91	11.0	2.95	-	1620
Q	74WA182	1482	101174	-	13.0	2.42	641	3050
K	74WA183	1483	111174	-	11.5	2.42	550	3120
I	74WA184	1484	1117	0.31	11.0	3.00	553	2900
D1	74WA185	1485	121174	-	11.0	2.75	463	1522
F1	74WA186	1486	121174	-	11.0	1.88	-	-
F2	74WA187	1487	121174	-	11.0	1.88	-	-
M	74WA188	1488	121174	0.16	11.8	3.0	-	4520
N	74WA189	1489	141174	4.0	14.0	2.50	-	1840
N	74WA190	1490	181174	4.0	10.1	2.55	-	2330
N	74WA192	1491	211174	7.91	10.5	2.5	-	2000
N	74WA193	1492	031274	338	9.5	3.09	-	600
N	74WA194	1493	131274	8.45	7.0	2.88	-	1750
N	74WA195	1494	201274	8.0	7.0	2.98	-	2000
G	74WA196	1495	201274	5	5.0	2.30	-	-

†This number is questionable.

Appendix I. Set 1 (cont'd.)

<u>I.D.</u>	<u>Date</u>	<u>Ca</u>	<u>Mg</u>	<u>Na</u>	<u>K</u>	<u>SO₄</u>	<u>HCO₃</u>	<u>Fe*</u>
Q	300874	-	-	-	-	-	-	350
P	300874	-	-	-	-	-	-	.549
R	300874	-	-	-	-	-	-	.058
N	310874	-	-	-	-	-	-	351
H	051174	9.5	4.0	3.90	0.35	30	0	.020
C	051174	9.8	15	5.40	0.40	333	0	25
B	051174	232	860	86	115	43050	0	10200
G	061174	69.5	185	17.5	21	7970	0	2260
J	061174	29.5	58	9.45	6.8	2530	0	680
G	071174	48	120	14.0	13.4	5280	0	1320
G	071174	42.5	98	12.6	11.4	4150	0	1090
N	081174	19	31	5.95	1.95	860	0	130
Q	101174	38	71	9.72	3.75	2260	0	418
K	111174	29.5	62.5	8.17	4.3	2050	0	460
I	1117	46.5	120	7.20	0.5	2390	0	210
DL	121174	28	39.5	7.60	0.3	819	0	140
F1	121174	62	160	19.4	20	6500	0	1900
F2	121174	61	145	18.9	17.6	6500	0	1770
M	141174	79	265	7.95	0.65	5750	0	1000
N	141174	28	54	8.40	3.55	1570	0	346
N	181174	26	51	7.88	3.60	1500	0	333
N	211174	22.5	45	7.35	3.10	1370	0	280
N	031274	7.2	8.0	2.40	0.55	246	0	39
N	131274	16	29.3	5.00	1.7	902	0	152
N	201274	19	36	5.32	3.42	1066	0	197
G	201274	43.5	111	12.0	11.7	4900	0	126

*Fe refers to total iron when no Fe(III) is given, otherwise it refers to Fe(II) only.

Appendix I. Set 1 (cont'd.)

<u>I.D.</u>	<u>Date</u>	<u>Mn</u>	<u>Zn</u>	<u>Cd</u>	<u>Cu</u>	<u>Al</u>	<u>SiO₂</u>	<u>D.O.</u>
Q	300874	5.42	55.9	.444	10.9	108	-	-
P	300874	.908	.528	-	.038	-	-	-
R	300874	.891	2.53	.019	.980	-	-	-
N	310874	2.50	55.9	.438	11.3	112	-	-
H	051174	.064	0.45	.008	.12	-	30	10.3
C	051174	.69	6.5	.056	2.28	24	32	10.5
B	051174	14	1750	12.3	148	1460	120	-
G	061174	5.68	310	2.25	8.6	278	78	11.0
J	061174	1.85	91.5	.68	2.5	93	37	11.8
G	071174	3.96	180	1.29	3.5	180	51	-
G	071174	3.38	150	1.09	3.5	158	45	-
N	081174	1.42	8.0	.20	4.3	45	31	-
Q	101174	4.00	69.0	.49	10.8	109	54	-
K	111174	2.44	60.0	.47	9.4	93	40	-
I	1117	5.85	24.0	.25	41.8	176	72	-
D1	121174	1.25	45.0	.24	3.9	29	38	-
F1	121174	5.0	260	1.82	4.5	272	75	-
F2	121174	5.0	250	1.70	4.4	240	79	-
M	141174	9.4	48	.515	115	358	110	-
N	141174	2.0	49	.372	7.54	80	76	-
N	181174	2.0	44	.355	7.13	75	40	-
N	211174	1.7	38	.315	6.01	65	36	-
N	031274	.43	4.5	.029	2.09	12	12	-
N	131274	1.13	25	.174	4.48	42	30	-
N	201274	1.34	27	.229	5.45	53	36	-
G	201274	3.32	186	1.27	5.70	170	62	-

Appendix I. Set 2

<u>I.D.</u>	<u>Log no.</u>	<u>Dataset</u>	<u>Date</u>	<u>Discharge (cfs)</u>	<u>Temp (°C)</u>	<u>pH</u>	<u>Eh (mv)</u>	<u>Conductivity (µS)</u>
U	74WA176	1496 U5	071174	-	12.8	7.46	-	74.6
T	74WA177	1497 T5	071174	-	12.5	7.46	-	76.0
S	74WA178	1498 S5	071174	-	12.0	6.2	-	168
O	74WA180	1499 O5	081174	-	13.2	2.75	-	1930
O	74WA181	1500 O5	081174	-	14.0	2.6	-	2400
J	74WA197	1501 J5	201274	-	6.0	3.00	-	-
L	74WA198	1502 L5	201274	-	7.0	3.45	-	-
N	74WA199	1503 N5	301274	10	5.0	3.23	-	1505
N	75WA1	1504 N5	240175	15	6.5	3.10	.688	1255
G	75WA2	1505 G5	240175	5	8.0	2.50	.631	6510
J	75WA3	1506 J5	240175	-	8.0	3.20	.637	1780
L	75WA4	1507 L5	240175	4	10.8	3.3	.831	2470
K	75WA5	1508 K5	240175	18	9.0	3.10	.638	1550
N	75WA6	1509 N5	050275	36	6.5	3.21	.657	825
N	75WA7	1510 N5	070275	132	6.5	3.30	.664	1510
J	75WA8	1511 J5	070275	70	6.0	3.30	.669	-
G	75WA9	1512 G5	070275	20.5	6.5	2.72	.652	2200
I	75WA10	1513 I5	070275	48.3	6.0	6.60	.393	41
B	75WA11	1514 B5	080275	0.16	22.0	1.00	.604	36000
N	75WA12	1515 N5	280275	35.0	12.0	2.92	-	1700
L	75WA128	1516 L5	030475	0.85	8.5	3.40	.825	1155
K	75WA129	1517 K5	030475	69	8.0	2.72	-	1385
N	75WA126	1518 N5	030475	75.4	8.0	2.72	.656	1385
J	75WA130	1519 J5	040475	68.1	5.0	2.70	.619	1480
G	75WA131	1520 G5	040475	13.1	4.8	2.35	.602	5480
I	75WA132	1521 I5	040475	49.1	5.0	5.85	.411	45.2

Appendix I. Set 2 (cont'd.)

<u>I.D.</u>	<u>Date</u>	<u>Ca</u>	<u>Mg</u>	<u>Na</u>	<u>K</u>	<u>SO₄</u>	<u>HCO₃</u>	<u>Fe</u>	<u>Fe(III)</u>
U	071174	8.5	4.2	5.10	1.1	3.73	0	-	-
T	071174	8.5	4.2	5.10	1.1	3.52	0	-	-
S	071174	14	7.5	4.95	0.95	76.2	0	-	-
O	081174	37	71.5	9.75	3.75	2260	0	420	-
O	081174	32.5	58	8.40	2.9	1780	0	310	-
J	201274	14.2	23	4.50	2.75	990	0	260	-
L	201274	47.2	134	6.00	0.48	2170	0	146	-
N	301274	15.5	23.5	5.00	1.3	700	0	125	-
N	240175	12.5	19.5	3.82	1.2	587	0	145	-
G	240175	34.3	71.2	9.60	8.3	3790	0	950	-
J	240175	10.4	15.5	4.10	1.9	1100	0	191	-
L	240175	39	103.5	5.62	0.48	2170	0	148	-
K	240175	12.8	21.5	3.60	1.5	1050	0	156	-
N	050275	8.5	10.5	3.70	0.65	287	0	51	-
N	070275	5.5	7.0	3.00	0.40	195	0	31	-
J	070275	5.0	5.8	2.35	0.48	195	0	44	-
G	070275	11.5	20.5	3.82	1.6	870	0	188	-
I	070275	2.5	1.5	1.78	0.15	10	0	-	-
B	080275	220	620	55	74	29500	0	7500	-
N	280275	8.5	12.0	3.22	1.0	882	0	67	-
L	030475	14.5	33	3.5	0.3	620	0	28.4	46.6
K	030475	5.0	8.7	3.2	1.5	560	0	80.0	42
N	030475	14.5	12	3.5	1.4	495	0	19.2	90.8
J	040475	5.2	8.7	3.3	1.6	510	0	80.0	43
G	040475	12	35	8.2	6.4	2400	0	416	304
I	040475	2.5	1.3	2.0	0.2	12.3	0	.016	.009

Appendix I. Set 2 (cont'd.)

<u>I.D.</u>	<u>Date</u>	<u>Mn</u>	<u>Zn</u>	<u>Cd</u>	<u>Cu</u>	<u>Al</u>	<u>SiO₂</u>	<u>D.O.</u>
U	071174	-	0.02	-	-	-	22	7.95
T	071174	-	0.01	-	-	-	22	7.8
S	071174	0.28	1.68	.008	0.24	0.80	18	9.5
O	081174	4.1	63	0.53	10.2	112	54	7.5
O	081174	3.1	50	0.40	8.5	92	44	6.5
J	201274	0.73	36	.266	1.25	36	25	-
L	201274	4.8	21	.197	34.5	170	84	-
N	301274	0.89	19	.140	4.20	35	30	-
N	240175	0.76	18	.126	3.13	30	25	-
G	240175	2.58	130	1.03	2.72	119	46	-
J	240175	0.59	26	.300	0.56	23	19	-
L	240175	4.7	20	.172	29.8	146	68	-
K	240175	0.94	21	.315	3.70	32	22	-
N	050275	0.37	7.6	.056	1.62	16	21	-
N	070275	0.26	4.4	.028	1.10	9.5	16	-
J	070275	0.17	5.7	.042	0.57	9	13	-
G	070275	0.71	24	.189	2.30	35	23	-
I	070275	-	0.05	-	-	-	9	-
B	080275	11.8	1090	9.0	182	960	130	-
N	280275	0.47	9.4	.076	1.80	18	18	-
L	030475	1.5	6.0	0.05	10.5	46	29	-
K	030475	0.25	13	0.09	0.32	14	8.5	-
N	030475	0.40	11	0.08	1.72	17	19	-
J	040475	0.25	12.5	0.09	0.35	14	8.5	-
G	040475	1.35	60	0.45	1.25	68	26	-
I	040475	-	0.10	-	-	-	13	-

Appendix I. Set 3

<u>I.D.</u>	<u>Log no.</u>	<u>Dataset</u>	<u>Date</u>	<u>Discharge (cfs)</u>	<u>Temp (°C)</u>	<u>pH</u>	<u>Eh (mv)</u>	<u>Conductivity (µS)</u>
N	75WA13	1522 N5	120575	25.0	12.2	2.83	.692	1562
J	75WA14	1523 J5	120575	19.0	12.6	2.78	.636	1970
G	75WA15	1524 G5	120575	4.97	14.0	2.25	.618	6100
N	75WA16	1525 N5	060675	9.71	18.5	2.85	-	2240
G	75WA20	1526 G5	230675	1.22	18.5	2.10	.648	-
J	75WA19	1527 J5	230675	4.87	18.5	2.98	.685	2880
L	75WA18	1528 L5	230675	0.29	19.5	2.98	.734	2505
K	75WA17	1529 K5	230675	5.35	21.0	2.86	.670	2550
N	75WA21	1530 N5	240675	6.94	13.5	2.89	.755	1920
N	75WA22	1531 N5	030775	5.39	23.0	2.76	-	-
N	75WA23	1532 N5	110775	-	28.8	2.68	.688	2660
G	75WA26	1533 G5	150875	-	24.0	2.10	.648	12250
J	75WA25	1534 J5	150875	-	22.0	2.72	.652	4220
N	75WA24	1535 N5	150875	-	25.0	2.80	.789	2980
N	75WA27	1536 N5	041075	2.5	22.0	2.41	.754	3700
J	75WA28	1537 J5	031075	-	14.0	2.10	.624	-
G	75WA29	1538 G5	031075	-	14.0	1.76	.620	-
B	75WA30	1539 B5	031075	-	23.0	1.10	.612	-
N	75WA31	1540 N5	171075	3.50	13.0	2.55	.684	3220
N	75WA32	1541 N5	301075	21.3	11.0	3.10	.731	1130
V	TD-1	1542 V5	160176	-	17.0	2.22	.678	5250
V1	TD-2	1543 V5	6017	-	14.0	2.40	.614	13000
W	TD-3	1544 W5	170176	-	9.5	3.65	.592	375
W1	TD-4	1545 W5	170176	-	8.0	3.50	.663	442
X	TD-5	1546 X5	170176	-	13.5	1.8	.709	12000
X1	TD-6	1547 X5	7017	-	6.0	2.0	.809	5650
I	SC A	1548 I5	261175	-	5.8	6.90	.391	-
B	RH	1549 B5	071275	-	25.5	1.10	.622	65000

Appendix I. Set 3 (cont'd.)

<u>I.D.</u>	<u>Date</u>	<u>Ca</u>	<u>Mg</u>	<u>Na</u>	<u>K</u>	<u>SO₄</u>	<u>HCO₃</u>	<u>Fe</u>	<u>Fe(III)</u>
N	120575	10.5	18.5	4.50	1.98	798	0	178	-
J	120575	8.5	14.0	4.35	2.6	779	0	215	-
G	120575	22	53.0	10.6	9.5	3410	0	910	-
N	060675	16	32.0	6.37	3.5	1320	0	325	-
G	230675	40	102	15.1	16.2	5490	0	148	-
J	230675	17	31	6.82	5.25	1660	0	455	-
L	230675	38	115	5.70	0.60	2210	0	208	-
K	230675	19	43.5	6.46	4.35	1770	0	425	-
N	240675	18	37.5	6.30	3.00	1240	0	246	-
N	030775	22	47	7.55	4.00	1660	0	390	-
N	110775	26	54.5	7.80	4.35	2500	0	410	-
G	150875	81.5	215	29.2	32.5	10900	0	1740	1780
J	150875	36.3	81	12.8	11.8	4080	0	670	530
N	150875	36.5	85	10.8	6.65	3000	0	6.12	613
N	041075	38.5	86	10.6	6.50	3090	0	5.00	595
J	031075	44.5	102	14.2	13.5	4910	0	454	666
G	031075	90	220	28.3	32.5	11250	0	1058	2042
B	031075	225	815	110	-	44600	0	7000	3700
N	171075	27.2	52.5	8.40	4.18	1850	0	400	40
N	301075	12.5	15	4.13	1.02	450	0	17.7	56.3
V	160176	64.5	43	5.25	1.90	2750	0	284	346
V1	6017	355	455	12.0	1.30	7070	0	2940	260
W	170176	22	5.0	4.05	0.3	155	0	16.4	-
W1	170176	22	5.0	4.80	0.3	158	0	11.8	-
X	170176	125	135	10.6	2.55	12050	0	358	2022
X1	7017	60	68	7.80	0.95	4700	0	10.4	1130
I	261175	7.5	2.5	3.15	0.20	28.5	0	.036	.064
B	071275	173	685	92.5	128	10170	0	9050	2650

Appendix I. Set 3 (cont'd.)

<u>I.D.</u>	<u>Date</u>	<u>Mn</u>	<u>Zn</u>	<u>Cd</u>	<u>Cu</u>	<u>Al</u>	<u>SiO₂</u>
N	120575	.68	21	.146	2.90	31	22
J	120575	.47	24	.177	.68	25	18
G	120575	1.78	92	.729	2.78	103	32
N	060675	1.31	34	.257	4.90	52	29
G	230675	3.30	171	1.22	3.30	178	50
J	230675	1.05	50	.423	1.48	55	25
L	230675	4.7	22	.200	36.8	164	62
K	230675	1.57	49	.355	6.45	59	32
N	240675	1.40	33	.229	6.00	57	30
N	030775	1.74	48	.337	7.28	75	34
N	110775	2.12	56	.400	9.81	85	42
G	150875	7.55	380	2.72	2.88	380	96
J	150875	2.93	117	.987	1.00	139	43
N	150875	3.10	78	.629	11.3	134	52
N	041075	2.93	88	.686	13.65	140	58
J	031075	2.55	166	1.22	13.50	172	52
G	031075	5.85	370	2.77	32	385	103
B	031075	-	1460	-	-	1450	140
N	171075	1.99	50	.389	7.04	89	42
N	301075	.76	12	.098	2.88	.21	20
V	160176	1.15	102	1.06	63	56	26
V1	6017	9.4	660	2.8	80	580	140
W	170176	.18	9.7	.044	3.9	30	30
W1	170176	.18	9.7	.038	3.9	3.0	28
X	170176	12.5	255	1.39	290	168	89
X1	7017	7.1	122	.66	135	89	52
I	261175	.043	1.20	-	-	-	15
B	071275	11.7	-	13.0	340	1400	-

Appendix I. Set 4

<u>I.D.</u>	<u>Log no.</u>	<u>Dataset</u>	<u>Date</u>	<u>Discharge (cfs)</u>	<u>Temp (°C)</u>	<u>pH</u>	<u>Eh (mv)</u>	<u>Conductivity (µS)</u>
G	BC-A	1412	261175	-	7.3	2.00	.628	11500
J1	SC-B	1413	261175	-	8.3	2.40	.629	8350
J2	SC-C	1414	261175	-	8.2	2.45	.647	3230
J3	SC-C1	1415	261175	-	8.4	2.46	.650	3140
J4	SC-D	1416	261175	-	9.5	2.48	.661	2970
J5	SC-E	1417	261175	-	6.8	2.53	.673	2720
L	SK-A	1418	261175	-	7.2	3.10	.769	2900
K	SC-F	1419	261175	-	6.5	2.62	.693	2670
N	SC-G	1420	261175	-	7.0	2.61	.774	2080
G	BC-A	1421	061275	3.90	10.0	2.25	.661	4000
J1	SC-B	1422	061275	-	9.5	2.90	.663	1110
J2	SC-C	1423	061275	15.1	9.5	2.90	.661	1148
J4	SC-D	1424	061275	17.6	9.5	2.90	.668	1102
J5	SC-E	1425	061275	18.5	9.0	2.90	.669	1140
L	SK-A	1426	061275	1.54	9.5	2.90	.696	1630
K	SC-F	1427	061275	20.0	9.0	2.90	.676	1038
N	SC-G	1428	061275	18.6	9.5	2.90	.689	1040
B	TD-7	1429	180176	-	24.0	1.10	.633	40000

Appendix I. Set 4 (cont'd.)

<u>I.D.</u>	<u>Date</u>	<u>Ca</u>	<u>Mg</u>	<u>Na</u>	<u>K</u>	<u>SO₄</u>	<u>HCO₃</u>	<u>Fe</u>	<u>Fe(III)</u>
G	261175	53	119	15.6	15.8	6190	0	1190	320
J1	261175	19	28.7	6.30	4.05	1420	0	300	112
J2	261175	18.5	28.1	6.30	4.01	1440	0	278	122
J3	261175	18.3	27.8	6.15	3.94	1410	0	267	129
J4	261175	18.3	27.5	6.15	3.95	1400	0	234	158
J5	261175	18.3	27.6	6.15	3.88	1390	0	182	204
L	261175	42.5	118	6.32	0.42	2190	0	7.2	176
K	261175	22	39.5	6.30	3.35	1400	0	140	220
N	261175	21	34.2	6.68	2.90	1260	0	4.9	247
G	061275	24	45.5	7.35	4.2	2140	0	299	231
J1	061275	8.5	9.5	3.30	1.06	431	0	55.4	49.5
J2	061275	8.5	9.5	3.30	1.05	431	0	52	50
J4	061275	8.5	9.5	3.30	1.10	443	0	48.8	51.2
J5	061275	8.5	9.0	3.30	1.09	414	0	41.6	51.4
L	061275	22	45.7	5.00	0.45	1020	0	9.48	74.5
K	061275	10	13	3.48	1.05	447	0	30.8	53.2
N	061275	10.2	12	4.05	0.88	437	0	17.8	59.2
B	180176	240	720	79	107	41000	0	7820	3180

Appendix I. Set 4 (cont'd.)

<u>I.D.</u>	<u>Date</u>	<u>Mn</u>	<u>Zn</u>	<u>Cd</u>	<u>Cu</u>	<u>Al</u>	<u>SiO₂</u>
G	261175	3.9	212	1.50	3.20	212	64
J1	261175	0.97	50	.372	.80	50	26
J2	261175	0.97	50	.369	.75	50	26
J3	261175	0.96	50	.369	.75	50	26
J4	261175	0.95	49	.369	.75	49	26
J5	261175	0.96	48	.369	.80	49	26
L	261175	5.0	22	.200	34.0	170	69
K	261175	1.56	46	.329	5.57	70	32
N	261175	1.35	37	.277	4.80	57	33
G	061275	1.65	56	.432	3.18	80	38
J1	061275	0.39	12	.084	.68	17	16
J2	061275	0.37	12	.084	.70	17	16
J4	061275	0.37	12	.084	.72	17	16
J5	061275	0.36	11	.084	.67	17	16
L	061275	2.25	10	.092	17.8	80	42
K	061275	0.53	10	.083	2.25	22	18
N	061275	0.50	10	.078	1.95	21	18
B	180176	11.0	1860	14	360	1410	140

Appendix I. Set 5

<u>I.D.</u>	<u>Log no.</u>	<u>Dataset</u>	<u>Date</u>	<u>Discharge (cfs)</u>	<u>Temp (°C)</u>	<u>pH</u>	<u>Eh (mv)</u>	<u>Conductivity (µS)</u>
J	S12/4930	1550 J5	041275	4.85	6.5	2.25	.619	3280
J	S12/41500	1551 J5	041275	4.95	7.8	2.24	.639	5050
J	S12/42100	1552 J5	041275	5.25	7.0	3.00	.667	905
J	S12/50330	1553 J5	051275	5.25	8.0	2.98	.668	822
J	S12/50945	1554 J5	051275	5.35	7.0	2.83	.667	1015
G	A12/40930	1555 G5	041275	-	6.8	1.90	.629	12500
G	A12/41500	1556 G5	041275	-	7.8	1.90	.629	9600
G	A12/42100	1557 G5	041275	-	7.5	2.50	.664	2550
G	A12/50330	1558 G5	051275	-	8.5	2.40	.660	3180
G	A12/50945	1559 G5	051275	-	7.5	2.38	.659	2740
D	B12/41030	1560 D5	041275	-	6.0	2.80	.699	1130
D	B12/41230	1561 D5	041275	-	6.0	2.80	.707	-
D	B12/41430	1562 D5	041275	-	6.0	2.70	.680	-
D	B12/41630	1563 D5	041275	-	6.0	2.72	.693	-
D	B12/41830	1564 D5	041275	-	6.0	2.71	.702	-
D	B12/42030	1565 D5	041275	-	6.0	2.71	.702	-
D	B12/42230	1566 D5	041275	-	6.0	2.76	.705	-
D	B12/50030	1567 D5	051275	-	6.0	2.80	.702	-
D	B12/50230	1568 D5	051275	-	6.0	2.80	.699	-
D	B12/50420	1569 D5	051275	-	6.0	2.80	.695	-
D	B12/50630	1570 D5	051275	-	6.0	2.76	.693	-
D	B12/50830	1571 D5	051275	-	6.0	2.78	.692	-
D	B12/51030	1572 D5	051275	-	6.0	2.71	.701	-
D	B 1,2,3	1573 D5	051275	-	6.0	2.77	.698	1470
D	B 4,5,6	1574 D5	051275	-	6.0	2.79	.700	1460
D	B 7,8,9	1575 D5	051275	-	6.0	2.75	.700	1485
D	B101112	1576 D5	051275	-	6.0	2.76	.700	1502
D	B141516	1577 D5	051275	-	6.0	2.75	.700	1515
D	B171819	1578 D5	051275	-	6.0	2.75	.700	1511

Appendix I. Set 5 (cont'd.)

<u>I.D.</u>	<u>Date</u>	<u>Ca</u>	<u>Mg</u>	<u>Na</u>	<u>K</u>	<u>SO₄</u>	<u>HCO₃</u>	<u>Fe</u>	<u>Fe(III)</u>
J	041275	18	31	6.45	4.05	1440	0	260	145
J	041275	24.5	52	8.40	6.55	2270	0	488	132
J	041275	8.0	6.5	2.65	1.00	340	0	46	31
J	051275	7.0	6.5	3.00	0.85	300	0	46	31
J	051275	8.0	9.0	3.16	1.02	410	0	62	3.3
G	041275	52	123	16.1	15.8	6170	0	1223	297
G	041275	44	107	14.2	12.5	5510	0	1094	226
G	041275	18	31.5	4.65	2.9	1330	0	198	172
G	051275	20	37.5	5.80	3.3	1650	0	242	178
G	051275	18	32.5	5.40	2.75	1420	0	198	132
D	041275	18.5	24	5.3	0.3	493	0	11.5	22.5
D	041275	19	23.5	5.45	1.18	499	0	7.2	24.3
D	041275	24	31	3.95	0.33	1090	0	90	125
D	041275	17.5	22.5	2.70	0.48	781	0	48.0	95
D	041275	14	19	2.65	0.43	667	0	33.0	89
D	041275	13.7	21	3.22	0.38	700	0	35.0	99
D	041275	11.7	18.5	4.05	0.27	565	0	21.0	76
D	051275	11.7	17.5	4.08	0.27	570	0	24.0	69
D	051275	11.8	18	4.10	0.27	559	0	28.0	67
D	051275	11.8	17.8	4.27	0.22	534	0	29.0	63
D	051275	13.0	19	4.06	0.15	608	0	44.0	64
D	051275	13.5	19.5	3.88	0.12	665	0	59.0	66
D	051275	11.5	17.5	3.48	0.24	608	0	43.0	71
D	051275	11.0	18.5	4.08	0.20	983	0	42.1	71.9
D	051275	11.7	21	4.95	0.13	652	0	38.3	75.7
D	051275	12.8	22	4.58	0.24	1091	0	39.8	76.2
D	051275	13.8	23	4.58	0.13	713	0	40.1	74.9
D	051275	14	24	4.65	0.18	718	0	39.2	72.8
D	051275	14	24	4.80	0.18	701	0	38.0	68

Appendix I. Set 5 (cont'd.)

<u>I.D.</u>	<u>Date</u>	<u>Mn</u>	<u>Zn</u>	<u>Cd</u>	<u>Cu</u>	<u>Al</u>	<u>SiO₂</u>
J	041275	1.03	50	.395	1.18	50	27
J	041275	1.70	82	.652	2.20	87	32
J	041275	0.37	10	.072	1.10	12	15
J	051275	0.31	11	.081	1.00	13	16
J	051275	0.38	14	.106	1.25	16	16
G	041275	3.95	221	1.57	5.20	223	55
G	041275	3.52	187	1.37	4.50	190	52
G	041275	1.45	48	.332	4.50	49	22
G	051275	1.45	55	.423	3.92	60	34
G	051275	1.25	47	.372	4.60	51	31
D	041275	0.98	8.0	.064	2.70	35	40
D	041275	1.0	8.0	.015	2.70	34	35
D	041275	1.45	72	.543	10.6	46	27
D	041275	1.10	37	.297	6.00	34	20
D	041275	0.95	25	.183	5.65	29	20
D	041275	0.92	21	.157	5.70	30	24
D	041275	0.76	16	.112	4.08	29	27
D	051275	0.72	17	.134	4.55	25	27
D	051275	0.74	17	.137	4.70	26	28
D	051275	0.73	17	.137	4.40	26	29
D	051275	0.78	20	.172	5.20	29	29
D	051275	0.78	22	.177	6.00	29	28
D	051275	0.76	17	.134	4.00	27	24
D	051275	0.70	10	.078	3.50	29	29
D	051275	0.72	6.2	.056	3.00	30	30
D	051275	0.82	6.0	.056	3.00	32	36
D	051275	0.86	6.0	.056	3.10	35	36
D	051275	0.90	6.1	.056	3.15	35	36
D	051275	0.95	6.2	.056	3.15	36	-

Appendix I. Set 6

<u>I.D.</u>	<u>Log no.</u>	<u>Dataset</u>	<u>Date</u>	<u>Discharge (cfs)</u>	<u>Temp (°C)</u>	<u>pH</u>	<u>Eh (mv)</u>	<u>Conductivity (µS)</u>
G	75WA35	1579 G5	111175	0.68	6.0	2.00	.378	9900
J	75WA34	1580 J5	111175	3.88	5.5	2.50	.650	2970
N	75WA33	1581 N5	111175	5.32	5.5	2.90	.770	1810
B2	75WA37	1582 B5	030476	-	20	1.10	.509	50000
B	75WA38	1583 B5	030476	-	23	1.10	.617	40000
B1	75WA39	1584 B5	030476	-	10	0.80	.644	75000
A	75WA33	1585 A5	040475	7.75	6.0	6.6	.433	54.5
B	75WA34	1586 B5	040475	0.6	31.0	1.02	.602	70000
C	75WA35	1587 C5	040475	-	7.5	3.49	.714	266
D	75WA36	1588 D5	040475	11.75	8.5	3.02	.725	460
E	75WA37	1589 E5	040475	-	14.0	3.68	.532	1040
F	75WA38	1590 F5	040475	10.51	9.0	1.75	.586	5900
Y	TD-8	1591 Y5	020476	-	10	2.58	.711	3000
Y1	TD-9	1592 Y5	020476	-	9.6	3.90	.675	290
Y2	TD-10	1593 Y5	020476	-	8	5.50	.580	100
Y3	TD-11	1594 Y5	020476	-	7	4.40	.568	270
Z	TD-12	1595 Z5	020476	-	8	3.58	.748	125
N		1596 N5	270276	43.2	8.5	3.15	.676	585
N		1597 N5	030476	14.2	6.0	3.17	.657	660

Appendix I. Set 6 (cont'd.)

<u>I.D.</u>	<u>Date</u>	<u>Ca</u>	<u>Mg</u>	<u>Na</u>	<u>K</u>	<u>SO₄</u>	<u>HCO₃</u>	<u>Fe</u>	<u>Fe(III)</u>
G	111175	45	107	14.2	13.8	5310	0	1280	-
J	111175	17	27.5	6.00	3.75	1280	0	260	94
N	111175	18	30.8	5.40	2.40	1080	0	208	-
B2	030476	222	585	57.5	86	5200	0	8720	1280
B	030476	227	595	56.5	83	3600	0	6480	1920
B1	030476	141	445	70.0	105	7600	0	5480	3720
A	040475	2.0	2.5	2.3	0.20	-	0	.012	-
B	040475	162	620	124	125	9800	0	5200	5800
C	040475	2.5	4.0	2.6	0.20	90	0	1.72	3.28
D	040475	3.0	8.0	2.9	0.22	180	0	3.48	20
E	040475	30	35.5	5.8	0.70	650	0	66.2	33.8
F	040475	18.5	36	8.3	6.95	2560	0	458	202
Y	020476	8.0	40	1.9	0.40	1270	0	138	-
Y1	020476	18	8.4	3.6	0.45	119	0	0.40	-
Y2	020476	6.5	1.5	3.2	0.3	41	0	-	-
Y3	020476	10	8.4	3.15	0.41	122	0	-	-
Z	020476	1.0	-	0.80	0.25	25.2	0	.032	.963
N	270276	1	4.0	2.1	0.48	187	0	35	-
N	030476	1	3.5	2.4	0.6	207	0	51	-

Appendix I. Set 6 (cont'd.)

<u>I.D.</u>	<u>Date</u>	<u>Mn</u>	<u>Zn</u>	<u>Cd</u>	<u>Cu</u>	<u>Al</u>	<u>SiO₂</u>
G	111175	3.4	180	1.29	2.75	188	55
J	111175	.82	44	.337	0.67	47	26
N	111175	1.9	31	.229	4.40	47	32
B2	030476	15.1	1210	9.5	4.23	1050	140
B	030476	11.0	1140	9.3	230	1030	140
B1	030476	8.3	1290	10.8	218	900	140
A	040475	0.05	0.03	-	0.03	-	15
B	040475	10.2	1260	10.2	222	1150	130
C	040475	0.1	0.8	.01	.60	5.0	18
D	040475	1.0	6.0	.05	1.30	11.0	28
E	040475	3.55	15	.08	1.48	33	84
F	040475	1.45	63	.50	1.28	70	27
Y	020476	2.4	22	-	14.3	74	72
Y1	020476	2.2	4.5	-	1.37	3.0	32
Y2	020476	0.55	0.8	-	0.38	0.25	21
Y3	020476	1.05	4.0	-	2.28	6.0	22
Z	020476	-	0.22	-	0.38	0.30	7.2
N	270276	0.1	3.7	-	0.61	9	14
N	030476	0.1	6.4	-	0.31	8.5	14

Appendix II

Measured Potentials (mv) in ZoBell's Solution from 8° to 84°C

Orion electrodes			
Temperature (°C)	No. 1	No. 2	Pt,Ag/AgCl
8.32	219.3	215.0	257.0
12.42	212.3	207.6	250.6
15.52	207.0	202.0	245.8
20.60	198.1	192.7	238.1
26.20	188.3	182.5	229.4
33.35	175.8	169.1	217.9
37.37	168.7	161.6	211.5
38.35	167.3	159.4	210.5
39.85	164.2	157.0	207.6
44.60	155.8	147.6	200.9
44.93	154.5	147.5	200.8
45.66	154.1	146.6	199.8
50.00			192.3
50.70	145.0	136.9	191.0
51.90	141.9	135.1	189.4
56.07	134.3	127.6	182.5
56.57	134.2	125.6	180.7
62.00	123.5	116.6	172.5
65.60		108.0	167.2
66.20	115.7	108.9	165.4
72.10	104.2	97.8	155.0
78.42	92.2	83.5	143.4
83.94		70.5	133.5
84.00			133.4
84.10	84.2	70.4	